doi.org/10.26434/chemrxiv.8219057.v1

BODIPY Fluorophores for Membrane Potential Imaging

Jenna Franke, Benjamin Raliski, Steven Boggess, Divya Natesan, Evan Koretsky, Patrick Zhang, Rishikesh Kulkarni, Parker Deal, Evan Miller

Submitted date: 03/06/2019 • Posted date: 04/06/2019

Citation information: Franke, Jenna; Raliski, Benjamin; Boggess, Steven; Natesan, Divya; Koretsky, Evan; Zhang, Patrick; et al. (2019): BODIPY Fluorophores for Membrane Potential Imaging. ChemRxiv. Preprint.

Fluorophores based on the BODIPY scaffold are prized for their tunable excitation and emission profiles, mild syntheses, and biological compatibility. Improving the water-solubility of BODIPY dyes remains an outstanding challenge. The development of water-soluble BODIPY dyes usually involves direct modification of the BODIPY fluorophore core with ionizable groups or substitution at the boron center. While these strategies are effective for the generation of water-soluble fluorophores, they are challenging to implement when developing BODIPY-based indicators: direct modification of BODIPY core can disrupt the electronics of the dye, complicating the design of functional indicators; and substitution at the boron center often renders the resultant BODIPY incompatible with the chemical transformations required to generate fluorescent sensors. In this study, we show that BODIPYs bearing a sulfonated aromatic group at the meso position provide a general solution for water-soluble BODIPYs. We outline the route to a suite of 5 new sulfonated BODIPYs with 2,6-disubstitution patterns spanning a range of electron-donating and -withdrawing propensities. To highlight the utility of these new, sulfonated BODIPYs, we further functionalize them to access 13 new, BODIPY-based voltage-sensitive fluorophores. The most sensitive of these BODIPY VF dyes displays a 48% ΔF/F per 100 mV in mammalian cells. Two additional BODIPY VFs show good voltage sensitivity (≥24% ΔF/F) and excellent brightness in cells. These compounds can report on action potential dynamics in both mammalian neurons and human stem cell-derived cardiomyocytes. Accessing a range of substituents in the context of a water soluble BODIPY fluorophore provides opportunities to tune the electronic properties of water-soluble BODIPY dyes for functional indicators.

File list (2)

BODIPY Fluorophores for Membrane Potential Imaging

Jenna M. Franke,[‡] Benjamin K. Raliski,[‡] Steven C. Boggess,[‡] Divya V. Natesan,[‡] Evan T. Koretsky,[‡] Patrick Zhang,[‡] Rishikesh U. Kulkarni,[‡] Parker E. Deal[‡] and Evan W. Miller[‡§†]*

Departments of [‡]Chemistry and [§]Molecular & Cell Biology and [†]Helen Wills Neuroscience Institute. University of California, Berkeley, California 94720, United States.

ABSTRACT: Fluorophores based on the BODIPY scaffold are prized for their tunable excitation and emission profiles, mild syntheses, and biological compatibility. Improving the water-solubility of BODIPY dyes remains an outstanding challenge. The development of water-soluble BODIPY dyes usually involves direct modification of the BODIPY fluorophore core with ionizable groups or substitution at the boron center. While these strategies are effective for the generation of water-soluble fluorophores, they are challenging to implement when developing BODIPY-based indicators: direct modification of BODIPY core can disrupt the electronics of the dye, complicating the design of functional indicators; and substitution at the boron center often renders the resultant BODIPY incompatible with the chemical transformations required to generate fluorescent sensors. In this study, we show that BODIPYs bearing a sulfonated aromatic group at the *meso* position provide a general solution for water-soluble BODIPYs. We outline the route to a suite of 5 new sulfonated BODIPYs with 2,6-disubstitution patterns spanning a range of electron-donating and -withdrawing propensities. To highlight the utility of these new, sulfonated BODIPYs, we further functionalize them to access 13 new, BODIPY-based voltage-sensitive fluorophores. The most sensitive of these BODIPY VF dyes displays a 48% ΔF/F per 100 mV in mammalian cells. Two additional BODIPY VFs show good voltage sensitivity (≥24% ΔF/F) and excellent brightness in cells. These compounds can report on action potential dynamics in both mammalian neurons and human stem cell-derived cardiomyocytes. Accessing a range of substituents in the context of a water soluble BODIPY fluorophore provides opportunities to tune the electronic properties of water-soluble BODIPY dyes for functional indicators.

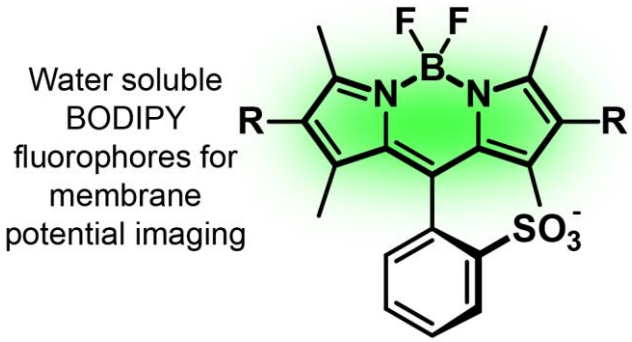

Introduction

Synthetic chemistry has long been a source of colorful compounds[1-3] whose ability to absorb light enable applications in far-ranging fields. Fluorescent dyes find wide-spread use in the modern research laboratory where features such as visible excitation and emission profiles, large molecular brightness values, and photostability are highly prized, along with biologically-compatible properties like water-solubility. Since the late 19th century, xanthene dyes like fluoresceins[4] and rhodamines[5-6] offered a fertile source of inspiration as scaffolds for biologically-useful dyes and indicators.[7-9] More recently, BODIPY, or 4,4-difluoro-4-bora-3a,4a,-diaza-*s*-indacene, (**Scheme 1**) dyes have emerged as a versatile complement to xanthene dyes. Owing to the relatively mild reaction conditions for the generation of BODIPY fluorophores,[10] a number of flexible synthetic routes afford the opportunity to install a range of substituents directly to the BODIPY core, tuning both the color and electronic properties of BODIPY dyes.

Since the initial report of BODIPY in 1968,[11] a proliferation of synthetic methods[10, 12-13] and conceptual understanding[14-15] enabled the application of BODIPYs as indicators for a number of important, biologically-relevant analytes and properties,[16-17] including pH,[18-19] cations like Na^+,[20-21] K^+,[20, 22] Mg^{2+},[23] and Ca^{2+};[24-25] transition metals;[26-28] reactive oxygen[29] and nitrogen

Scheme 1. Design of H_2O-soluble BODIPYs

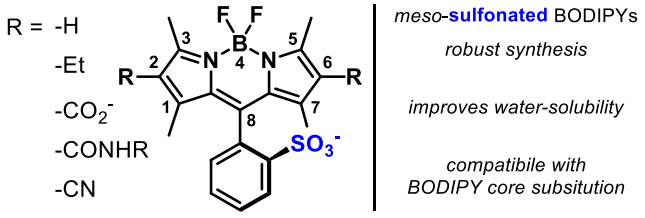

species,[14] electron transfer reactions,[30] and membrane viscosity.[31] Because of the broad tunability of BODIPY-based scaffolds, we thought these fluorophores would make an excellent choice for incorporation into a molecular wire-based, photo-induced electron transfer (PeT) membrane potential sensing framework.[32] Previous work in our lab showed that tuning the relative electron affinities between a fluorescein-based reporter and electronically-orthogonal phenylenevinylene molecular wire voltage-sensing domain profoundly altered the voltage sensitivities of fluorescein based dyes. However, the limited synthetic scope of sulfonated fluorescein only allowed access to a narrow range of substituents (H, F, Cl, Me).[33]

Here, we introduce new, water-soluble sulfonated BODIPYs with substituents ranging from highly electron donating (R = Et) to

Scheme 2. Synthesis of BODIPY VoltageFluor dyes with Et, H and CN at the 2,6-positions

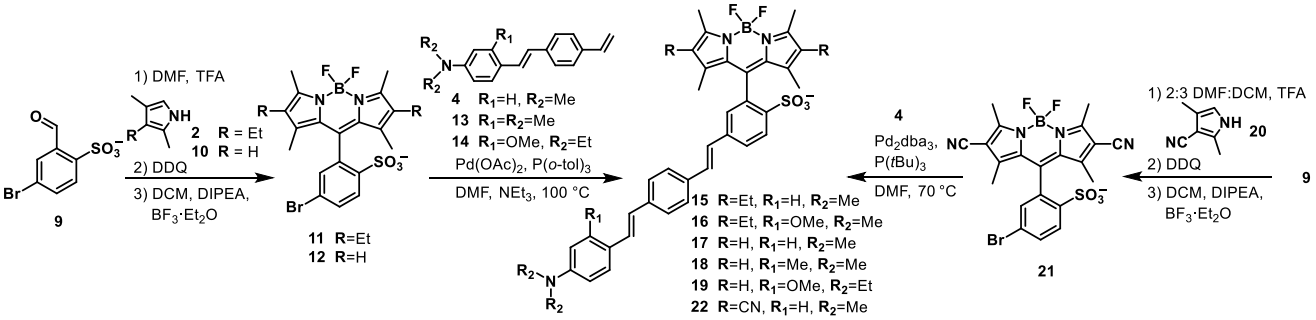

withdrawing (R = CN). We incorporate the new, sulfonated BODIPYs into a molecular wire voltage-sensing scaffold to provide the first examples of PeT-based voltage-sensitive BODIPYs. The most sensitive of these dyes displays a 48% ΔF/F per 100 mV in HEK cells, and two others possess ≥24% ΔF/F, making them useful for voltage sensing applications in both neurons and cardiomyocytes.

Design of water soluble BODIPYs

We prepared a total of 13 BODIPY-based Voltage-sensitive Fluorophores, or BODIPY-VF dyes. All of the BODIPY compounds feature a common *ortho*-sulfonic acid substituted *meso* aromatic ring (8-position, **Scheme 1**) and substitution patterns at the 2,6 positions that include hydrogen, ethyl, carboxylate, amide, and cyano functionalities (**Scheme 1**). Our initial attempts to access BODIPY-based VoltageFluor indicators centered around the development of water-soluble tetramethyl, diethyl BODIPY fluorophores. Ionizable groups, such as sulfonates or carboxylates, are essential for the proper orientation of VF-type dyes in cellular membranes.[34-35] We first sought to introduce water-solubilizing groups centered on substitution at boron.[36-38] However, in our hands, these modifications proved incompatible with many of the subsequent reaction conditions required for installation of voltage-sensing phenylenevinylene molecular wires. Functionalization of the 2 and 6 positions of the BODIPY core offered a route to the installation of water-solubilizing groups like sulfonates[39] or carboxylates,[40] but direct functionalization of the BODIPY core can profoundly alter redox properties, confounding the tuning of fluorophore redox potential[15, 33] with installation of water solubilizing groups. One solution is to include a sulfonate on the *meso* aromatic ring (**Scheme 1**), which we hypothesized would improve solubility, be generalizable across a range of 2,6-substitution patterns on the BODIPY core, and aid in the proper orientation within cellular plasma membranes.

Synthesis of H- and Et-BODIPY VoltageFluors

Owing to the commercial availability of the 3-ethyl-2,4-dimethyl-*1H*-pyrrole precursors (kryptopyrrole), we first synthesized BODIPY **3** (**Scheme S1**) and **11** (**Scheme 2**) for use in subsequent coupling with phenylenevinylene molecular wires. The sulfonated benzaldehyde precursor, **9** (**Scheme 2**, and related *para*-isomer, **1**, **Scheme S1**), was completely insoluble in CH_2Cl_2 and toluene, the most commonly used solvents for BODIPY condensations. [10, 14, 20, 31, 41-44] We screened polar solvents for the TFA-catalyzed condensation of aldehyde **9** (or **1**) with kryptopyrrole **2** (**Scheme 2** and **S1**). DMF gave the best conversion to the dipyrromethane. Oxidation with DDQ to form the corresponding dipyrromethene followed by BF_2 chelation with boron trifluoride diethyl etherate ($BF_3{\cdot}OEt_2$) in CH_2Cl_2 solvent gave *ortho*-sulfonated BODIPY **3** (Br *para* to BODIPY, **Scheme S1**) in 49% yield and **11** (Br *meta* to BODIPY, **Scheme 2**) in 33% yield.

A Pd-catalyzed Heck coupling between BODIPY **3** and substituted styrenes **4** and **5** gave two different 2,6-diethyl, *para* molecular wire BODIPY VoltageFluors: Et*p*H (**6**) and Et*p*OMe (**7**) in 92 and 25% isolated yield, respectively (**Scheme S1**). The naming convention represents the ethyl groups at the 2,6-positions, molecular wire *para* from the fluorophore, and the identity of the R_1 substituent. Derivatives with the molecular wire *meta* from the fluorophore were prepared via a similar route from BODIPY **11** (**Scheme 2**; Et*m*H **15**, 26% yield, and Et*m*OMe **16**, 29%). Tetramethyl BODIPY VoltageFluors **17**-**19** (R = H) were prepared first by reacting 2,4-dimethyl-*1H*-pyrrole **10** with sulfonated aldehyde **9**, resulting in a 38% yield of *ortho*-sulfonated tetramethyl BODIPY **12**. Heck coupling with substituted styrene **4**, **13**, or **14** then gave TM*m*H (**17**), TM*m*Me (**18**), and TM*m*OMe (**19**) in 35-62% yield after silica gel chromatography.

Synthesis of CN-BODIPY VoltageFluor

Access to electron-withdrawing BODIPY derivatives provide a useful counterpoint to H- and ethyl-substituted BODIPYs and may produce lower levels of reactive $^1O_2$ than more electron-rich derivatives.[40] Synthesis of cyano VoltageFluor derivative **22** was more challenging than either H- or Et-substituted BODIPY VoltageFluors. Because of the poor nucleophilicity of 2,4-dimethyl-*1H*-pyrrole-3-carbonitrile (**20**), no reaction with sulfonated benzaldehyde **9** was observed unless heated to 60 °C. The heated condensation resulted in only an 8% isolated yield of 2,6-dicyano BODIPY **21**. Switching the solvent to a 2:3 DMF:CH_2Cl_2 mixture and adding an excess of TFA (100 µL, 6 equiv.) allowed the synthesis to proceed at room temperature and increased the isolated yield to 29% (**Scheme 2**).

BODIPY **21** is less stable than 2,6-diethyl and tetramethyl BODIPYs **11** and **12**, possibly due to the lower effective charges on the dipyrromethene nitrogen atoms.[45] When subjected to the Pd-catalyzed Heck coupling conditions that afforded previous BODIPY VF dyes, dicyano BODIPY **21** decomposed before conversion to product. Lowering the reaction temperature from 100 °C to 70 °C did not prevent decomposition. By exposing dicyano BODIPY **21** to Heck reaction conditions and systematically removing single reaction components, we determined that the presence of trimethylamine (NEt_3) was initiating decomposition of dicyano BODIPY **21**. Replacing NEt_3 with inorganic bases (Cs_2CO_3, K_2CO_3) or bulky amine bases (1,8-bis(dimethylamino)naphthalene) resulted in scant improvement in conversion; decomposition of **21** remained a problem. To circumvent the sensitivity of dicyano BODIPY **21**,

Scheme 3. Synthesis of BODIPY VoltageFluor dyes with CO_2H and CONHR at the 2,6-positions.

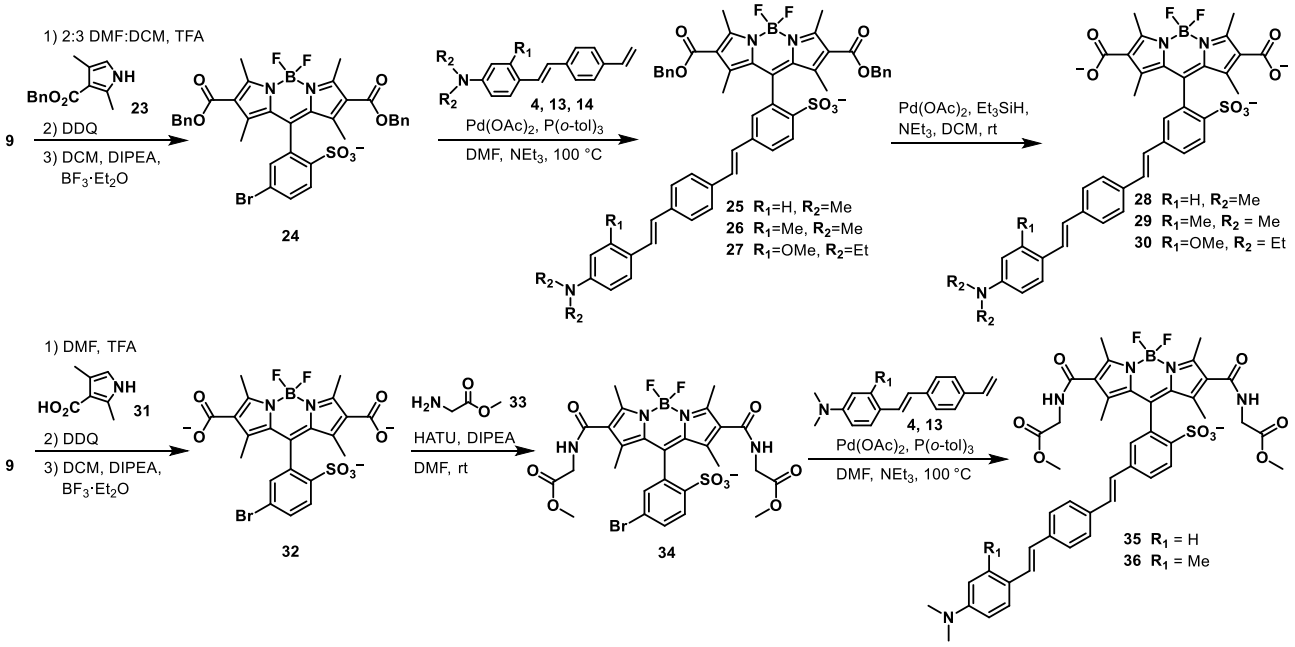

we attempted a base-free Heck coupling, relying only on the substituted aniline of styrene reactant **4** to buffer generated HBr. The resulting Heck coupling was low yielding (6%), but provided sufficient cyano*m*H **22** to purify and characterize (**Scheme 2**).

Synthesis of dicarboxy- and diamido-BODIPY VoltageFluors

The 2,6-dicarboxy VoltageFluor series was synthesized via two different routes. Initially, 2,6-dicarboxy BODIPY **32** was synthesized in a 49% yield from aldehyde **9** and 2,4-dimethylpyrrole-3-carboxylic acid **31** (**Scheme 3**), then subjected to the same base-free Heck coupling conditions as the dicyano BODIPY **21**, giving the 2,6-dicarboxylic acid VoltageFluor, carboxy*m*H **28** in a 6% yield after preparative thin layer chromatography (pTLC). Subsequent Heck couplings with unprotected BODIPY **32** gave inconsistent results: either unmodified starting material or decomposition. We suspected the carboxylates could be chelating the palladium catalyst and decided to switch to a protecting group approach, which would likely improve the Heck coupling and allow for more facile purification of intermediates by normal phase chromatography.

Benzyl ester protected pyrrole **23** is less nucleophilic than its carboxylic acid precursor. We performed the BODIPY condensation in 2:3 DMF:CH_2Cl_2, providing benzyl-protected BODIPY **24** in a 61% isolated yield (**Scheme 3**). Benzyl-protected BODIPY **24** proceeds cleanly through Heck coupling, even in the presence of NEt_3. Benzyl-protected intermediates **26** and **27** were isolated in a 30 and 43% yield following column chromatography. Cleavage of the benzyl groups with Pd/C under hydrogen atmosphere also reduced one of the alkenes of the molecular wire, evidenced by a mass 2 m/z higher than the desired product (**Figure S1**) and increased brightness of the resulting dye. A Birkofer reduction[46-47] with $Pd(OAc)_2$, Et_3SiH, NEt_3 in CH_2Cl_2 at room temperature gave the cleanest conversion to the free carboxylate product with minimal over-reduction of the alkenes of the molecular wire. Carboxy*m*Me **29** and carboxy*m*OMe **30** were isolated 31 and 14% yield after pTLC.

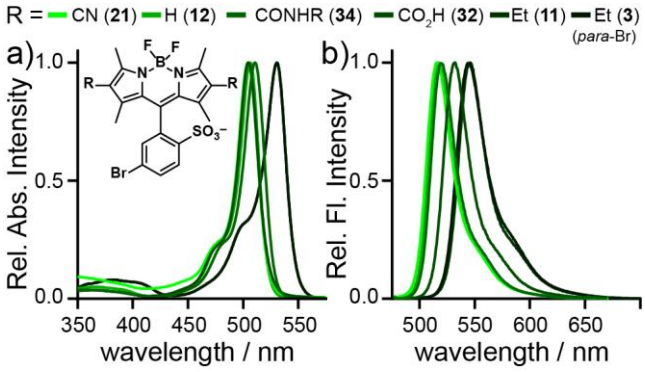

Figure 1. Plots of normalized **a)** absorption and **b)** emission of sulfonated BODIPY fluorophores **3**, **11**, **12**, **32**, **34**, and **21**. Spectra were acquired in PBS pH 7.4. Dye concentration is 1 μM.

Glycyl-amido BODIPY VoltageFluors **35** and **36** were synthesized via Heck coupling between styrenes **4** or **13** and 2,6-diamido BODIPY **34**, which was accessed in 82% yield from a HATU-mediated amide bond formation between dicarboxy BODIPY **32** and glycine methyl ester **33**. Like benzyl-protected BODIPY **24**, the amide-substituted BODIPY withstands the presence of NEt_3 in the Pd-catalyzed cross-coupling, which returns amide*m*H (**35**) and amide*m*Me (**36**) in 21% and 34% isolated yields, respectively (**Scheme 3**).

Spectroscopic characterization of sulfonated BODIPYs

The absorption and the emission of BODIPY fluorophores (**Figure 1**, **Table 1**) and VoltageFluors (**Figure 2a**, **Figure S2**, **Table 2**) varied with the 2,6-substituents. Consistent with a Dewar formalism,[48-50] electron-withdrawing groups at the 2,6-positions result in a hypsochromatic shift (λ_{max} = 502 nm for dicyano-BODIPY **21**) and electron donating groups like Et (BODIPY **3** and **11**) yield bathochromic shifts (λ_{max} = 530 nm). Emission trends mirror the absorption profiles, with the electron-rich 2,6-ethyl BODIPY **3** and **11** emitting around 544 nm, and 2,6-cyano BODIPY **21**, the most electron-poor, emitting at

Table 1. Spectral properties of sulfonated BODIPYs

	R	λ_{max} abs [a]	λ_{max} em [a]	ε (M^{-1} cm^{-1})[b]	ϕ_{fl}[a]
3	Et	530	544	53000	0.72
11	Et	530	545	60000	0.70
12	H	503	515	70000	0.99
32	CO_2H	517	532	77000	0.95
34	$CONHCH_2$ CO_2Me	507	519	84000	0.92
21	CN	502	517	41000	0.93

a acquired in PBS pH 7.4. **b** acquired in ethanol.

517 nm. The absorption and emission profiles of the complete BODIPY VF dyes closely match the spectra of the parent BODIPY fluorophores, with absorption profiles centered at 502 to 528 nm and the phenylene vinylene molecular wire absorbing near 400 nm (**Figure 2a**, **Figure S2**, and **Table 2**). The *ortho*-sulfonated BODIPY fluorophores have impressive fluorescence quantum yields (ϕ_{fl}) of 0.70—0.99 (**Table 1**), but after the addition of the phenylene vinylene molecular wire the quantum yields drop dramatically, supporting the presence of PeT within the compounds (**Table 2**). In general, ϕ_{fl} decreased as the fluorophore electron density decreased, such as from Et*m*H **15** to TM*m*H **17**, and decreased further whenever the standard phenylene vinylene molecular wire **4** was replaced with more electron-rich methyl-substituted **13** or methoxy-substituted **14**.

Cellular performance of BODIPY VF Dyes

All BODIPY VF dyes localize to cell membranes (**Figure 2a, Figure S3a**,**b-S8a,b**) and display different cellular brightness (**Table 2**, **Figure S9a**). Despite having the highest ϕ_{fl}, BODIPY VF Et*p*H **6** was one of the dimmest dyes in cells (relative brightness in cells = 0.4, compared to BODIPY VF TM*m*OMe **19**), likely due to its poor solubility in aqueous buffer even in the presence of detergent (**Table 2**). On the other hand, 2,6-dicarboxy BODIPY VF dyes **28** – **30** possessed the largest cellular brightness (relative brightness up to 12x, **Table 2**, **Figure S9a**). We speculate that the increased anionic character of the dicarboxy BODIPY VFs **28** – **30**, with three negative charges, improves the water solubility of the dyes, enabling more efficient delivery to cellular membranes.

After confirming BODIPY VoltageFluors localize to the cell membrane, we next investigated their voltage sensitivity using whole cell voltage-clamp electrophysiology in tandem with epifluorescence microscopy (**Figure 2c,d Figure S3c,d-S8c,d**). We stepped the membrane potential of a single HEK cell stained with 2 μM BODIPY VoltageFluor from a holding potential of -60 mV to ±100 mV while recording dye fluorescence intensity. 2,6-diethyl BODIPY VF dyes (**6**, **7**, **15**, and **16**) demonstrate little to no voltage sensitivity. BODIPYs Et*p*H (**6**) and Et*p*OMe (**7**), with a *para* molecular wire configuration, show no voltage sensitivity (**Figure S3c**), while BODIPYs Et*m*H (**15**) and Et*m*OMe (**16**) display modest voltage sensitivities of 1.5 and 5 % ΔF/F per 100 mV (**Figure S4c,d** and **Table 2**).

We hypothesized replacing the 2,6-diethyl BODIPY with progressively more electron-poor BODIPYs would increase PeT and therefore increase % ΔF/F. Gratifyingly, we see a 67% increase in voltage sensitivity from Et*m*H **16** to TM*m*H **17**, from 1.5 to 2.5 % ΔF/F (**Figure S5c,d** and **Table 2**). Strengthening

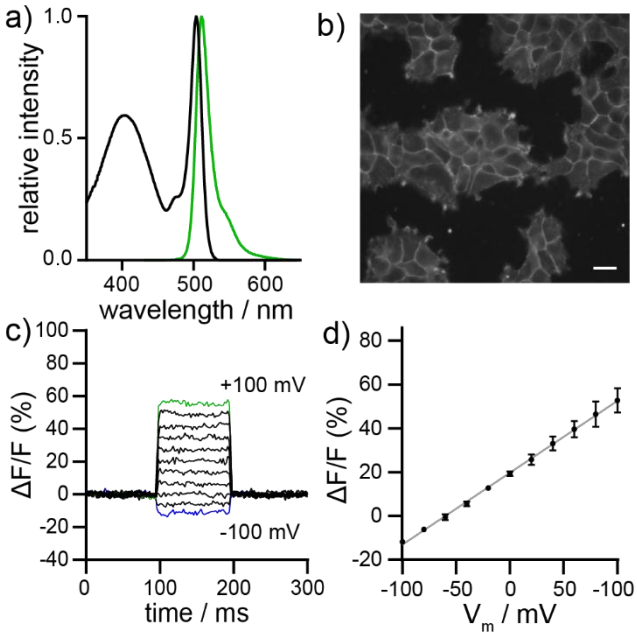

Figure 2. Spectroscopic, cellular, and functional characterization of TM*m*OMe BODIPY VF **19**. **a)** Plot of normalized absorbance and emission intensity for TM*m*OMe BODIPY VF **19** (1 μM, ethanol). Excitation is provided at 470 nm. **b)** Widefield fluorescence micrograph of HEK cells stained with TM*m*OMe BODIPY VF **19** (1 μM). **c)** Plot of fractional change in fluorescence of TM*m*OMe BODIPY VF **19** (ΔF/F) vs. time for 100 ms hyper- and depolarizing steps (±100 mV in 20 mV increments) from a holding potential of -60 mV in a single HEK cell under whole-cell voltage-clamp mode. **d)** Plot of fractional change in fluorescence (ΔF/F) vs final membrane potential. Data represent the mean ΔF/F, ±S.E.M. for n = 3 separate cells. Grey line is the line of best fit.

the electron-donating ability of the aniline by addition of a methyl or methoxy group increased the voltage-sensitivity to 6.2 % for TM*m*Me **18** and 33 % ΔF/F for TM*m*OMe **19** (**Figure 2**).

More electron-deficient cyano BODIPY VF cyano*m*H **22** displayed extremely low cellular brightness (**Table 2**, **Figure S6b, S9a**) and required increasing both illumination intensity and camera exposure time in order to obtain a reasonable estimate of its voltage sensitivity, which was low: 3.8 % ΔF/F per 100 mV (**Table 2**, **Figure S6c,d**). While dicyano BODIPY VF dye **22** was slightly more voltage sensitive than its analogous precursors, Et*m*H **15** and TM*m*H **17**, its extremely low cellular brightness prohibited further use as a voltage-sensitive dye in cells.

We then evaluated the 2,6-dicarboxy and diamido BODIPY series, hoping to find an electronic "sweet spot" between the tetramethyl and cyano series. The carboxy VoltageFluors carboxy*m*H **28**, carboxy*m*Me **29**, and carboxy*m*OMe **30** had voltage sensitivities of 4.4%, 9.9%, and 24% ΔF/F per 100 mV, respectively (**Figure S7c,d** and **Table 2**). While dicarboxy BODIPY VF dyes display a similar range of voltage sensitivities to their tetramethyl precursors, the most striking quality of the dicarboxy VoltageFluors was their cellular brightness—they were 5-12x brighter compared to the cellular fluorescence intensity of TM*m*OMe **19** (**Table 2**). The *in vitro* fluorescence quantum yields of the carboxy VoltageFluors are slightly lower than the tetramethyl VoltageFluors, so this increase in brightness is likely due to improved hydrophilicity and cell loading

Table 2. Properties of BODIPY VoltageFluor (VF) dyes

	Name	R	R_1	isomer	λ_{max} abs[a]	λ_{max} em[a]	ϕ_{fl}[a]	% $\Delta F/F$[bc]	Cell brightness[cd]
6	Et*p*H	Et	H	*para*	528	541	0.14	0	0.43 ± 0.02[f]
7	Et*p*OMe	Et	OMe	*para*	527	541	0.07	0	0.76 ± 0.03[f]
15	Et*m*H	Et	H	*meta*	528	541	0.15	1.8 ± 0.1	4.4 ± 0.3[f]
16	Et*m*OMe	Et	OMe	*meta*	527	541	0.05	5.4 ± 0.6	0.60 ± 0.03[f]
17	TM*m*H	H	H	*meta*	503	518	0.11	2.5 ± 0.1	0.62 ± 0.08
18	TM*m*Me	H	Me	*meta*	504	517	0.07	6.2 ± 0.4	1.5 ± 0.2
19	TM*m*OMe	H	OMe	*meta*	504	512	0.05	33 ± 0.7	1.0 ± 0.1
28	carboxy*m*H	COOH	H	*meta*	503	516	0.07	4.4 ± 0.2	12 ± 2
29	carboxy*m*Me	COOH	Me	*meta*	503	517	0.03	9.9 ± 0.4	5.1 ± 0.9
30	carboxy*m*OMe	COOH	OMe	*meta*	509	522	0.06	24 ± 0.5	7.1 ± 0.8
35	amide*m*H	$CONHCH_2CO_2Me$	H	*meta*	508	521	0.06	48 ± 2	1.0 ± 0.1
36	amide*m*Me	$CONHCH_2CO_2Me$	Me	*meta*	509	521	0.03	5.1 ± 0.4	1.0 ± 0.1
22	cyano*m*H	CN	H	*meta*	502	519	0.08	3.8[e]	0.34 ± 0.002

a Determined in ethanol. **b** Per 100 mV depolarization. **c** Determined in HEK cells. **d** Relative to TM*m*OMe **19**. **e** Increased exposure time and light intensity required to make measurement. **f** Pluronic F-127 (0.01%) used during loading

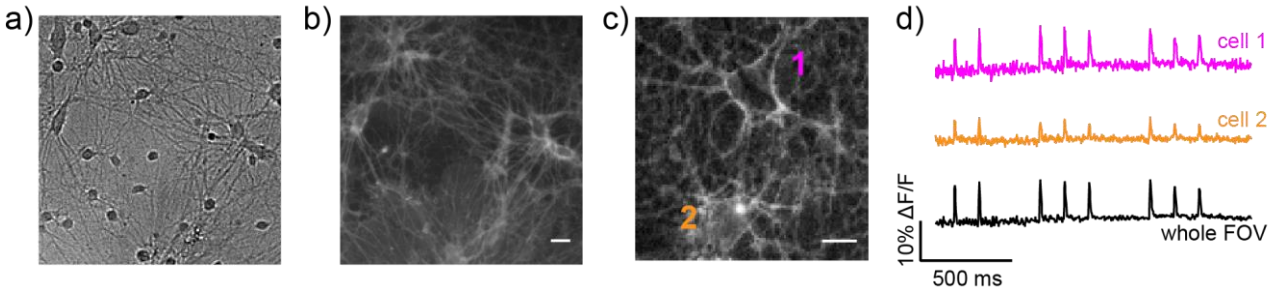

Figure 3. Voltage imaging in mammalian neurons with carboxy*m*OMe BODIPY VF **30**. **a)** Transmitted light and **b)** widefield epifluorescence image of cultured rat hippocampal neurons stained with 500 nM carboxy*m*OMe BODIPY VF **30**. Scale bar is 20 μm. **c)** Widefield epifluorescence image of neurons stained with 1 μM carboxy*m*OMe BODIPY VF **30** and imaged at 500 Hz. Image is a single frame from this high-speed acquisition. Scale bar is 20 μm. **d)** Plot of fractional change in fluorescence ($\Delta F/F$) for the cells identified in panel (c) or for the entire field of view (FOV).

efficiency. We found that amide-substituted BODIPY VF **35** (amide*m*H, **Figure S8c,d**) possesses voltage sensitivity 10x greater than the corresponding carboxy*m*H **28**, with a fractional sensitivity of 48% $\Delta F/F$ per 100 mV in HEK cells (compared to 4.4% for carboxy*m*H **28**). Introduction of a more electron-rich molecular wire (methyl substitution) results in a loss of voltage sensitivity for amide*m*Me **36**, which displays only nominal voltage sensitivity (5.1% $\Delta F/F$ per 100 mV).

Functional Imaging in Neurons and Cardiomyocytes

We evaluated the ability of BODIPY VF dyes to report on voltage dynamics in electrically excitable cells: mammalian neurons and human induced pluripotent stem cell-derived cardiomyocytes (hiPSC-CMs). Three BODIPY VoltageFluors stood out as good candidates for functional imaging: TM*m*OMe BODIPY VF **19** and amide*m*H BODIPY VF **35** because of their high $\Delta F/F$ (33 and 48%, respectively), and carboxy*m*OMe BODIPY VF **30** because of its combination of cellular brightness (7x brighter than TM*m*OMe and amide*m*H) and good sensitivity (24% $\Delta F/F$).

We evaluated the photostability of these BODIPY VF dyes in HEK cells. Based on previous reports,[40] we predicted photostability would decrease from amide*m*H **35** > TM*m*OMe **19** > carboxy*m*OMe **30**. Indeed, we find amide*m*H BODPIY **35** to be the most photostable in HEK cells, maintaining near 100% fluorescence after 6 min of constant illumination, although with some photobrightening (**Figure S9b**). TM*m*OMe BODIPY **19** displays photostability comparable to fluorescein-based VF2.1.Cl[32] (**Figure S9b**). Carboxy-substituted BODIPY **35** bleaches the most rapidly, dropping to about 20% of original fluorescence values after 2 minutes (**Figure S9b**). However, because of the high starting brightness of carboxy*m*OMe BODIPY **35**, this indicator retains its utility for functional voltage imaging.

In cultured rat hippocampal neurons stained with BODIPY VFs, both TM*m*OMe **19** and amide*m*H **35** were too dim to capture evoked neuronal action potentials with sufficient signal-to-noise. Carboxy*m*OMe **30** displayed bright, membrane-localized staining in neurons isolated from rat hippocampi (**Figure 3a** and **b**). Carboxy*m*OMe **30** responded to electrically-evoked neuronal action potentials (**Figure 3c** and **d**), which could be detected when analyzing single cell regions of interest (ROIs) or when viewing the entire field of neurons.

We also evaluated the performance of BODIPY VF dyes TM*m*OMe **19**, carboxy*m*OMe **30**, and

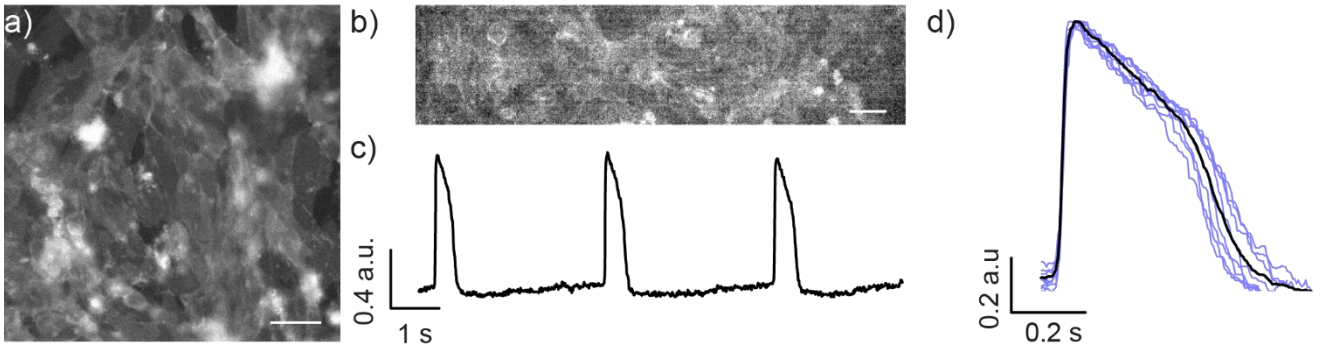

Figure 4. Voltage imaging in human induced pluripotent stem cell-derived cardiomyocytes (hiPSC-CMs) with TM*m*OMe BODIPY VF **19**. **a)** Widefield, epifluorescence micrograph of hiPSC-CMs stained with 500 nM TM*m*OMe BODIPY VF **19**. Scale bar is 50 µm. **b)** Single frame of a movie collected at 200 Hz for functional imaging of hiPSC-CM spontaneous action potentials. Scale bar is 50 µm. **c)** Trace of mean pixel intensity (arbitrary fluorescence units, a.u.) from full region of interest (ROI) in panel (b) plotted vs time during 10 second acquisition, corrected for photobleach. **d)** Averaged action potential trace (black) from three 10 second recordings from 3 separate ROIs over individual AP events from each recording (blue).

amide*m*H **35** in human induced pluripotent stem cell-derived cardiomyocytes (hiPSC-CMs). All three BODIPY VFs stain the membranes of hiPSC-CMs (**Figure 4a**, **Figure S10a,b**). High-speed fluorescence microscopy (200 Hz frame rate) demonstrates that all three BODIPY VFs can report on spontaneously-generated cardiac action potentials in hiPSC-CMs (**Figure 4** and **Figure S10**) during 10 second bouts of imaging.

We found BODIPY VF TM*m*OMe **19** was the best suited voltage reporter because of its robust 33% ΔF/F and good signal-to noise (**Figure 4c**). Additionally, under longer-term imaging (60 sec of continuous imaging), TM*m*OMe **19** displays the least phototoxic effects among the BODIPYs tested under constant illumination. Under these conditions, the photostability of TM*m*OMe BODIPY VF **19** was comparable to VF2.1.Cl,[32] although with lower signal to noise than either VF2.1.Cl or fVF 2[51] (**Figure S11**). Like VF2.1.Cl, TM*m*OMe BODIPY VF **19** also slightly alters the shape and magnitude of cardiac action potentials under prolonged illumination (**Figure S11**). These effects are not seen during shorter imaging sessions (**Figure 4d**).

Discussion

We designed and synthesized 5 new sulfonated BODIPY dyes with variable 2,6-subsitution patterns. These sulfonated fluorophores represent a generalizable solution to improving BODIPY water solubility while simultaneously avoiding modification to the boron center or fluorophore core. We incorporated these fluorophores into 13 new BODIPY voltage-sensitive fluorophores for evaluation in live-cell imaging, but the tunable, water-soluble BODIPYs presented here may have applications beyond voltage sensing. Amide*m*H BODIPY VF **35** is the most sensitive BODIPY-based voltage indicator to date,[52-53] but its low cellular brightness precludes its ready adoption for functional imaging in electrically excitable cells like neurons or cardiomyocytes. Two other indicators developed in this study, TM*m*OMe BODIPY VF **19**, with its slightly lower sensitivity (33% ΔF/F per 100 mv), but good brightness, and carboxy-*m*OMe BODIPY VF **30**, which retains good voltage sensitivity (24% ΔF/F per 100 mV) and exceptional brightness (~7x brighter than **19** or **35**) are better suited for functional imaging in cardiomyocytes or neurons, where they can each report on action potential dynamics in single trials.

The voltage sensitivity of the BODIPY VF dyes correlates with the electron-withdrawing character of the 2,6-substitution pattern in the BODIPY fluorophore. More electron-withdrawing substituents increase voltage sensitivity in the order of -Et < -H < -CO_2H < -CONHR > -CN. The extremely electron-withdrawing character of nitrile substitution makes for a poorly sensitive BODIPY VF. We find that calculated values of HOMO energies (**Figure S12**) for the BODIPY fluorophores—lacking the molecular wire—correlate extremely well with either *meta* or *para* Hammett constants (σ_m or σ_p),[54] validating the use of tabulated Hammett constants for analysis of the relative electron density of a particular BODIPY fluorophore (**Figure S13a** and **b**). Correlation between calculated HOMO energies and σ_m or σ_p values is best when evaluating neutral BODIPYs (Et, H, CONHR, or CN), with correlation coefficients (R^2) >0.99 for both σ_m and σ_p compared to HOMO. If carboxy-substituted BODIPYs are included, the correlation (R^2) between HOMO level and Hammett parameter drops to 0.92 (σ_m) and 0.78 (σ_p) (**Figure S13a** and **b**).

The average ΔF/F for a class of BODIPY fluorophore (R = Et, H, CO_2H, CONHR, or CN) displays a parabolic relationship with calculated HOMO energy levels (**Figure S13c**), with maximum voltage sensitivity at around -4.75 eV (or σ = 0.2 - 0.4). BODIPY VF dyes that have very large and negative ΔG_{PeT},[14] either by a combination of electron deficient fluorophores (R = CN) with mildly donating anilines (R = H) as in the case of BODIPY VF **22**, or by with moderately withdrawing fluorophores (R = CONHR) with electron-rich anilines (R = Me) in the case of amide*m*Me BODIPY **35**, will have low voltage sensitivity. These results suggest that amide*m*H **35** occupies a "sweet spot" of PeT to optimize the voltage sensitivity for BODIPY VoltageFluors, and any further lowering of the fluorophore HOMO (such as amide BODIPY to cyano BODIPY) or raising the HOMO of the aniline PeT donor (unsubstituted aniline to methyl-substituted aniline) is detrimental to the voltage sensitivity.

Despite its impressive 48% ΔF/F of amide*m*H BODIPY **35** in HEK cells, its low cellular brightness (12x less bright than dicarboxy BODIPY VFs) precludes its direct use in functional imaging. The low cellular brightness likely results from poor solubility of the dye, because the highly charged dicarboxy BODIPY VFs displayed greater cellular brightness. The structure of the diamido BODIPY VFs lend themselves to introduction of additional water-solubilizing groups, without significantly perturbing the electronics of the 2,6-diamide substitution

pattern. Experiments are underway to expand the utility of amide-substituted BODIPYs in the context of voltage imaging and beyond.

ASSOCIATED CONTENT

Supporting Information. Support figures, spectra, synthetic methods and imaging details. This material is available free of charge via the Internet at http://pubs.acs.org.

AUTHOR INFORMATION

Corresponding Author

* evanwmiller@berkeley.edu

ACKNOWLEDGMENT

Research in the Miller lab is supported by the National Institutes of Health (R35GM119855). J.M.F, B.K.R., S.C.B., and R.U.K. were supported in part by a training grant from the National Institutes of Health (T32GM066698). We thank Dr. Kathy Durkin and Dr. David Small for assisting with calculations performed in the Molecular Graphics and Computation Facility in the UC Berkeley College of Chemistry (NIH S10OD023532).

REFERENCES

1. Perkin, W. H., Producing a New Coloring Matter for Dyeing with a Lilac or Purple Color Stuffs of Silk, Cotton, Wool, or other Materials. *British Patent* **1856,** *No. 1984*.
2. Cliffe, W. H., In the Footsteps of Perkin. *Journal of the Society of Dyers and Colourists* **1956,** *72* (12), 563-566.
3. Welham, R. D., The Early History of the Synthetic Dye Industry*. *Journal of the Society of Dyers and Colourists* **1963,** *79* (3), 98-105.
4. Baeyer, A., Ueber eine neue Klasse von Farbstoffen. *Berichte der deutschen chemischen Gesellschaft* **1871,** *4* (2), 555-558.
5. Ceresole, M., Verfahren zur Darstellung von Farbstoffen aus der Gruppe des Meta-amidophenolphtaleïns. *German Patent* **1887,** *No. 44002*.
6. Sandmeyer, T., Red dye. *US Patent* **1896,** *No. US573299A*.
7. Tsien, R. Y., Building and breeding molecules to spy on cells and tumors. *FEBS Lett* **2005,** *579* (4), 927-32.
8. Lavis, L. D.; Raines, R. T., Bright building blocks for chemical biology. *ACS Chem Biol* **2014,** *9* (4), 855-66.
9. Lavis, L. D., Teaching Old Dyes New Tricks: Biological Probes Built from Fluoresceins and Rhodamines. *Annu Rev Biochem* **2017,** *86* (1), 825-843.
10. Loudet, A.; Burgess, K., BODIPY dyes and their derivatives: syntheses and spectroscopic properties. *Chem Rev* **2007,** *107* (11), 4891-932.
11. Treibs, A.; Kreuzer, F. H., Di- and Tri-Pyrrylmethene Complexes with Di-Fluoro Boron. *Liebigs Ann Chem* **1968,** *718* (Dec), 208-+.
12. Ziessel, R.; Ulrich, G.; Harriman, A., The chemistry of Bodipy: a new El Dorado for fluorescence tools. *New J Chem* **2007,** *31* (4), 496-501.
13. Ulrich, G.; Ziessel, R.; Harriman, A., The chemistry of fluorescent bodipy dyes: Versatility unsurpassed. *Angew Chem Int Edit* **2008,** *47* (7), 1184-1201.
14. Gabe, Y.; Urano, Y.; Kikuchi, K.; Kojima, H.; Nagano, T., Highly Sensitive Fluorescence Probes for Nitric Oxide Based on Boron Dipyrromethene Chromophore-Rational Design of Potentially Useful Bioimaging Fluorescence Probe. *J Am Chem Soc* **2004,** *126* (10), 3357-3367.
15. Lincoln, R.; Greene, L. E.; Krumova, K.; Ding, Z.; Cosa, G., Electronic excited state redox properties for BODIPY dyes predicted from Hammett constants: estimating the driving force of photoinduced electron transfer. *J Phys Chem A* **2014,** *118* (45), 10622-30.
16. Boens, N.; Leen, V.; Dehaen, W., Fluorescent indicators based on BODIPY. *Chem Soc Rev* **2012,** *41* (3), 1130-1172.
17. Kowada, T.; Maeda, H.; Kikuchi, K., BODIPY-based probes for the fluorescence imaging of biomolecules in living cells. *Chem Soc Rev* **2015,** *44* (14), 4953-4972.
18. Kollmannsberger, M.; Gareis, T.; Heinl, S.; Breu, J.; Daub, J., Electrogenerated chemiluminescence and proton-dependent switching of fluorescence: Functionalized difluoroboradiaza-s-indacenes. *Angew Chem Int Edit* **1997,** *36* (12), 1333-1335.
19. Urano, Y.; Asanuma, D.; Hama, Y.; Koyama, Y.; Barrett, T.; Kamiya, M.; Nagano, T.; Watanabe, T.; Hasegawa, A.; Choyke, P. L.; Kobayashi, H., Selective molecular imaging of viable cancer cells with pH-activatable fluorescence probes. *Nat Med* **2008,** *15*, 104.
20. Kollmannsberger, M.; Rurack, K.; Resch-Genger, U.; Rettig, W.; Daub, J., Design of an efficient charge-transfer processing molecular system containing a weak electron donor: spectroscopic and redox properties and cation-induced fluorescence enhancement. *Chem Phys Lett* **2000,** *329* (5-6), 363-369.
21. Baruah, M.; Qin, W.; Vallée, R. A. L.; Beljonne, D.; Rohand, T.; Dehaen, W.; Boens, N., A Highly Potassium-Selective Ratiometric Fluorescent Indicator Based on BODIPY Azacrown Ether Excitable with Visible Light. *Org Lett* **2005,** *7* (20), 4377-4380.
22. Müller, B. J.; Borisov, S. M.; Klimant, I., Red- to NIR-Emitting, BODIPY-Based, K+-Selective Fluoroionophores and Sensing Materials. *Adv Funct Mater* **2016,** *26* (42), 7697-7707.
23. Lin, Q.; Buccella, D., Highly selective, red emitting BODIPY-based fluorescent indicators for intracellular Mg2+ imaging. *J Mater Chem B* **2018,** *6* (44), 7247-7256.
24. Basarić, N.; Baruah, M.; Qin, W.; Metten, B.; Smet, M.; Dehaen, W.; Boens, N., Synthesis and spectroscopic characterisation of BODIPY® based fluorescent off–on indicators with low affinity for calcium. *Org Biomol Chem* **2005,** *3* (15), 2755-2761.
25. Kamiya, M.; Johnsson, K., Localizable and Highly Sensitive Calcium Indicator Based on a BODIPY Fluorophore. *Anal Chem* **2010,** *82* (15), 6472-6479.
26. Zeng, L.; Miller, E. W.; Pralle, A.; Isacoff, E. Y.; Chang, C. J., A Selective Turn-On Fluorescent Sensor for Imaging Copper in Living Cells. *J Am Chem Soc* **2006,** *128* (1), 10-11.
27. Wu, Y.; Peng, X.; Guo, B.; Fan, J.; Zhang, Z.; Wang, J.; Cui, A.; Gao, Y., Boron dipyrromethene fluorophore based fluorescence sensor for the selective imaging of Zn(ii) in living cells. *Org Biomol Chem* **2005,** *3* (8), 1387-1392.
28. Dodani, S. C.; He, Q.; Chang, C. J., A Turn-On Fluorescent Sensor for Detecting Nickel in Living Cells. *J Am Chem Soc* **2009,** *131* (50), 18020-18021.
29. Sun, Z.-N.; Liu, F.-Q.; Chen, Y.; Tam, P. K. H.; Yang, D., A Highly Specific BODIPY-Based Fluorescent Probe for the Detection of Hypochlorous Acid. *Org Lett* **2008,** *10* (11), 2171-2174.
30. Belzile, M. N.; Godin, R.; Durantini, A. M.; Cosa, G., Monitoring Chemical and Biological Electron Transfer Reactions with a Fluorogenic Vitamin K Analogue Probe. *J Am Chem Soc* **2016,** *138* (50), 16388-16397.
31. Yang, Z.; He, Y.; Lee, J.-H.; Park, N.; Suh, M.; Chae, W.-S.; Cao, J.; Peng, X.; Jung, H.; Kang, C.; Kim, J. S., A Self-Calibrating Bipartite Viscosity Sensor for Mitochondria. *J Am Chem Soc* **2013,** *135* (24), 9181-9185.
32. Miller, E. W.; Lin, J. Y.; Frady, E. P.; Steinbach, P. A.; Kristan, W. B., Jr.; Tsien, R. Y., Optically monitoring voltage in neurons by photo-induced electron transfer through molecular wires. *Proc Natl Acad Sci U S A* **2012,** *109* (6), 2114-9.
33. Woodford, C. R.; Frady, E. P.; Smith, R. S.; Morey, B.; Canzi, G.; Palida, S. F.; Araneda, R. C.; Kristan, W. B.; Kubiak, C. P.; Miller, E. W.; Tsien, R. Y., Improved PeT Molecules for Optically Sensing Voltage in Neurons. *J Am Chem Soc* **2015,** *137* (5), 1817-1824.
34. Deal, P. E.; Kulkarni, R. U.; Al-Abdullatif, S. H.; Miller, E. W., Isomerically Pure Tetramethylrhodamine Voltage Reporters. *J Am Chem Soc* **2016,** *138* (29), 9085-8.
35. Kulkarni, R. U.; Yin, H.; Pourmandi, N.; James, F.; Adil, M. M.; Schaffer, D. V.; Wang, Y.; Miller, E. W., A Rationally Designed, General Strategy for Membrane Orientation of Photoinduced Electron Transfer-Based Voltage-Sensitive Dyes. *ACS Chem Biol* **2017,** *12* (2), 407-413.

36. Niu, S. L.; Ulrich, G.; Ziessel, R.; Kiss, A.; Renard, P. Y.; Romieu, A., Water-soluble BODIPY derivatives. *Org Lett* **2009,** *11* (10), 2049-52.

37. Brizet, B.; Bernhard, C.; Volkova, Y.; Rousselin, Y.; Harvey, P. D.; Goze, C.; Denat, F., Boron functionalization of BODIPY by various alcohols and phenols. *Org Biomol Chem* **2013,** *11*, 7729.

38. Courtis, A. M.; Santos, S. A.; Guan, Y.; Hendricks, J. A.; Ghosh, B.; Szantai-Kis, D. M.; Reis, S. A.; Shah, J. V.; Mazitschek, R., Monoalkyl BODIPYs-A Fluorophore Class for Bioimaging. *Bioconj Chem* **2014,** *25*, 1043-1051.

39. Li, L.; Han, J.; Nguyen, B.; Burgess, K., Syntheses and spectral properties of functionalized, water-soluble BODIPY derivatives. *J Org Chem* **2008,** *73* (5), 1963-70.

40. Komatsu, T.; Oushiki, D.; Takeda, A.; Miyamura, M.; Ueno, T.; Terai, T.; Hanaoka, K.; Urano, Y.; Mineno, T.; Nagano, T., Rational design of boron dipyrromethene (BODIPY)-based photobleaching-resistant fluorophores applicable to a protein dynamics study. *Chem Commun* **2011,** *47* (36), 10055-7.

41. Wagner, R. W.; Lindsey, J. S., Boron-dipyrromethene dyes for incorporation in synthetic multi-pigment light-harvesting arrays. *Pure Appl Chem* **1996,** *68* (7), 1373-1380.

42. D'Souza, F.; Smith, P. M.; Zandler, M. E.; McCarty, A. L.; Itou, M.; Araki, Y.; Ito, O., Energy Transfer Followed by Electron Transfer in a Supramolecular Triad Composed of Boron Dipyrrin, Zinc Porphyrin, and Fullerene: A Model for the Photosynthetic Antenna-Reaction Center Complex. *J Am Chem Soc* **2004,** *126* (25), 7898-7907.

43. Lou, Z.; Hou, Y.; Chen, K.; Zhao, J.; Ji, S.; Zhong, F.; Dede, Y.; Dick, B., Different Quenching Effect of Intramolecular Rotation on the Singlet and Triplet Excited States of Bodipy. *J Phys Chem C* **2018,** *122* (1), 185-193.

44. Bricks, J. L.; Kovalchuk, A.; Trieflinger, C.; Nofz, M.; Büschel, M.; Tolmachev, A. I.; Daub, J.; Rurack, K., On the Development of Sensor Molecules that Display FeIII-amplified Fluorescence. *J Am Chem Soc* **2005,** *127* (39), 13522-13529.

45. Rumyantsev, E. V.; Alyoshin, S. N.; Marfin, Y. S., Kinetic study of Bodipy resistance to acids and alkalis: Stability ranges in aqueous and non-aqueous solutions. *Inorg Chim Acta* **2013,** *408*, 181-185.

46. Birkofer, L.; Bierwirth, E.; Ritter, A., Siliciumorganische Verbindungen .8. Decarbonbenzoxylierungen Mit Triathylsilan. *Chem Ber-Recl* **1961,** *94* (3), 821-824.

47. Coleman, R. S.; Shah, J. A., Chemoselective cleavage of benzyl ethers, esters, and carbamates in the presence of other easily reducible groups. *Synthesis-Stuttgart* **1999**, 1399-1400.

48. Dewar, M. J. S., Colour and Constitution .1. Basic Dyes. *J Chem Soc* **1950,** (Sep), 2329-2334.

49. Hung, J.; Liang, W.; Luo, J.; Shi, Z.; Jen, A. K. Y.; Li, X., Rational Design Using Dewar's Rules for Enhancing the First Hyperpolarizability of Nonlinear Optical Chromophores. *J Phys Chem C* **2010,** *114* (50), 22284-22288.

50. Olsen, S., A quantitative quantum chemical model of the Dewar–Knott color rule for cationic diarylmethanes. *Chem Phys Lett* **2012,** *532*, 106-109.

51. Boggess, S. C. G., Shivaani, S.; Siemons, Brian A.; , New Molecular Scaffolds for Fluorescent Voltage Indicators. *ACS Chem Biol* **2019,** *14*, 390-396.

52. Bai, D.; Benniston, A. C.; Clift, S.; Baisch, U.; Steyn, J.; Everitt, N.; Andras, P., Low molecular weight Neutral Boron Dipyrromethene (Bodipy) dyads for fluorescence-based neural imaging. *J Mol Struct* **2014,** *1065-1066*, 10-15.

53. Sirbu, D.; Butcher, J. B.; Waddell, P. G.; Andras, P.; Benniston, A. C., Locally Excited State–Charge Transfer State Coupled Dyes as Optically Responsive Neuron Firing Probes. *Chem Eur J* **2017,** *23* (58), 14639-14649.

54. Hansch, C.; Leo, A.; Taft, R. W., A Survey of Hammett Substituent Constants and Resonance and Field Parameters. *Chem Rev* **1991,** *91*, 165-195.

Water soluble BODIPY fluorophores for membrane potential imaging

Supplemental Information for

BODIPY Fluorophores for Membrane Potential Imaging

Authors

Jenna M. Franke,[‡] Benjamin K. Raliski,[‡] Steven C. Boggess,[‡] Divya V. Natesan,[‡] Evan T. Koretsky,[‡] Patrick Zhang,[‡] Rishikesh U. Kulkarni,[‡] Parker E. Deal,[‡] and Evan W. Miller[‡§†]*

Departments of [‡]Chemistry and [§]Molecular & Cell Biology and [†]Helen Wills Neuroscience Institute. University of California, Berkeley, California 94720, United States.

DOI placeholder

Table of Contents

Methods

Chemical synthesis and characterization

Chemical reagents and anhydrous solvents were purchased from commercial suppliers and used without further purification. Compounds **1**, **4**, **5**, **9**, **14**, **20**, and **23** were prepared according to literature procedures.[1–5] 2,4-dimethylpyrrole-3-carboxylic acid was purchased from CombiBlocks. All reactions were carried out in flame-dried flasks sealed with septa and conducted under an inert nitrogen atmosphere. Thin layer chromatography (TLC, Silicycle, F254, 250 µm) and preparative thin layer chromatography (pTLC, Silicycle, F254, 1000 µm) were performed on glass-backed plates pre-coated with silica gel and were visualized by fluorescence quenching under UV light. Flash column chromatography was performed on Silicycle Silica Flash F60 (230-400 Mesh) using a forced flow of air at 0.5–1.0 bar.

NMR spectra were measured on a Bruker AVQ-400, AVB-400, AV-500, AV-600, or AV-700 MHz instrument, indicated for each compound. CoC-NMR is supported in part by NIH S10-OD024998. NMR spectra measured on Bruker AVII-900 MHz, 225 MHz, equipped with a TCI cryoprobe accessory, were performed by Dr. Jeffrey Pelton (QB3). Funds for the QB3 900 MHz NMR spectrometer were provided by the NIH through grant GM68933. Chemical shifts are expressed in parts per million (ppm) and are referenced to either d_6-DMSO, 2.5 ppm, $CDCl_3$, 7.26 ppm, acetone-d_6, 2.05 ppm, or MeOD, 3.31 ppm. Coupling constants are reported in Hertz (Hz). Splitting patterns are indicated as follows: s, singlet; d, doublet; t, triplet; sep, septet; dd, doublet of doublets; ddd, doublet of doublet of doublets; dt, doublet of triplets; td; triplet of doublets; m, multiplet.

High-resolution mass spectra (HR-ESI-MS) were obtained by Dr. Rita Nichiporuk (QB3 Mass Spectrometry Facility at University of California, Berkeley). High performance liquid chromatography (HPLC) and low resolution ESI Mass Spectrometry were performed on an Agilent Infinity 1200 analytical instrument coupled to an Advion CMS-L ESI mass spectrometer. The column used for the analytical HPLC was Phenomenex Luna 5 µm C18(2) (4.6 mm I.D. × 75 mm) with a flow rate of 1.0 mL/min. The mobile phases were MQ-H_2O with 0.05% trifluoroacetic acid (eluent A) and HPLC grade acetonitrile with 0.05% trifluoroacetic acid (eluent B). Signals were monitored at 254, 400, and 500 nm over 13 min with a gradient of 10-100% eluent B, unless otherwise noted. Ultra-high performance liquid chromatography (UHPLC) for purification of final compounds was performed using a Waters Acquity Autopurificaiton system equipped with a Waters XBridge BEH 5 µm C18 column (19 mm I.D. x 250 mm) with a flow rate of 30.0 mL/min, made available by the Catalysis Facility of Lawrence Berkeley National Laboratory (Berkeley, CA). The mobile phases were MQ-H_2O with 0.05% formic acid (eluent A) and HPLC grade acetonitrile with 0.05% formic acid (eluent B). Signals were monitored at 400 and 500 nm over 20 min with a gradient of 10-100% eluent B, unless otherwise noted.

Spectroscopic studies

Stock solutions of BODIPY fluorophores and VoltageFluors were prepared in DMSO (500 µM–2 mM) and diluted with PBS (10 mM KH_2PO_4, 30 mM $Na_2HPO_4 \cdot 7H_2O$, 1.55 M NaCl, pH 7.4) or filtered absolute ethanol. UV-Vis absorbance and fluorescence spectra were recorder using a Shimadzu 2501 Spectrophotometer and a Quantamaster 4L-format scanning spectrofluorimeter (Photon Technologies International). The fluorimeter is equipped with an LPS-220B 75-W xenon lamp and power supply, a 1010B lamp housing with integrated igniter, switchable 814 photon-counting/analog photomultiplier detection unit, and MD5020 motor driver. Samples were measured in 1-cm path length quartz cuvettes (Starna Cells).

Relative quantum yields (Φ_{Fl}) were calculated by comparison to fluorescein (Φ_{Fl} = 0.93 in 0.1 M NaOH) and rhodamine 123 (Φ_{Fl} = 0.90 in ethanol) as references.[6,7] Briefly, stock solutions of standards were

prepared in DMSO (0.25-1.25 mM) and diluted with appropriate solvent (1:1000 dilution). Absorption and emission (excitation = 470 nm) were taken at 5 concentrations. The absorption value at the excitation wavelength (470 nM) was plotted against the integration of the area of fluorescence curve (475-700 nm). The slope of the linear best fit of the data was used to calculate the relative Φ_{Fl} by the equation $\Phi_{Fl(X)} = \Phi_{Fl(R)}(S_R/S_X)(\eta_X/\eta_R)^2$, where S_R and S_X are the slopes of the reference compound and unknown, respectively, and η is the refractive index of the solution. This method was validated by cross-referencing the reported Φ_{Fl} values of fluorescein and rhodamine 123 to the calculated Φ_{Fl} using the one standard as a reference for the other and vice versa. Calculated Φ_{Fl} within 10% of the reported value for both standards ensured that Φ_{Fl} calculated for BODIPY fluorophores and VoltageFluors was reliable within 10% error.

Cell culture

All animal procedures were approved by the UC Berkeley Animal Care and Use Committees and conformed to the NIH Guide for the Care and Use and Laboratory Animals and the Public Health Policy.

Human embryonic kidney (HEK) 293T cells were acquired from the UC Berkeley Cell Culture Facility. Cells were passaged and plated onto 12 mm glass coverslips coated with Poly-D-Lysine (PDL; 1 mg/mL; Sigma-Aldrich) to a confluency of ~15% and 50% for electrophysiology and imaging, respectively. HEK293T cells were plated and maintained in Dulbecco's modified eagle medium (DMEM) supplemented with 4.5 g/L D-glucose, 10% fetal bovine serum (FBS), and 1% Glutamax.

Hippocampi were dissected from embryonic day 18 Sprague Dawley rats (Charles River Laboratory) in cold sterile HBSS (zero Ca^{2+}, zero Mg^{2+}). All dissection products were supplied by Invitrogen, unless otherwise stated. Hippocampal tissue was treated with trypsin (2.5%) for 15 min at 37 °C. The tissue was triturated using fire polished Pasteur pipettes, in minimum essential media (MEM) supplemented with 5% fetal bovine serum (FBS; Thermo Scientific), 2% B-27, 2% 1M D-glucose (Fisher Scientific) and 1% glutamax. The dissociated cells were plated onto 12 mm diameter coverslips (Fisher Scientific) pre-treated with PDL (as above) at a density of 30-40,000 cells per coverslip in MEM supplemented media (as above). Neurons were maintained at 37 °C in a humidified incubator with 5% CO_2. At 1 day in vitro (DIV) half of the MEM supplemented media was removed and replaced with Neurobasal media containing 2% B-27 supplement and 1% glutamax. Evoked activity experiments were performed on 12-15 DIV neurons. Unless stated otherwise, for loading of HEK cells, BODIPY VoltageFluors were diluted in DMSO to 1 mM, and then diluted 1:1000 in HBSS and imaging experiments were performed in HBSS. For loading of hippocampal neurons, BODIPY VoltageFluors were diluted in DMSO to 500 µM, then diluted 1:1000 in HBSS and imaging experiments were performed in HBSS.

Differentiation of hiPSC into cardiomyocytes and culture: WTC11 hiPSCs were cultured on Matrigel (1:100 dilution; Corning)-coated 6 well-plates in StemFlex medium (Gibco). When the cell confluency reached 80–90%, which is referred as day 0, the medium was switched to RPMI 1640 medium (Life Technologies) containing B27 minus insulin supplement (Life Technologies) and 8 µM CHIR99021 GSK3 inhibitor (Peprotech). At day 1, the medium was changed to RPMI 1640 medium containing B27 minus insulin supplement only. At day 3, medium was replaced to RPMI 1640 medium containing B27 supplement without insulin, and 5 µM IWP4 (Peprotech) for 2 days without medium change. On day 5, medium was replaced to RPMI 1640 medium containing B27 minus insulin supplement for 2 days without medium change. On day 7, medium was replaced toRPMI 1640 containing B27 with insulin supplement. After day 7, the medium was changed every other day. Confluent contracting sheets of beating cells appear between days 7 to 15 and are ready for dissociation after this time. Confluent sheets were dissociated with 0.25% trypsin-EDTA (8-30 minutes, depending on density and quality of tissue) and plated onto Matrigel (1:100)-coated Ibidi ® 24 well µ-plates (cat no. 82406) in RPMI 1640 medium containing B27 supplement and 10 µM Y27632. The following day, medium was exchanged for RPMI 1640 plus B27. Medium was

changed every 2 days until imaging. For loading hiPSC cardiomyocytes, VoltageFluor dyes (BODIPY, VF2.1.Cl, or fVF 2) were diluted in DMSO to 500 μM, and then diluted 1:1000 in RPMI 1640 with B27 supplement minus Phenol Red. Imaging experiments were performed in RPMI 1640 with B27 supplement minus Phenol Red.

Epifluorescence microscopy

For HEK293T cells, epifluorescence imaging was performed on an AxioExaminer Z-1 (Zeiss) equipped with a Spectra-X Light engine LED light (Lumencor), controlled with Slidebook (v6, Intelligent Imaging Innovations). Images were acquired with either a W-Plan-Apo 20x/1.0 water objective (Zeiss). Images were focused onto either an OrcaFlash4.0 sCMOS camera (sCMOS; Hamamatsu) or an eVolve 128 EMCCD camera (EMCCD; photometrix). For rat hippocampal neurons, μManager (V1.4, open-source, Open Imaging) was used to control the microscope.[8] For BODIPY-VF images, the excitation light was delivered from a LED at 510/25 nm and emission was collected with a triple emission filter (473/22, 543/19, 648/98 nm) after passing through a triple dichroic mirror (475/30, 540/25, 642/96 nm).

Membrane staining and photostability in HEK293T cells

HEK293T cells were incubated with a HBSS solution (Gibco) containing BODIPY VoltageFluors (1 μM) at 37°C for 20 min prior to transfer to fresh HBSS (no dye) for imaging. Microscopic images were acquired with a W-Plan-Apo 20x/1.0 water objective (Zeiss) and OrcaFlash4.0 sCMOS camera (Hamamatsu). For image intensity measurements, regions of interest were drawn around cells and the mean fluorescence was calculated in ImageJ (FIJI, NIH).[9] Background fluorescence was subtracted by measuring the fluorescence from regions of interest containing no cells.

For photostability experiments, HEK293T cells were incubated separately with VF2.1.Cl (1 μM), fVF 2 (1 μM), Et*m*H (1 μM), TM*m*OMe (1 μM), carboxy*m*OMe (1 μM), or amide*m*H (1 μM) in HBSS at 37°C for 20 min. Data were acquired with a W-Plan-Apo 20x/1.0 water objective (Zeiss) and OrcaFlash4.0 sCMOS camera (Hamamatsu). Images were taken every 5 seconds for 6 minutes with constant illumination of teal LED (2.48 mW/mm^2; 25 ms exposure time). The obtained fluorescence curves (background subtracted) were normalized with the fluorescence intensity at t = 0 and averaged (three rafts of cells of each dye).

Voltage sensitivity in HEK293T cells and Neurons

Analysis of voltage sensitivity in HEK cells was performed using ImageJ (FIJI).[9] Briefly, a region of interest (ROI) was selected manually based on fluorescence intensity and applied as a mask to all image frames. Fluorescence intensity values were calculated at known baseline and voltage step epochs. For analysis of voltage responses in neurons, regions of interest encompassing cell bodies (all of approximately the same size) were drawn in ImageJ and the mean fluorescence intensity for each frame extracted. ΔF/F values were calculated by first subtracting a mean background value from all raw fluorescence frames, to give a background subtracted trace (bkgsub). A baseline fluorescence value (Fbase) is calculated from the median of all the frames and subtracted from each timepoint of the bkgsub trace to yield a ΔF trace. The ΔF was then divided by Fbase to give ΔF/F traces. No averaging has been applied to any voltage traces.

Voltage imaging in cardiomyocytes

Functional recordings using VoltageFluor indicators (BODIPY, fVF 2, and VF2.1.Cl) were performed on an inverted epifluoresence microscope (AxioObserver Z-1; Zeiss) equipped with a Spectra-X light engine LED light (Lumencore) and controlled with μManager software (V1.4, open source, Open Imaging). Image series were acquired using a Plan-Apochromat 20/0.8 air objective (20X, Zeiss) focused onto an OrcaFlash4.0 sCMOS camerea (sCMOS, Hamamatsu). Sampling rate of 200 Hz (4x4 binning and restricted to 512x125 pixel frame for high-speed acquisition) was used. Analysis of action potential data

was performed using in-house MATLAB scripts used previously (Boggess et al., *ACS Chem Biol.* **2019**, *14*, 390-6), which are available upon request.

Electrophysiology

For electrophysiological experiments, pipettes were pulled from borosilicate glass (Sutter Instruments, BF150-86-10), with a resistance of 5–8 MΩ, and were filled with an internal solution; (in mM) 125 potassium gluconate, 1 EGTA, 10 HEPES, 5 NaCl, 10 KCl, 2 ATP disodium salt, 0.3 GTP trisodium salt (pH 7.25, 275 mOsm).

Recordings were obtained with an Axopatch 200B amplifier (Molecular Devices) at room temperature. The signals were digitized with Digidata 1332A, sampled at 50 kHz and recorded with pCLAMP 10 software (Molecular Devices) on a PC. Fast capacitance was compensated in the on-cell configuration. For all electrophysiology experiments, recordings were only pursued if series resistance in voltage clamp was less than 30 MΩ. For whole-cell, voltage clamp recordings in HEK 293T cells, cells were held at -60 mV and 100 ms hyper- and de-polarizing steps were applied from -100 to +100 mV in 20 mV increments.

Functional Imaging in Neurons

Extracellular field stimulation was delivered by a SD9 Grass Stimulator connected to a recording chamber containing two platinum electrodes (Warner), with triggering provided through the same Digidata 1332A digitizer and pCLAMP 9 software (Molecular Devices) that ran the electrophysiology. Action potentials were triggered by 1 ms 60 V field potentials delivered at 5 Hz. To prevent recurrent activity, the HBBS bath solution was supplemented with synaptic blockers; 10 μM 2,3-Dioxo-6-nitro-1,2,3,4-tetrahydrobenzo[f]quinoxaline-7-sulfonamide (NBQX; Santa Cruz Biotechnology) and 25 μM D(-)-2-Amino-5-phosphonopentanoic acid (D(-)-APV; Sigma-Aldrich). Functional Imaging of BODIPY-VFs was performed using the OrcaFlash4.0 sCMOS camera (sCMOS; Hamamatsu) and W-Plan-Apo 20x/1.0 water objective (Zeiss). Images were binned 4x4 to allow sampling rates of 0.5 kHz and 2500 frames (5 s) were acquired for each recording.

Computation

Gaussian 16 software[1] was used to draw BODIPY fluorophore structures. Bromines on the *meso*-aromatic ring were omitted because they are not present in the final VoltageFluor structure. Sodium counter-cations were added to the 1,3,5,7-tetramethyl-2,6-carboxylate BODIPY structure. All BODIPYs were assigned a –1 charge, then geometry optimizations, frequency calculations, and HOMO/LUMO orbital calculations were performed in Gaussian in an inert, gas-phase environment using WB97XD functional[2] and def2svp basis set.[3] Visualizations of BODIPY HOMOs (Figure S12) were generated with GaussView 6.

Supporting Scheme

Scheme S1 Synthesis of 2,6-diethyl para wire VoltageFluors

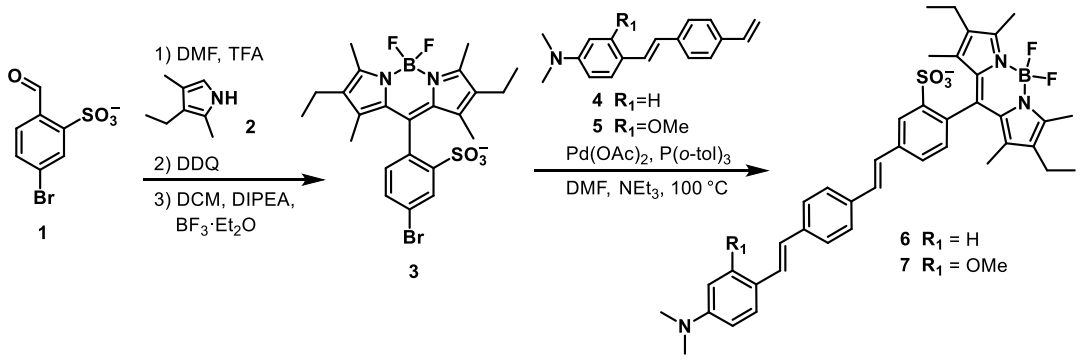

Scheme S2 Proposed synthetic route to more hydrophilic amidemH derivative

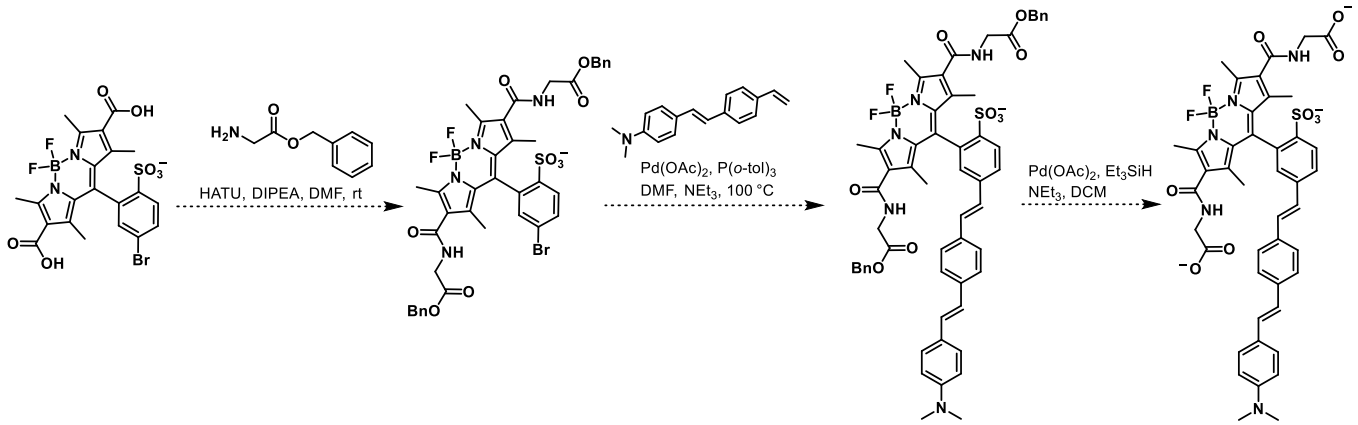

Supplementary Figures.

Figure S1. Reduction of molecular wire under Pd/C & H_2 benzyl removal conditions

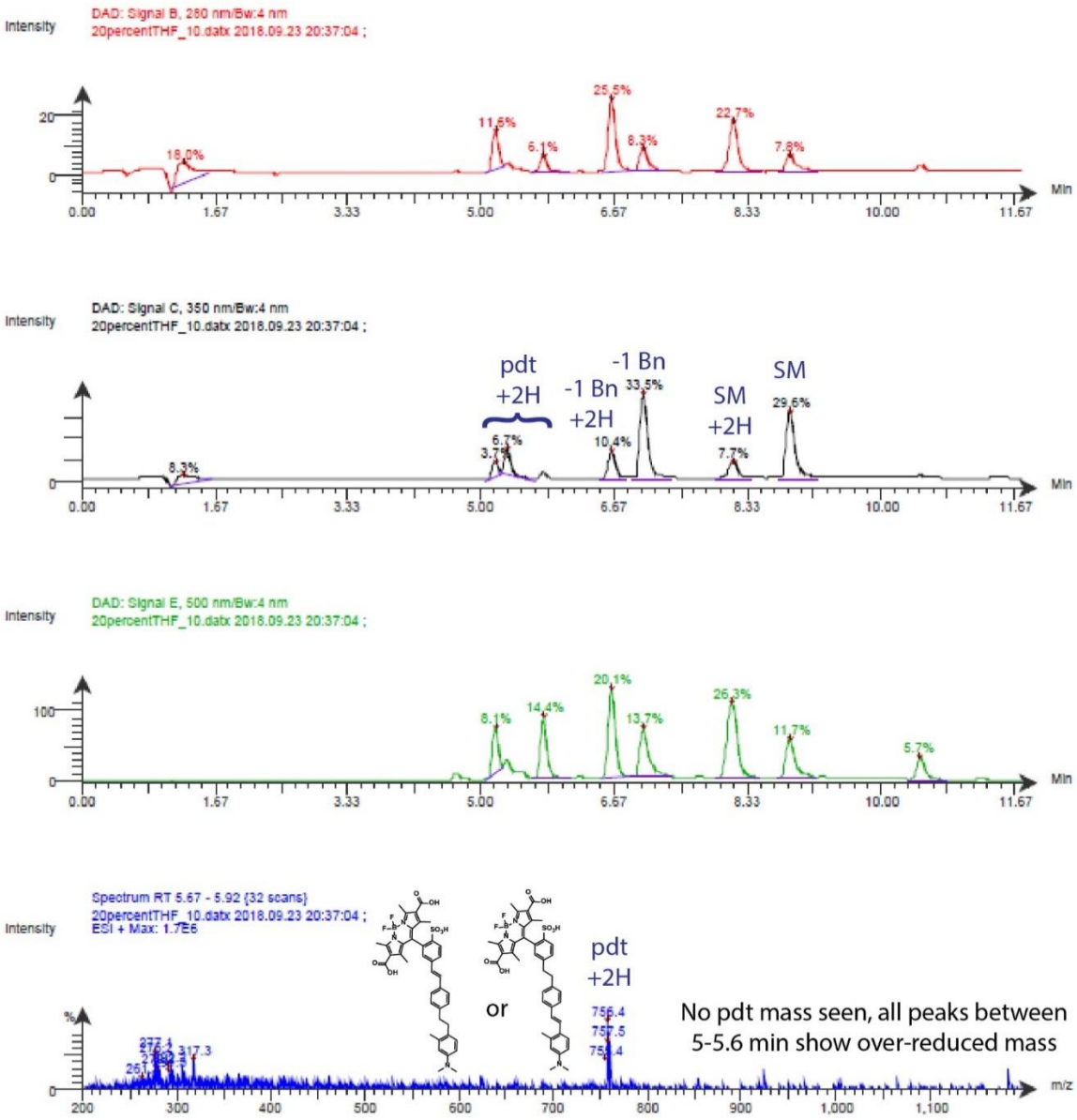

Figure S1. LC-MS of treating OBn*m*Me **26** with 20 mol% Pd/C under hydrogen atmosphere. While one benzyl group is successfully cleaved with only partial over-reduction of the molecular wire, no doubly deprotected product was obtained. All peaks between 5-6 min displayed 756 m/z, corresponding to cleaving both benzyl groups and also reducing an alkene.

Figure S2. Absorption and emission spectra of BODIPY VoltageFluors.

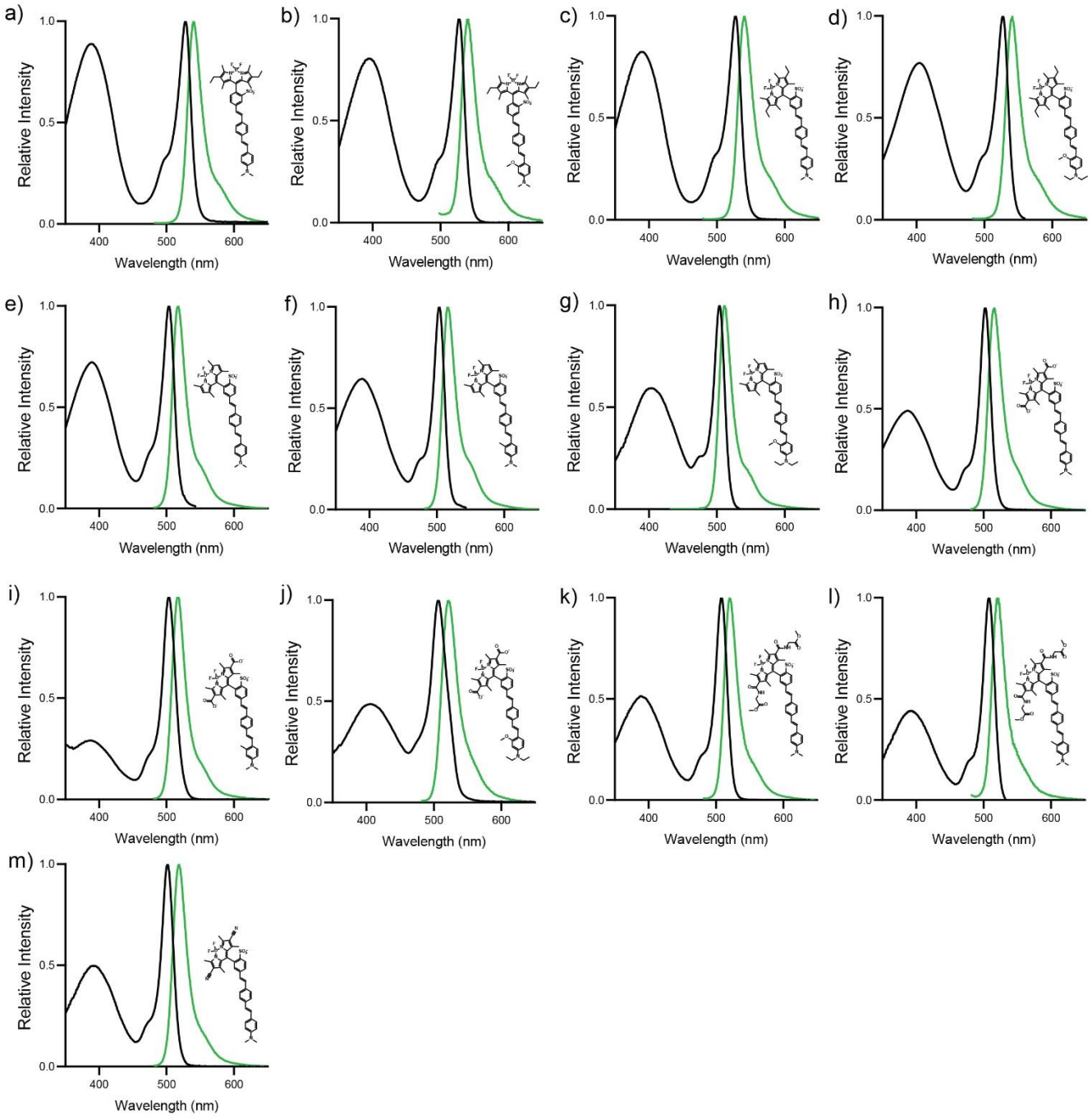

Figure S2. Absorption and emission spectra of **a)** Et*p*H, **b)** Et*p*OMe, **c)** Et*m*H, **d)** Et*m*OMe, **e)** TM*m*H, **f)** TM*m*Me, **g)** TM*m*OMe, **h)** carboxy*m*H, **i)** carboxy*m*Me, **j)** carboxy*m*OMe, **k)** amide*m*H, **l)** amide*m*Me, and **m)** cyano*m*H BODIPY VoltageFluors. Spectra were acquired in ethanol with 1 µM dye.

Figure S3. Cellular characterization of ethyl-substituted (para) BODIPY VF dyes 6 and 7

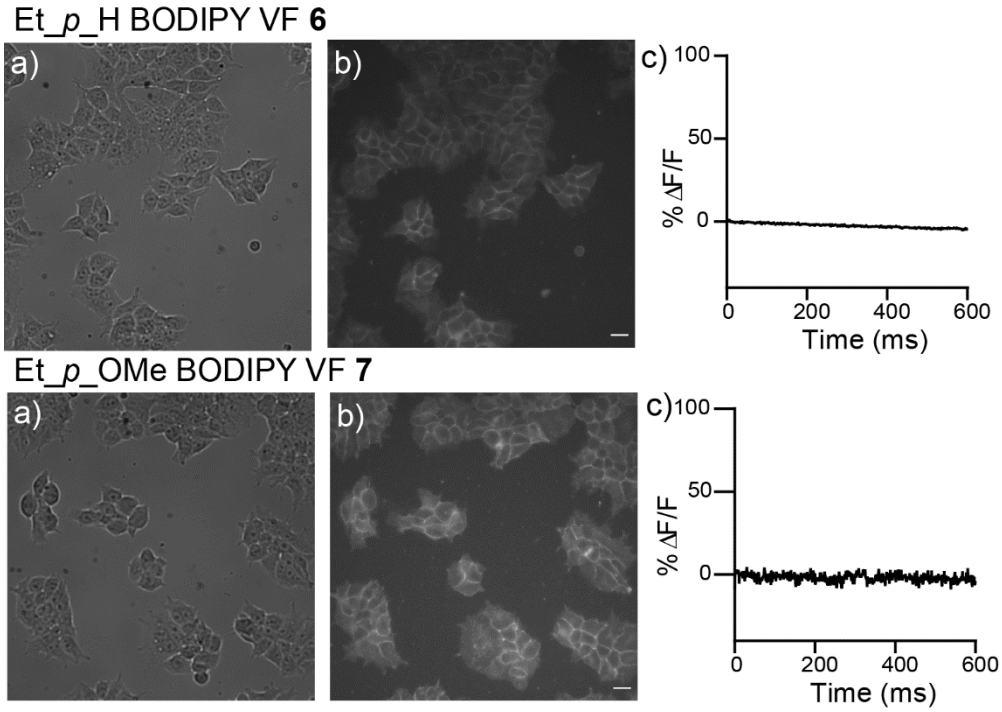

Figure S3. Cellular characterization of ethyl-substituted (*para*) BODIPY VF dyes Et*p*H **6** and Et*p*OMe **7**. HEK293T cells stained with 1 μM BODIPY VF are visualized under **a)** transmitted light and **b)** widefield fluorescence microscopy. Fluorescence images are adjusted to allow membrane staining to be seen. Scale bars are 20 μm. **c)** Plot of fractional change in fluorescence (ΔF/F) vs. time for hyper- and depolarizing steps (±100 mV in 20 mV increments) from a holding potential of -60 mV in a single HEK cell under whole-cell voltage-clamp mode. BODIPY VoltageFluors with < 5% ΔF/F are shown as unconcatenated, non-bleach corrected traces. All plots are scaled from -40 to 100% ΔF/F to facilitate comparison of voltage sensitivity.

Figure S4. Cellular characterization of ethyl-substituted (meta) BODIPY VF dyes 15 and 16.

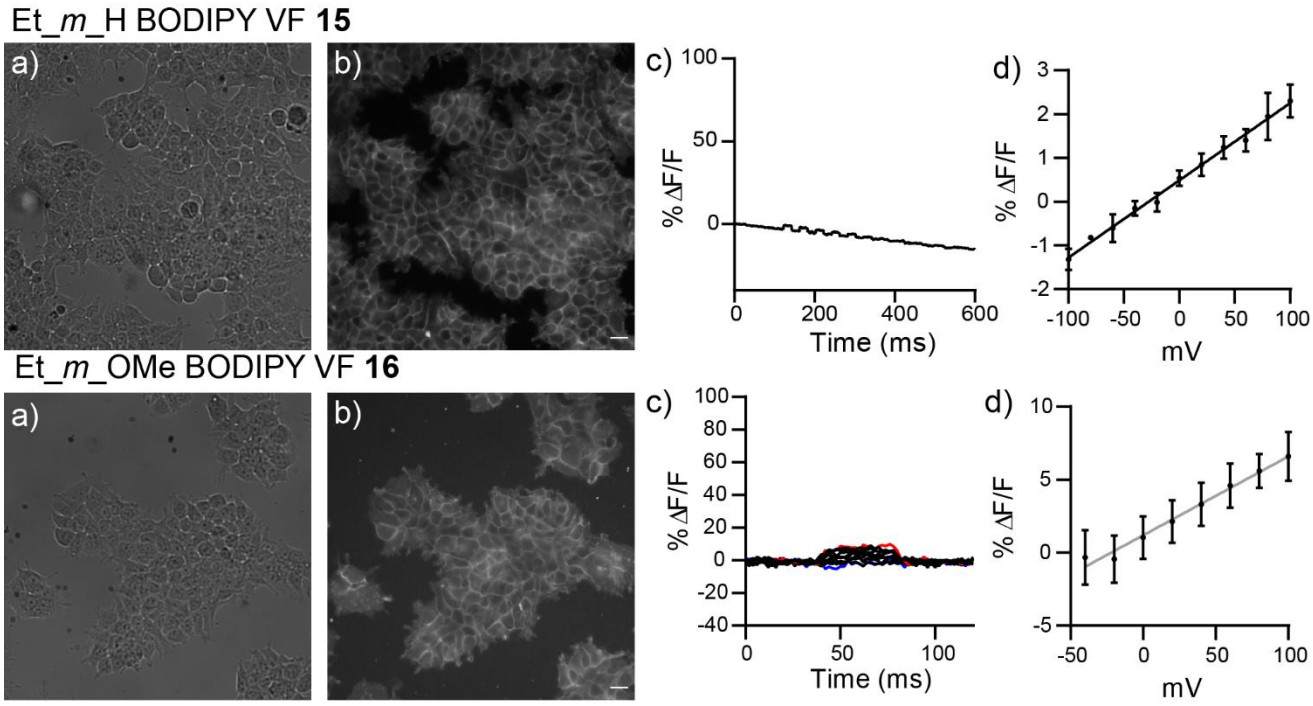

Figure S4. Cellular characterization of ethyl-substituted (*meta*) BODIPY VF dyes Et*m*H **15** and Et*m*OMe **16**. HEK293T cells stained with 1 μM BODIPY VF are visualized under **a)** transmitted light and **b)** widefield fluorescence microscopy. Fluorescence images are adjusted to allow membrane staining to be seen. Scale bars are 20 μm. **c)** Plot of fractional change in fluorescence (ΔF/F) vs. time for hyper- and depolarizing steps (±100 mV in 20 mV increments) from a holding potential of -60 mV in a single HEK cell under whole-cell voltage-clamp mode. BODIPY VoltageFluors with < 5% ΔF/F are shown as unconcatenated, non-bleach corrected traces. All plots are scaled from -40 to 100% ΔF/F to facilitate comparison of voltage sensitivity. **d)** Plot of fractional change in fluorescence (ΔF/F) vs. final membrane potential. Data represent the mean ΔF/F, ± S.E.M., for a minimum of n = 3 separate cells. Grey line is the line of best fit.

Figure S5. Cellular characterization of H-substituted BODIPY VF dyes 17, 18, and 19.

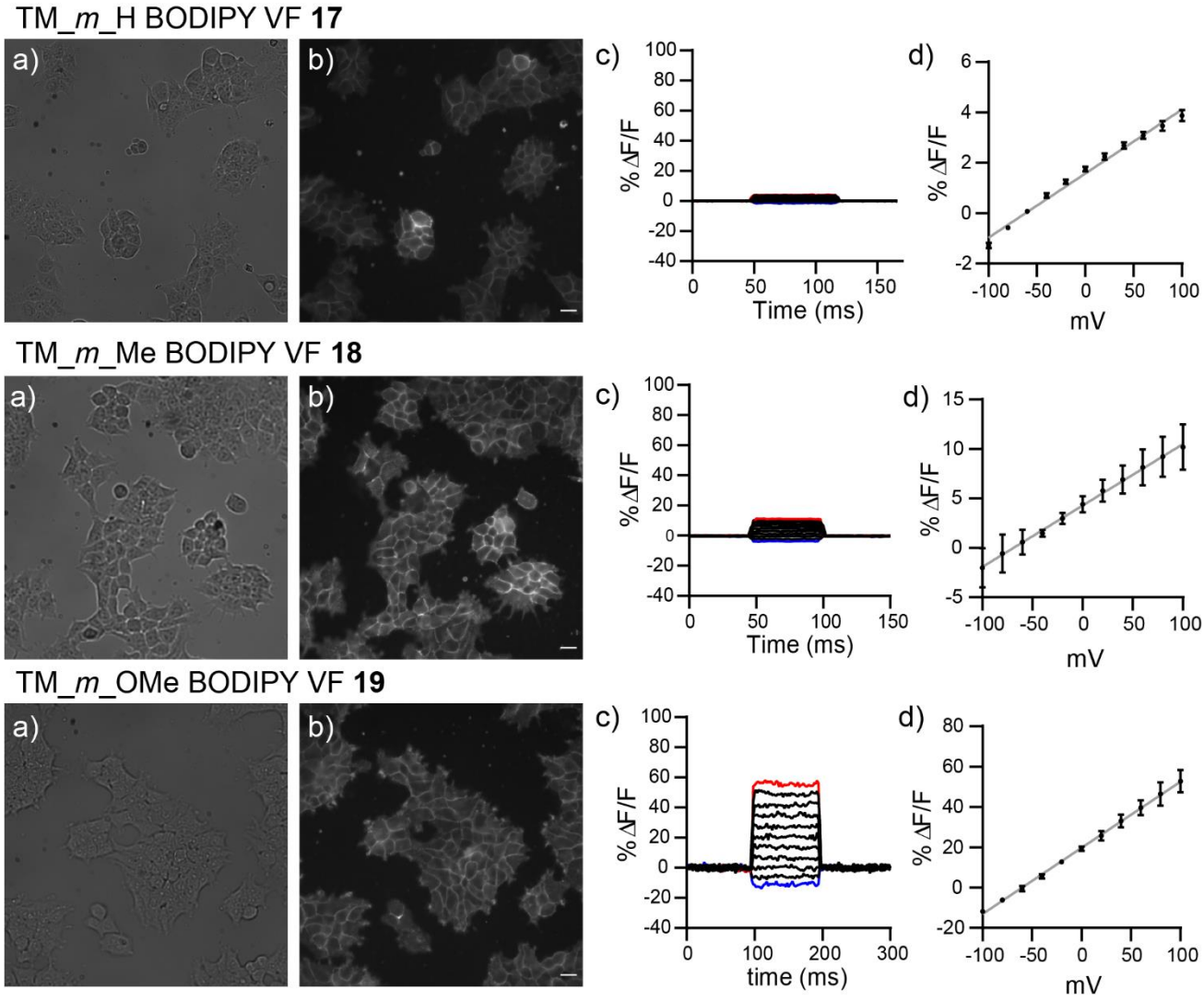

Figure S5. Cellular characterization of H-substituted BODIPY VF dyes **17**, **18**, and **19**. HEK293T cells stained with 1 μM BODIPY VF are visualized under **a)** transmitted light and **b)** widefield fluorescence microscopy. Fluorescence images are adjusted to allow membrane staining to be seen. Scale bars are 20 μm. **c)** Plot of fractional change in fluorescence (ΔF/F) vs. time for hyper- and depolarizing steps (±100 mV in 20 mV increments) from a holding potential of -60 mV in a single HEK cell under whole-cell voltage-clamp mode. All plots are scaled from -40 to 100% ΔF/F to facilitate comparison of voltage sensitivity. **d)** Plot of fractional change in fluorescence (ΔF/F) vs. final membrane potential. Data represent the mean ΔF/F, ± S.E.M., for a minimum of n = 3 separate cells. Grey line is the line of best fit.

Figure S6. Cellular characterization of cyano-substituted BODIPY VF dye 22.

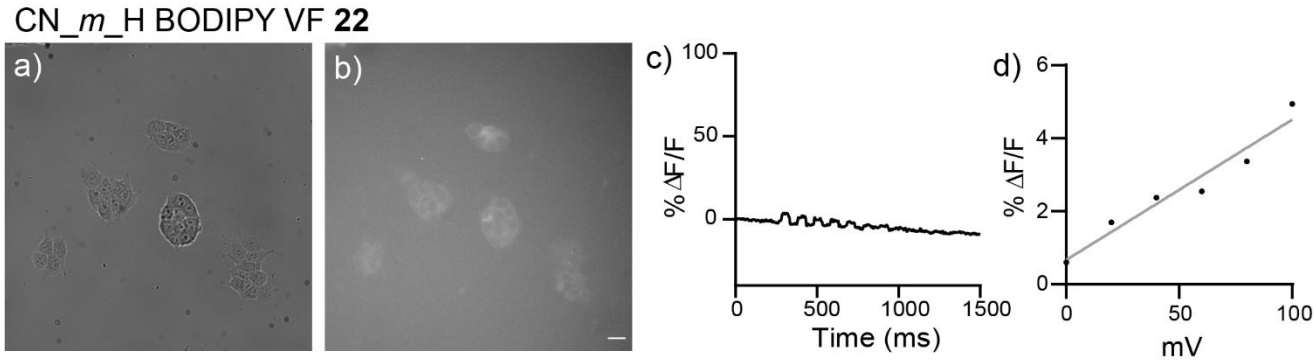

Figure S6. Cellular characterization of cyano-substituted BODIPY VF dye **22**. HEK293T cells stained with 1 μM BODIPY VF are visualized under **a)** transmitted light and **b)** widefield fluorescence microscopy. Fluorescence images are adjusted to allow membrane staining to be seen. Scale bars are 20 μm. **c)** Plot of fractional change in fluorescence (ΔF/F) vs. time for hyper- and depolarizing steps (±100 mV in 20 mV increments) from a holding potential of -60 mV in a single HEK cell under whole-cell voltage-clamp mode. BODIPY VoltageFluors with < 5% ΔF/F are shown as unconcatenated, non-bleach corrected traces. All plots are scaled from -40 to 100% ΔF/F to facilitate comparison of voltage sensitivity. **d)** Plot of fractional change in fluorescence (ΔF/F) vs. final membrane potential for n = 1 cell. Grey line is the line of best fit.

Figure S7. Cellular characterization of carboxy-substituted BODIPY VF dyes 28, 29, and 30.

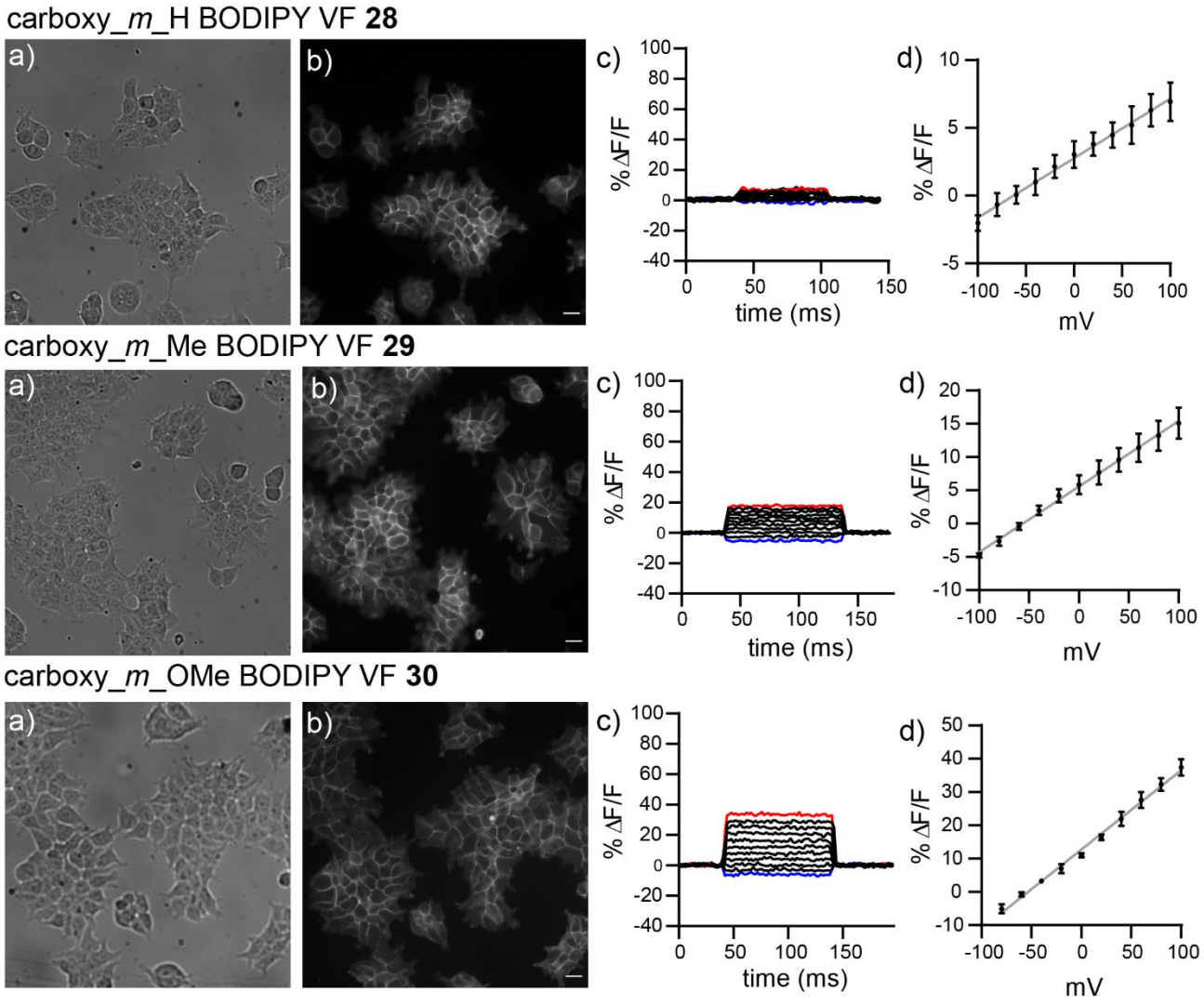

Figure S7. Cellular characterization of carboxy-substituted BODIPY VF dyes **28**, **29**, and **30**. HEK293T cells stained with 1 μM BODIPY VF are visualized under **a)** transmitted light and **b)** widefield fluorescence microscopy. Fluorescence images are adjusted to allow membrane staining to be seen. Scale bars are 20 μm. **c)** Plot of fractional change in fluorescence (ΔF/F) vs. time for hyper- and depolarizing steps (±100 mV in 20 mV increments) from a holding potential of -60 mV in a single HEK cell under whole-cell voltage-clamp mode. All plots are scaled from -40 to 100% ΔF/F to facilitate comparison of voltage sensitivity. **d)** Plot of fractional change in fluorescence (ΔF/F) vs. final membrane potential. Data represent the mean ΔF/F, ± S.E.M., for a minimum of n = 3 separate cells. Grey line is the line of best fit.

Figure S8. Cellular characterization of amide-substituted BODIPY VF dyes 35 and 36.

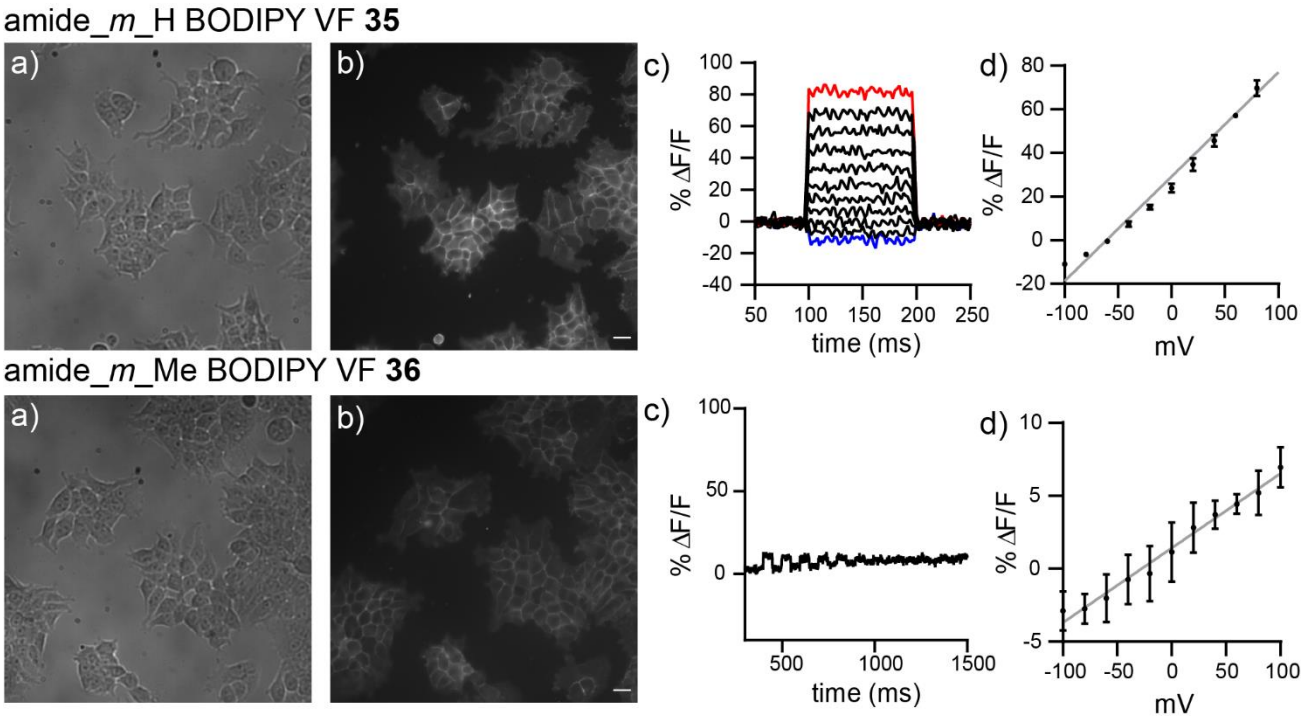

Figure S8. Cellular characterization of amide-substituted BODIPY VF dyes **35** and **36**. HEK293T cells stained with 1 μM BODIPY VF are visualized under **a)** transmitted light and **b)** widefield fluorescence microscopy. Fluorescence images are adjusted to allow membrane staining to be seen. Scale bars are 20 μm. **c)** Plot of fractional change in fluorescence (ΔF/F) vs. time for hyper- and depolarizing steps (±100 mV in 20 mV increments) from a holding potential of -60 mV in a single HEK cell under whole-cell voltage-clamp mode. BODIPY VoltageFluors with < 5% ΔF/F are shown as unconcatenated, non-bleach corrected traces. All plots are scaled from -40 to 100% ΔF/F to facilitate comparison of voltage sensitivity. **d)** Plot of fractional change in fluorescence (ΔF/F) vs. final membrane potential. Data represent the mean ΔF/F, ± S.E.M., for a minimum of n = 3 separate cells. Grey line is the line of best fit.

Figure S9. Relative brightness and photostability of BODIPY VoltageFluors

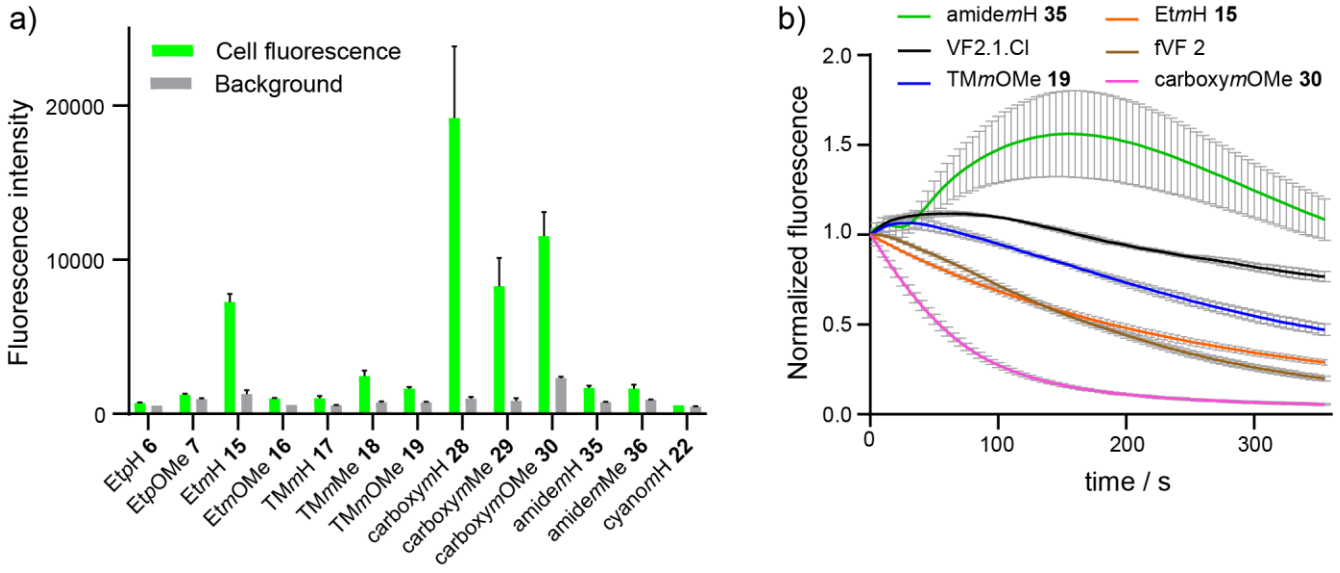

Figure S9. Relative brightness and photostability of BODIPY VoltageFluors. **a)** Average fluorescence intensity of BODIPY VoltageFluors in HEK293T cells for n = 3 images. Cells were loaded with 1 µM of each dye, and images acquired with teal LED/100 ms exposure time. **b)** Relative photobleaching of 1 µM BODIPY VoltageFluors as well as 1 µM of two dichlorofluorescein-based voltage indicators, VF2.1Cl (Miller, et al. *Proc Natl Acad Sci USA*, **2011**, *109*, 2114-2119) and fVF 2 (Boggess et al., *ACS Chem Biol*, **2019**, *14*, 390-396).

Figure S10. Voltage imaging in human induced pluripotent stem cell-derived cardiomyocytes (hiPSC-CMs) with selected BODIPY VF dyes.

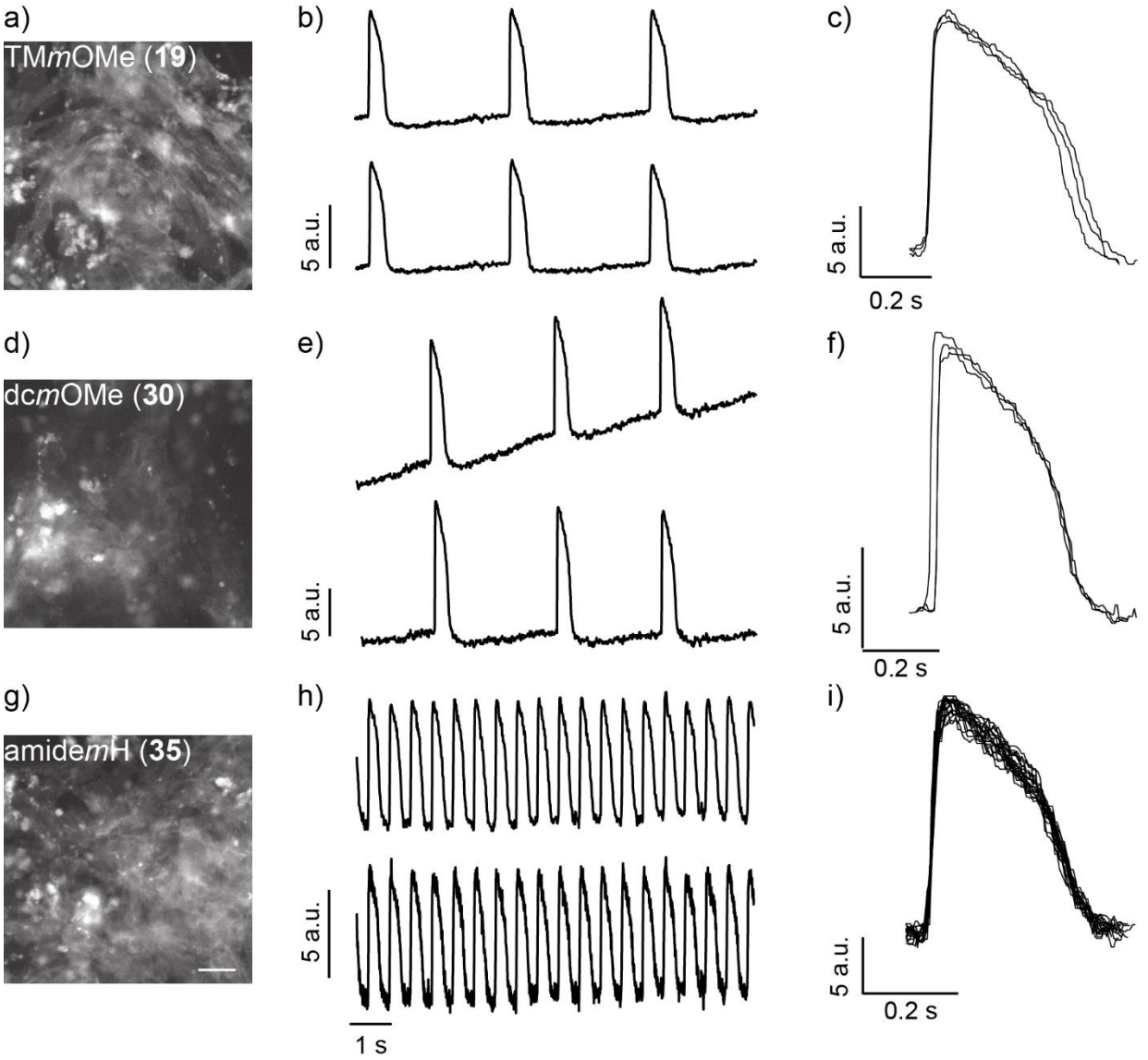

Figure S10. Voltage imaging in human induced pluripotent stem cell-derived cardiomyocytes (hiPSC-CMs) with selected BODIPY VF dyes. Panels **a**, **d**, and **g** show the widefield, epifluorescence micrographs of hiPSC-CMs stained with **a)** TM*m*OMe BODIPY VF **19** (different image from that shown in **Figure 4a** of main text; provided here for comparison), **d)** carboxy*m*OMe BODIPY VF **30**, or **g)** amide*m*H BODIPY VF **35**. All dyes were loaded at a concentration of 500 nM. Scale bar for these images is 50 μm. Panels **b**, **e**, and **h** display plot of mean pixel intensity (arbitrary fluorescence units, a.u.) across an entire field of view (similar to that shown in **Figure 4b** in the main text) vs. time during a 10 second acquisition (500 frames/s). The upper trace is the raw, median-filtered signal. The lower trace has been bleach-corrected. (panel b, lower trace, is reproduced from **Figure 4c** in the main text, for comparison). Panels c, f, and i depict individual action potentials from the bleach corrected traces.

Figure S11. Extended voltage imaging in hiPSC-CMs with TMmOMe BODIPY VF, fVF 2, and VF2.1.Cl.

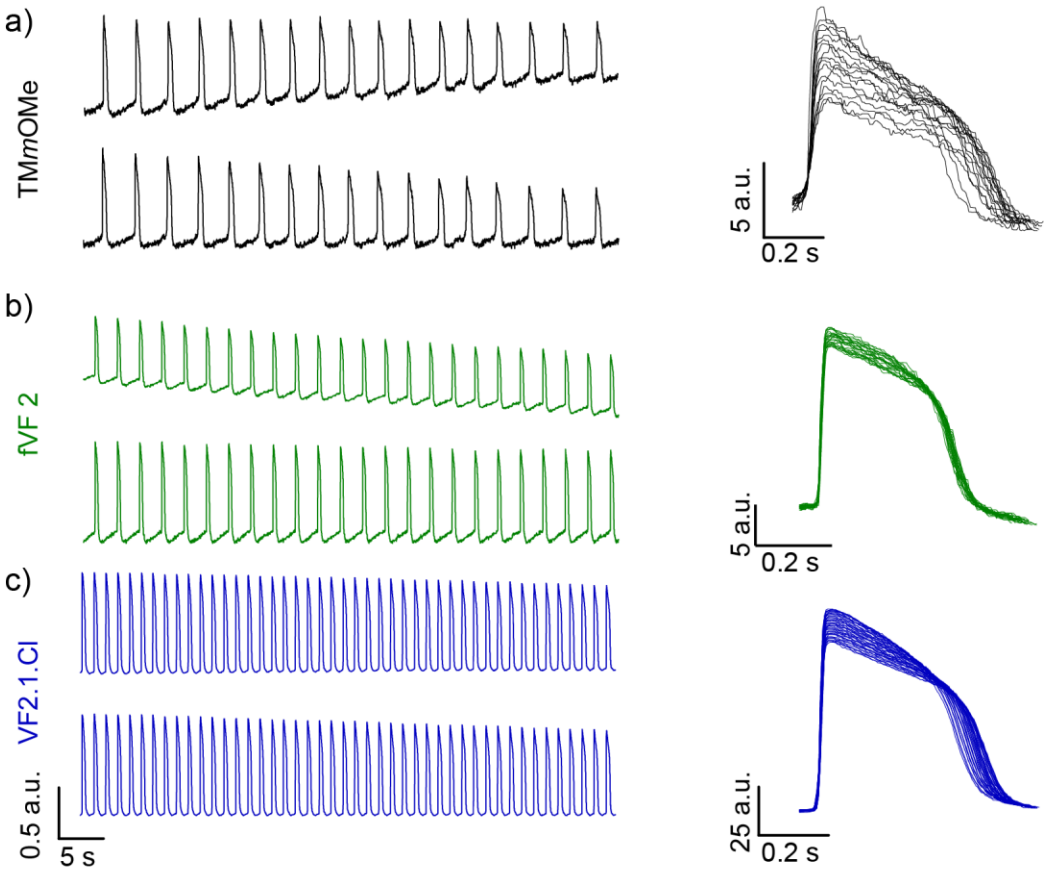

Figure S11. Extended voltage imaging in hiPSC-CMs with TM*m*OMe BODIPY VF, fVF 2, and VF2.1.Cl. Analysis of continuous voltage imaging in hiPSC-CMs for **a)** TM*m*OMe BODIPY VF **19** (black), **b)** fVF 2 (green; from Boggess et al., *ACS Chem Biol*, **2019**, *14*, 390-396), and **c)** VF2.1.Cl (blue; from Miller, et al. *Proc Natl Acad Sci USA*, **2011**, *109*, 2114-2119). The plots on the left depict the mean pixel intensity from an entire field of view (similar to **Figure 4b**, main text) vs. time during a 60 second acquisition (all dyes loaded at 500 nM, and under identical illumination conditions); upper traces are median-filtered values; lower traces are corrected for bleaching. The plots on the right are the concatenated action potentials from the bleach-corrected traces.

Figure S12. Computed HOMO energy levels for BODIPY fluorophores

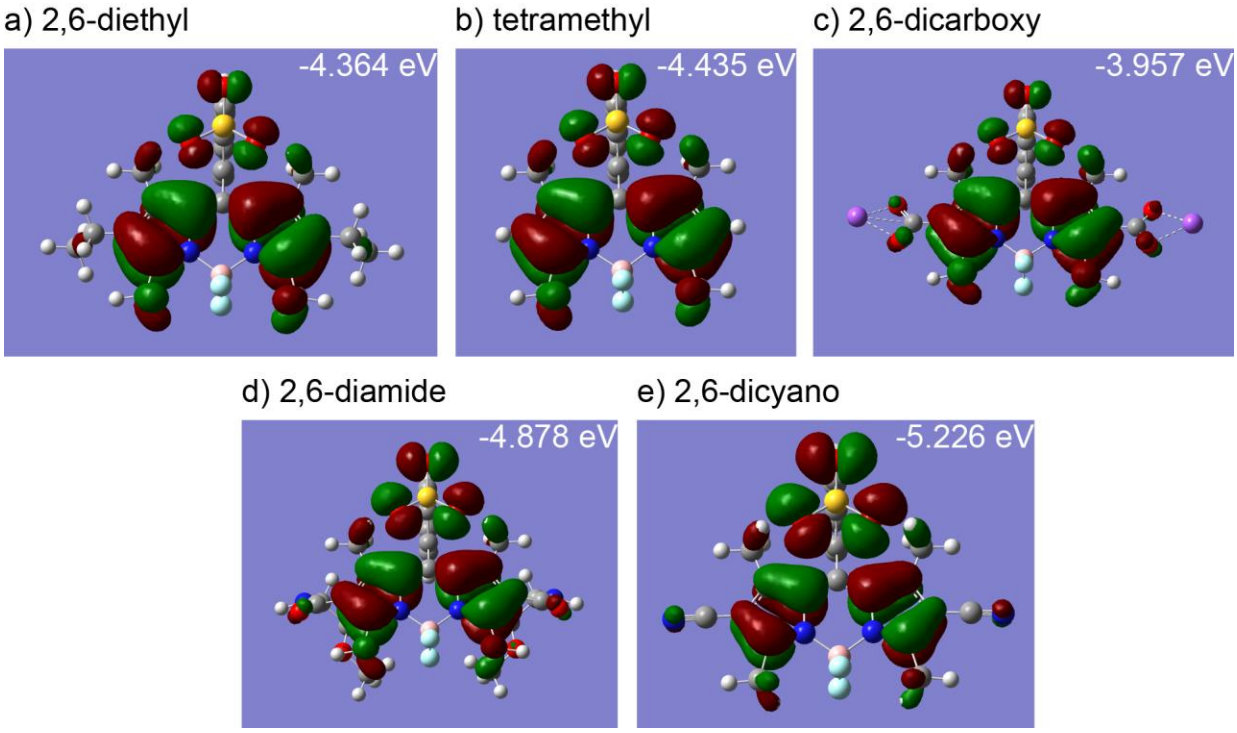

Figure S12. Computed HOMO energy levels for BODIPY fluorophores. Calculations are for sulfonated BODIPY dyes **11**, **12**, **32**, **34**, and **21**, but without Br. Calculations performed with the WB97XD functional and def2svp basis set. Calculated HOMO energies and associated orbital visualizations for **a)** 2,6-diethyl BODIPY **11**, **b)** 2,6-hydrogen (tetramethyl) BODIPY **12**, **c)** 2,6-dicarboxy BODIPY **32**, **d)** 2,6-diamide BODIPY **34** (methyl amide), and **e)** 2,6-dicyano BODIPY **21**.

Figure S13. Computational analysis of sulfonated BODIPY energy levels

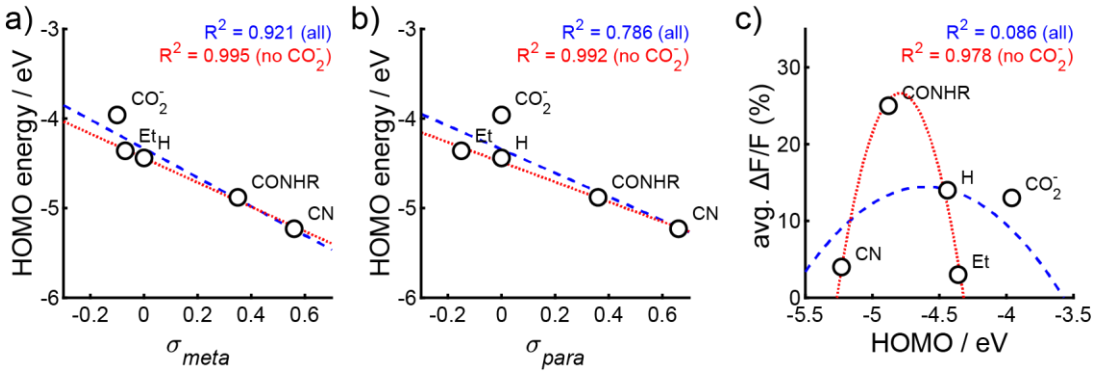

Figure S13. Computational analysis of sulfonated BODIPY energy levels. Plots of calculated HOMO energy (eV) vs. **a)** σ_{meta} or **b)** σ_{para}. Blue dashed lines indicate line of best fit including all data points. Red dotted lines depict the line of best fit, excluding σ parameters for carboxylates ($-CO_2^-$). R-squared parameters for each fit are indicated at the top of the plot. Values fo σ_{meta} or σ_{para} are taken from Hansch, et al., *Chem. Rev.*, **1991**, *91*, 165-195. **c)** Plot of average voltage sensitivity (in units of ΔF/F per 100 mV) for particular 2,6-substitutions on BODIPY vs. the calculated HOMO level of that type of BODIPY. Blue dashed line indicates binomial fit including all data. Red dotted line excludes the calculated HOMO level for carboxylate-containing BODIPYs ($-CO_2^-$).

Synthesis of BODIPY dyes

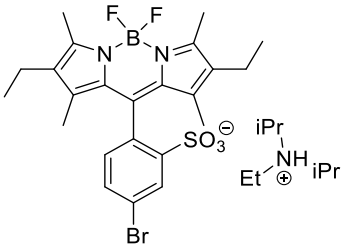

1,3,5,7-tetramethyl-2,6-diethyl-*p*-bromo BODIPY (3). *Para*-bromo sulfonated aldehyde **1** (256 mg, 0.97 mmol, 1 eq) was added to a flame-dried 25 mL round-bottom flask. Flask was evacuated and backfilled with N_2 3x, then DMF (5 mL), 3-ethyl-2,4-dimethyl-*1H*-pyrrole (287 µL, 2.12 mmol, 2.2 eq) and TFA (2 drops) were added via syringe, and reaction stirred under nitrogen atmosphere overnight. DDQ (219 mg, 0.97 mmol, 1 eq) was then added, stirred for 5 min, then concentrated under reduced pressure. An optional silica plug (3-10% MeOH in DCM gradient) yielded the dipyrromethene as a pink, green iridescent solid, which was taken onto the next step directly.

The dipyrromethene was dissolved in DCM (20 mL), DIPEA (1.91 mL, 11 mmol, 11 eq) and $BF_3{\cdot}Et_2O$ (2 mL, 15.5 mmol, 16 eq) were added via syringe and the solution became green fluorescent. After 10 min, reaction was quenched by addition of water, and organics were washed with 0.25N HCl (3 x 30 mL), brine (40 mL), dried over Na_2SO_4, and concentrated under reduced pressure. Flash chromatography on silica gel (3-7% MeOH in DCM gradient) yielded the BODIPY **3** as a pink, green iridescent solid (252 mg, 49%).

^{1}H NMR (400 MHz, MeOD) δ 8.24 (d, *J* = 2.06 Hz, 1H), 7.76 (dd, *J* = 2.06, 8.20 Hz, 1H), 7.17 (d, *J* = 8.20 Hz, 1H), 3.68 (sep, *J* = 6.64 Hz, 1H, $NEt(iPr)_2H^+$ salt), 3.18 (q, *J* = 7.41 Hz, 2H, $NEt(iPr)_2H^+$ salt), 2.45 (s, 6H), 2.33 (q, *J* = 7.52 Hz, 4H), 1.42 (s, 6H), 1.33 – 1.28 (m, 12H, $NEt(iPr)_2H^+$ salt), 0.98 (t, *J* = 7.51 Hz, 6H). **^{13}C NMR** (400 MHz, MeOD) δ 154.1, 147.2, 140.3, 140.1, 135.2, 133.64, 133.59, 133.3, 133.0, 132.5, 123.9, 55.8 ($NEt(iPr)_2H^+$ salt), 43.8 ($NEt(iPr)_2H^+$ salt), 18.0, 15.2, 13.1, 12.7, 12.1 ppm. **ESI-HR(-)**, calculated for $C_{23}H_{25}BBrF_2N_2O_3S^-$: 537.0836, found: 537.0825.

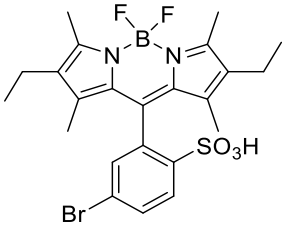

1,3,5,7-tetramethyl-2,6-diethyl-*m*-bromo BODIPY (11). *Meta*-bromo sulfonated aldehyde **9** (160 mg, 0.60 mmol, 1 eq) was added to a flame-dried 25 mL round-bottom flask. Flask was evacuated and backfilled with N_2 3x, then DMF (5 mL), 3-ethyl-2,4-dimethyl-*1H*-pyrrole (179 µL, 2.12 mmol, 2.2 eq) and TFA (2 drops) were added via syringe, and reaction stirred under nitrogen atmosphere overnight. DDQ (137 mg, 0.60 mmol, 1 eq) was then added, stirred for 5 min, then concentrated under reduced pressure. An optional silica plug (3-10% MeOH in DCM gradient) yielded the dipyrromethene as a pink, green iridescent solid, which was taken onto the next step directly.

The dipyrromethene was dissolved in DCM (20 mL), DIPEA (1.2 mL, 6.9 mmol, 10.4 eq) and $BF_3{\cdot}Et_2O$ (1.19 mL, 9.7 mmol, 16 eq) were added via syringe, and the solution became green fluorescent. After 10 min, reaction was quenched by addition of water, and organics were washed with 0.25N HCl (3 x 10 mL), brine (20 mL), dried over Na_2SO_4, and concentrated under reduced pressure. Flash chromatography on silica gel (3% MeOH in DCM) yielded the BODIPY **11** as a pink, green iridescent solid (126 mg, 33%).

^{1}H NMR (500 MHz, DMSO-d_6) δ 8.47 (d, J = 8.42 Hz, 1H), 8.16 (dd, J = 2.08, 8.48 Hz, 1H), 7.85 (d, J = 2.10 Hz, 1H), 2.91 (s, 6H), 2.76 (q, J = 7.56 Hz, 4H), 1.88 (s, 6H), 1.42 (t, J = 7.54 Hz, 6H). **^{13}C NMR** (900 MHz, DMSO-d_6) δ 162.8, 155.7, 149.7, 149.2, 145.6, 142.3, 142.2, 142.0, 141.64, 141.55, 133.5, 27.2, 24.8, 22.3, 21.5 **ESI-HR(-)**, calculated for $C_{23}H_{25}BBrF_2N_2O_3S^-$: 537.0836, found: 537.0837.

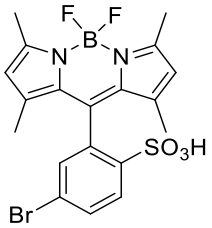

1,3,5,7-tetramethyl-*m*-bromo BODIPY (12). *Meta*-bromo sulfonated aldehyde **9** (504.9 mg, 1.9 mmol, 1 eq) was added to a flame-dried 25 mL round-bottom flask. Flask was evacuated and backfilled with N_2 3x, then DMF (5 mL), 2,4-dimethyl-*1H*-pyrrole (432 µL, 4.2 mmol, 2.2 eq) and TFA (3 drops) were added via syringe, and reaction stirred under nitrogen atmosphere overnight. DDQ (432 mg, 1.9 mmol, 1 eq) was then added, stirred for 5 min, then concentrated under reduced pressure. An optional silica plug (2-14% MeOH in DCM gradient) yielded the dipyrromethene as a pink, green iridescent solid, which was taken onto the next step directly.

The dipyrromethene was dissolved in DCM (40 mL), DIPEA (3.6 mL, 21 mmol, 11 eq) and $BF_3{\cdot}Et_2O$ (3.8 mL, 30 mmol, 16 eq) were added via syringe and the solution became green fluorescent. After 10 min, reaction was quenched by addition of 10 mL iPrOH. Organics were washed with 0.25N HCl (2 x 20 mL), brine (20 mL), dried over Na_2SO_4, and concentrated under reduced pressure. Flash chromatography on silica gel (1-7% MeOH in DCM gradient) yielded the BODIPY **12** as a pink, green iridescent solid (350 mg, 38%). **^{1}H NMR** (400 MHz, MeOD) δ 8.47 (d, J = 8.44 Hz, 1H), 8.16 (dd, J = 2.08, 8.47 Hz, 1H), 7.87 (d, J = 7.87 Hz, 1H), 6.44 (s, 2H), 2.91 (s, 6H), 1.96 (s, 6H). **^{13}C NMR** (900 MHz, DMSO-d_6) δ 164.5, 155.8, 153.9, 151.2, 144.8, 142.3, 142.1, 141.9, 141.6, 133.4, 131.0, 24.24, 24.21. **ESI-HR(-)**, calculated for $C_{19}H_{17}BBrF_2N_2O_3S^-$: 481.0210, found: 481.0211.

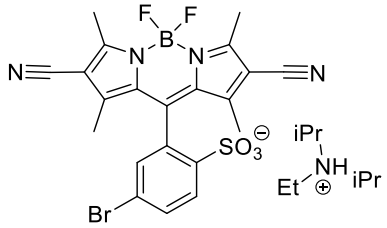

1,3,5,7-tetramethyl-2,6-cyano-*m*-bromo BODIPY (21). *Meta*-bromo sulfonated aldehyde **9** (256 mg, 0.22 mmol, 1 eq) and 2,4-dimethyl-*1H*-pyrrole-3-carbonitrile (**31**) (58.3 mg, 0.49 mmol, 2.2 mmol) were added to an oven-dried 25 mL round-bottom flask. Flask was evacuated and backfilled with N_2 three times, then dissolved in DMF (680 µL) and DCM (1.01 mL). TFA (100 µL) was added via syringe and reaction stirred under inert N_2 atmosphere overnight. DDQ was then added (50.1 mg, 0.22 mmol, 1 eq), stirred for 5 min, then solution was concentrated under reduced pressure.

The dipyrromethene was dissolved in DCM (5 mL), then DIPEA (423 µL, 2.4 mmol, 11 eq) and $BF_3{\cdot}Et_2O$ (436 µL, 3.5 mmol, 16 eq) were added and reaction stirred for 1.5 hrs. Reaction was quenched by addition of water, and organics were washed with water (3 x 30 mL), dried over Na_2SO_4, and concentrated under reduced pressure. Flash chromatography on silica gel (1-7% MeOH in DCM gradient) yielded the BODIPY **21** as a pink, green iridescent solid (33.8 mg, 29%).

^{1}H NMR (400 MHz, Methanol-d_4) δ 8.04 (d, J = 8.5 Hz, 1H), 7.89 (dd, J = 8.5, 2.0 Hz, 1H), 7.61 (d, J = 2.0 Hz, 1H), 3.71 (p, J = 6.6 Hz, 1H, $NEt(iPr)_2H^+$ salt), 3.20 (q, J = 7.4 Hz, 2H, $NEt(iPr)_2H^+$ salt), 2.66 (s, 6H), 1.70 (s, 6H), 1.40 – 1.25 (m, 15H, $NEt(iPr)_2H^+$ salt). **^{13}C NMR** (400 MHz, Methanol-d_4) δ 160.2, 150.9, 146.8, 144.3, 134.9, 133.4, 133.3, 132.5, 132.2, 126.5, 114.7, 106.9, 56.0 ($NEt(iPr)_2H^+$ salt), 55.0 ($NEt(iPr)_2H^+$ salt), 43.9, 14.2, 13.9, 13.3 ppm. **ESI-HR(-)**, calculated for $C_{21}H_{15}BBrF_2N_4O_3S^-$: 531.0115, found: 531.0110.

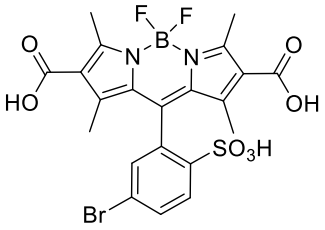

1,3,5,7-tetramethyl-2,6-carboxy-*m*-bromo BODIPY (32). *Meta*-bromo sulfonated aldehyde **9** (357 mg, 1.4 mmol, 1 eq) and 2,4-dimethylpyrrole-3-carboxylic acid **31** (412 mg, 3.0 mmol, 2.2 eq) were added to a flame-dried 25 mL round-bottom flask. Flask was evacuated and backfilled with N_2 3x, then DMF (10 mLand TFA (100 µL) were added via syringe and reaction stirred under nitrogen atmosphere overnight. DDQ (306 mg, 1.4 mmol, 1 eq) was added and solution stirred for 5 min then was concentrated under reduced pressure. An optional silica plug (15% MeOH + 1% AcOH in DCM) yielded the dipyrromethene as a pink, green iridescent solid, which was taken onto the next step directly.

DCM (50 mL) was added to 250 mL round-bottom flask containing the dipyrromethene and the solution was sonicated to suspend the material. DIPEA (2.6 mL, 15 mmol, 11 eq) and $BF_3{\cdot}Et_2O$ (2.7 mL, 22 mmol, 16 eq) were added via syringe and the solution became green fluorescent. After 10 min, reaction was quenched by addition of 10 mL iPrOH and solution was concentrated under reduced pressure. Flash chromatography on silica gel (10-20% MeOH in DCM + 1% AcOH, gradient) yielded the BODIPY **32** as a pink, green iridescent solid (380 mg, 49%). This material was >90% pure by analytical HPLC and was used without further purification in the next synthetic step. For NMR and spectroscopic characterization, was purified by reverse phase preparative HPLC (10-100% MeCN in water, 0.05% formic acid additive).

^{1}H NMR (400 MHz, Methanol-d_4) δ 8.01 (d, J = 8.5 Hz, 1H), 7.82 (dd, J = 8.5, 2.1 Hz, 1H), 7.52 (d, J = 2.0 Hz, 1H), 2.75 (s, 6H), 1.80 (s, 6H). **^{13}C NMR** (900 MHz, Methanol-d_4) δ 170.3, 158.9, 145.8, 144.5, 143.6, 135.6, 133.6, 133.2, 132.9, 132.0, 125.9, 14.8, 13.6 ppm. **ESI-HR(-)**, calculated for $C_{21}H_{17}BBrF_2N_2O_7S^-$: 569.0006, found: 569.0008).

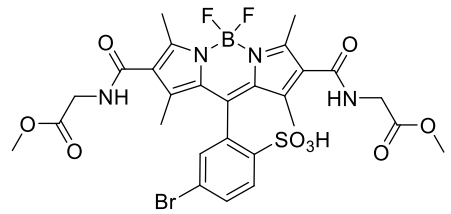

1,3,5,7-tetramethyl-2,6-amido-*m*-bromo BODIPY (34). 1,3,5,7-tetramethyl-2,6-dicarboxy BODIPY **32** (23 mg, 0.04 mmol), glycine methyl ester (11.3 mg, 0.09 mmol, 2.25 eq), and HATU (34.4 mg, 0.09 mmol, 2.25 eq) were dissolved in DMF (0.5 mL), then DIPEA (70 µL, 0.4 mmol, 10 eq) were added and reaction stirred at rt for 3.5 hrs. Reaction was concentrated to near-dryness under reduced pressure, then 10 mL DCM was added and solution was washed with water (2 x 5 mL), dried over Na_2SO_4, and concentrated under reduced pressure. Preparative TLC (15% MeOH in DCM) yielded amide BODIPY **34** as an orange, green iridescent solid (24 mg, 82%). This material was >95% pure by analytical HPLC and

was used without further purification in the next synthetic step. For NMR and spectroscopic characterization, a small amount was further purified by reverse phase preparative HPLC (10-100% MeCN in water, 0.05% formic acid additive).

^{1}H NMR (700 MHz, Methanol-*d*$_4$) δ 8.02 (d, J = 8.5 Hz, 1H), 7.83 (dd, J = 8.5, 2.1 Hz, 1H), 7.54 (d, J = 2.1 Hz, 1H), 4.12 – 3.99 (m, 4H), 3.73 (s, 6H), 2.61 (s, 6H), 1.63 (s, 6H). **^{13}C NMR** (600 MHz, Methanol-*d*$_4$) δ 171.6, 168.1, 155.9, 143.9, 142.9, 133.9, 133.0, 132.7, 132.1, 129.5, 126.1, 52.6, 42.0, 13.5, 13.1 ppm. **LR-MS (ESI+)** calculated for $C_{27}H_{29}BF_2BrN_4O_9S^+$: 713.09, found 713.4. **Analytical HPLC retention time:** 5.02 min (10-100% MeCN in water, 0.05% TFA additive).

Synthesis of BODIPY VoltageFluors

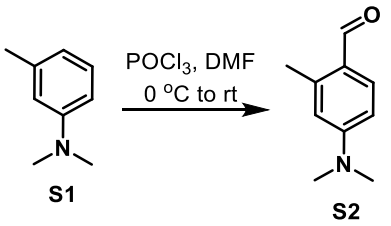

4-(dimethylamino)-2-methylbenzaldehyde (S2). A flame-dried round-bottom flask was charged with *N,N*-dimethyl-*m*-toluidene **S1** (4 g, 29.6 mmol, 1 eq) and evacuated/backfilled with N_2 3x. DMF (45 mL) was added and solution was cooled to 0 °C in an ice-water bath. $POCl_3$ (4.98 mL, 53.6 mmol, 1.8 eq) was added dropwise via syringe and reaction stirred at rt 18 hr. Reaction was poured into ice water (500 mL) and adjusted to pH 9 with 1M NaOH. The resulting precipitate was filtered, washed with water (50 mL), then dried *in vacuo,* yielding **S2** as a white solid (3.19 g, 66%).

^{1}H NMR (400 MHz, Chloroform-*d*) δ 9.98 (s, 1H), 7.67 (d, *J* = 8.7 Hz, 1H), 6.57 (dd, *J* = 8.7, 2.6 Hz, 1H), 6.43 (d, *J* = 2.6 Hz, 1H), 3.07 (s, 6H), 2.63 (s, 3H). **^{13}C NMR** (400 MHz, $CDCl_3$) δ 190.37, 153.52, 142.77, 134.60, 123.34, 113.42, 108.83, 39.96, 20.38. **ESI-HR(+)**, calculated for $C_{10}H_{14}O_1N_1^+$: 164.1070, found: 164.1068.

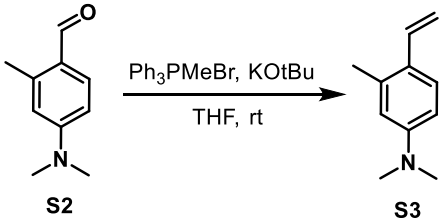

***N,N*,3-trimethyl-4-vinylaniline (S3).** A flame-dried round-bottom flask was charged with Ph_3PMeBr (11.17 g, 31 mmol, 1.6 eq) and evacuated/backfilled 3x with N_2. Anhydrous THF (18 mL) and KOtBu (3.5 g, 31 mmol, 1.6 eq) were added and stirred for 15 min. Aldehyde **S2** was added slowly via a funnel, which was rinsed with THF (8 mL). After 2.5 hrs, solvent was removed under reduced pressure, hexanes were added, filtered through a pad of alumina, and concentrated. Resulting residue was purified further with an alumina column (3 – 5% EtOAc in hexanes gradient), yielding styrene **S3** as a light yellow oil (2.9 g, 92%).

^{1}H NMR (400 MHz, Chloroform-*d*) δ 7.43 (dd, *J* = 8.7, 1.7 Hz, 1H), 6.89 (ddd, *J* = 17.4, 11.0, 1.9 Hz, 1H), 6.60 (dt, *J* = 8.6, 2.1 Hz, 1H), 6.52 (t, *J* = 2.1 Hz, 1H), 5.50 (dq, *J* = 17.4, 1.4 Hz, 1H), 5.10 (dq, *J* = 10.9, 1.4 Hz, 1H), 2.96 (d, *J* = 1.4 Hz, 6H), 2.35 (d, *J* = 1.8 Hz, 3H). **^{13}C NMR** (400 MHz, Chloroform-

d) δ 150.31, 137.99, 134.48, 126.23, 125.54, 114.07, 111.07, 110.69, 40.65, 20.38. **ESI-HR(+)**, calculated for $C_{11}H_{16}N_1^+$: 162.1277, found: 162.1275.

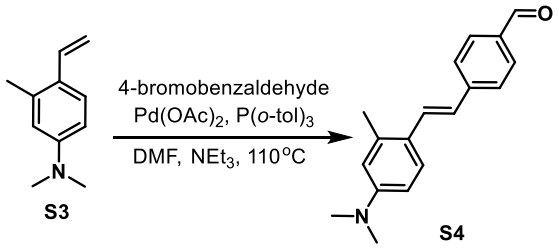

(E)-4-(4-(dimethylamino)-2-methylstyryl)benzaldehyde (S4). A flame-dried Schlenk flask was charged with **S3** (2.9 g, 18 mmol, 1 eq), 4-bromobenzaldehyde (3.3 g, 18 mmol, 1 eq), $Pd(OAc)_2$ (40.4 mg, 0.18 mmol, 1 mol%), and P(*o*-tol)$_3$ (109 mg, 0.36 mmol, 2 mol%). Flask was evacuated and backfilled with N_2 3x, DMF (20 mL) and NEt_3 (8 mL) were added, and reaction stirred at 110 °C 18 hr. Reaction was concentrated under reduced pressure, then residue was dissolved in EtOAc (200 mL) and washed with water (2 x 225 mL) and brine (200 mL). Organics were dried with Na_2SO_4 and concentrated under reduced pressure. Flash chromatography (5 – 20% EtOAc in hexanes, gradient) yielded **S4** as an orange solid (1.55 g, 32%).

^{1}H NMR (400 MHz, Chloroform-*d*) δ 9.97 (s, 1H), 7.87 – 7.80 (m, 2H), 7.61 (d, *J* = 8.1 Hz, 2H), 7.57 (d, *J* = 8.7 Hz, 1H), 7.47 (d, *J* = 16.1 Hz, 1H), 6.90 (d, *J* = 16.1 Hz, 1H), 6.61 (dd, *J* = 8.7, 2.8 Hz, 1H), 6.53 (d, *J* = 2.6 Hz, 1H), 3.00 (s, 6H), 2.45 (s, 3H). **^{13}C NMR** (400 MHz, $CDCl_3$) δ 191.8, 150.7, 145.0, 137.7, 134.7, 130.4, 130.1, 129.7, 126.7, 126.5, 124.1, 123.9, 114.0, 110.6, 40.5, 20.6 ppm. **ESI-HR(+)**, calculated for $C_{18}H_{20}O_1N_1^+$: 266.1539, found: 266.1526.

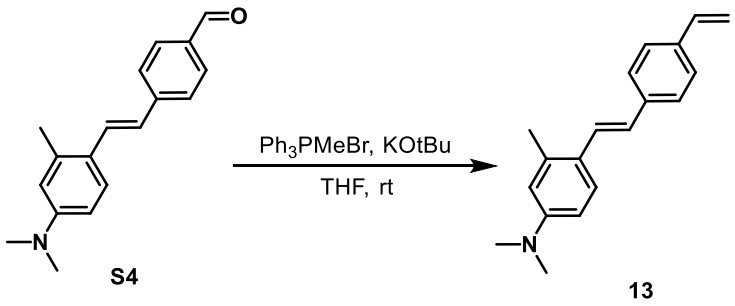

***(E)-N,N*,3-trimethyl-4-(4-vinylstyryl)aniline (13).** A flame-dried round-bottom flask was charged with Ph_3PMeBr (474 mg, 1.3 mmol, 1.6 eq) and evacuated/backfilled 3x with N_2. Anhydrous THF (1.8 mL) and KOtBu (149 mg, 1.3 mmol, 1.6 eq) were added and stirred for 15 min. Aldehyde **S4** was dissolved in THF (1 mL + 1mL rinse) and pipetted into reaction flask. After 20 hrs, solvent was removed under reduced pressure, hexanes were added, filtered through a pad of celite, and concentrated. Flash chromatography on silica (3 – 5% EtOAc in hexanes gradient), yielded **13** as a yellow solid (141 mg, 65%).

^{1}H NMR (400 MHz, Chloroform-*d*) δ 7.65 (d, *J* = 8.7 Hz, 1H), 7.57 (d, *J* = 8.2 Hz, 2H), 7.50 (d, *J* = 8.2 Hz, 2H), 7.42 (d, *J* = 16.1 Hz, 1H), 6.97 (d, *J* = 16.1 Hz, 1H), 6.83 (dd, *J* = 17.6, 10.9 Hz, 1H), 6.72 (dd, *J* = 8.7, 2.7 Hz, 1H), 6.65 (d, *J* = 2.7 Hz, 1H), 5.87 (dd, *J* = 17.6, 0.9 Hz, 1H), 5.34 (dd, *J* = 10.8, 1.0 Hz, 1H), 3.07 (s, 6H), 2.54 (s, 3H). **^{13}C NMR** (400 MHz, $CDCl_3$) δ 150.15, 138.22, 136.92, 136.71, 136.09, 126.59, 126.47, 126.32, 126.30, 125.44, 124.82, 114.08, 113.18, 110.73, 40.51, 20.58. **ESI-HR(+)**, calculated for $C_{19}H_{22}N_1^+$: 264.1747, found: 264.1742.

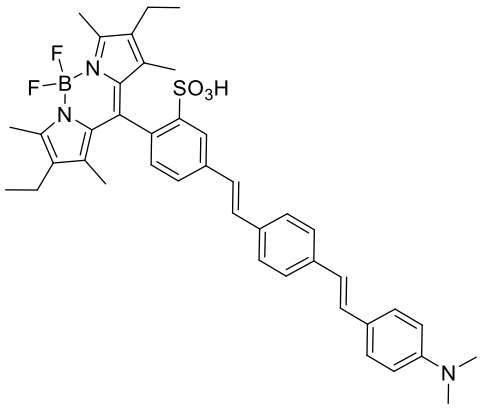

Ethyl BODIPY *p*-normal wire (6). To a flame-dried 10 mL Schlenk flask were added 1,3,5,7-tetramethyl-2,6-diethyl-*p*-bromo BODIPY **3** (87.5 mg, 0.16 mmol, 1 eq), molecular wire **4** (44.5 mg, 0.18 mmol, 1.1 eq), $Pd(OAc)_2$ (3.2 mg, 0.015 mmol, 9 mol%), and P(*o*-tol)$_3$ (8.9 mg, 0.029 mmol, 18 mol%). The flask was evacuated and backfilled with N_2 3x before addition of DMF (1.1 mL) and NEt_3 (60 µL). The Schlenk flask was sealed shut and heated to 70 °C overnight. The DMF was removed *in vacuo* and the residue dissolved in DCM (10 mL). Washed with water (3 x 10 mL), dried over Na_2SO_4, and concentrated under reduced pressure. Flash chromatography on silica gel (4% MeOH in DCM) yielded Et*p*H **6** as a reddish orange solid (105.7 mg, 92%).

^{1}H NMR (400 MHz, Chloroform-*d*) δ 9.83 (s, 1H), 8.42 (d, *J* = 1.8 Hz, 1H), 7.63 (dd, *J* = 8.0, 1.8 Hz, 1H), 7.54 – 7.46 (m, 4H), 7.43 (d, *J* = 8.4 Hz, 2H), 7.29 (d, *J* = 16.7 Hz, 2H), 7.22 – 7.13 (m, 2H), 7.09 (d, *J* = 16.2 Hz, 1H), 6.92 (d, *J* = 16.2 Hz, 1H), 6.73 (d, *J* = 8.2 Hz, 2H), 2.99 (s, 6H), 2.86 (qd, *J* = 7.2, 4.3 Hz, 6H, Et_3HN^+ salt), 2.49 (s, 6H), 2.32 – 2.25 (m, 4H), 1.46 (s, 6H), 1.08 (t, J = 7.3 Hz, 9H, Et_3HN^+ salt), 0.95 (t, *J* = 7.4 Hz, 6H). **^{13}C NMR** (400 MHz, Chloroform-*d*) δ 152.4, 143.8, 140.5, 140.1, 138.6, 138.2, 135.5, 132.3, 131.4, 130.4, 129.8, 129.1, 128.4, 127.8, 127.4, 127.2, 126.6, 126.5, 124.1, 112.6, 46.2, 40.6, 29.9, 17.2, 14.9, 12.5, 11.7, 8.32 ppm. **ESI-HR(-)**, calculated for $C_{41}H_{43}BF_2N_3O_3S^-$: 706.3092, found: 706.3074. **Analytical HPLC retention time:** 8.39 min. Estimated purity >99%.

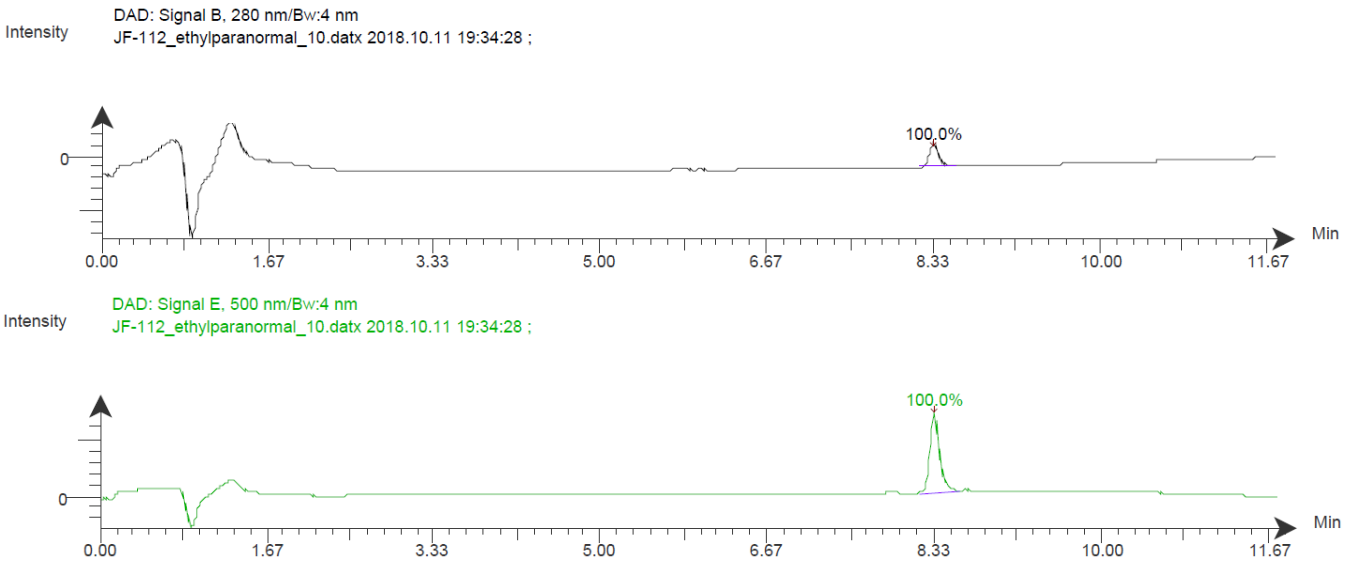

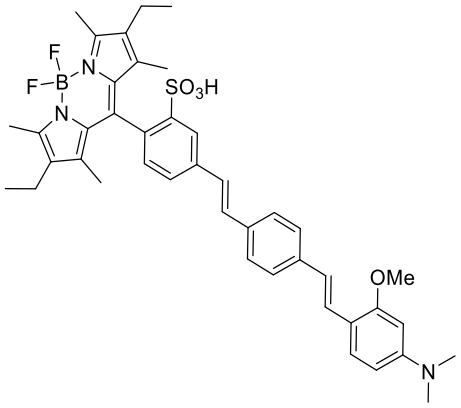

Ethyl BODIPY *p*-methoxy wire (7) To a flame-dried 10 mL Schlenk flask were added 1,3,5,7-tetramethyl-2,6-diethyl-*p*-bromo BODIPY **3** (44.4 mg, 0.08 mmol, 1 eq), methoxy molecular wire **5** (22.6 mg, 0.09 mmol, 1.1 eq), $Pd(OAc)_2$ (1.7 mg, 0.007 mmol, 9 mol%), and P(*o*-tol)$_3$ (4.5 mg, 0.015 mmol, 18 mol%). The flask was evacuated and backfilled with N_2 3x before addition of DMF (0.6 mL) and NEt_3 (300 µL). The Schlenk flask was sealed shut and heated to 70 °C overnight. The DMF was removed *in vacuo* and the residue dissolved in DCM (10 mL). Washed with water (3 x 10 mL), dried over Na_2SO_4, and concentrated under reduced pressure. Flash chromatography on silica gel (4% MeOH in DCM) yielded Et*p*OMe **7** as a reddish orange solid (17.1 mg, 25%).

^{1}H NMR (400 MHz, Chloroform-*d*) δ 8.39 (s, 1H), 7.63 (dd, *J* = 7.9, 1.7 Hz, 1H), 7.55 – 7.40 (m, 6H), 7.26 (apps, 1H), 7.19 – 7.09 (m, 2H), 6.95 (d, *J* = 16.4 Hz, 1H), 6.36 (dd, *J* = 8.7, 2.4 Hz, 1H), 6.23 (d, *J* = 2.4 Hz, 1H), 3.90 (s, 3H), 3.00 (s, 6H), 2.91 – 2.80 (m, 5H, Et_3HN^+ salt), 2.48 (s, 6H), 2.27 (q, *J* = 7.6 Hz, 4H), 1.45 (s, 6H), 1.08 (t, *J* = 7.3 Hz, 7H, Et_3HN^+ salt), 0.95 (t, *J* = 7.5 Hz, 6H). **^{13}C NMR** (600 MHz, Chloroform-*d*) δ 158.2, 152.4, 151.5, 143.5, 140.2, 139.8, 138.8, 138.5, 135.0, 132.2, 131.3, 131.2, 130.4, 129.7, 128.2, 127.3, 127.2, 127.0, 126.4, 126.2, 124.3, 123.9, 115.2, 105.2, 95.6, 77.2, 76.8, 55.4, 46.0, 40.5, 17.0, 14.7, 12.3, 11.6, 8.2 ppm. **ESI-HR(-)**, calculated for $C_{42}H_{45}BF_2N_3O_4S^-$: 736.3197, found: 736.3183. **Analytical HPLC retention time:** 8.63 min. Estimated purity 94%.

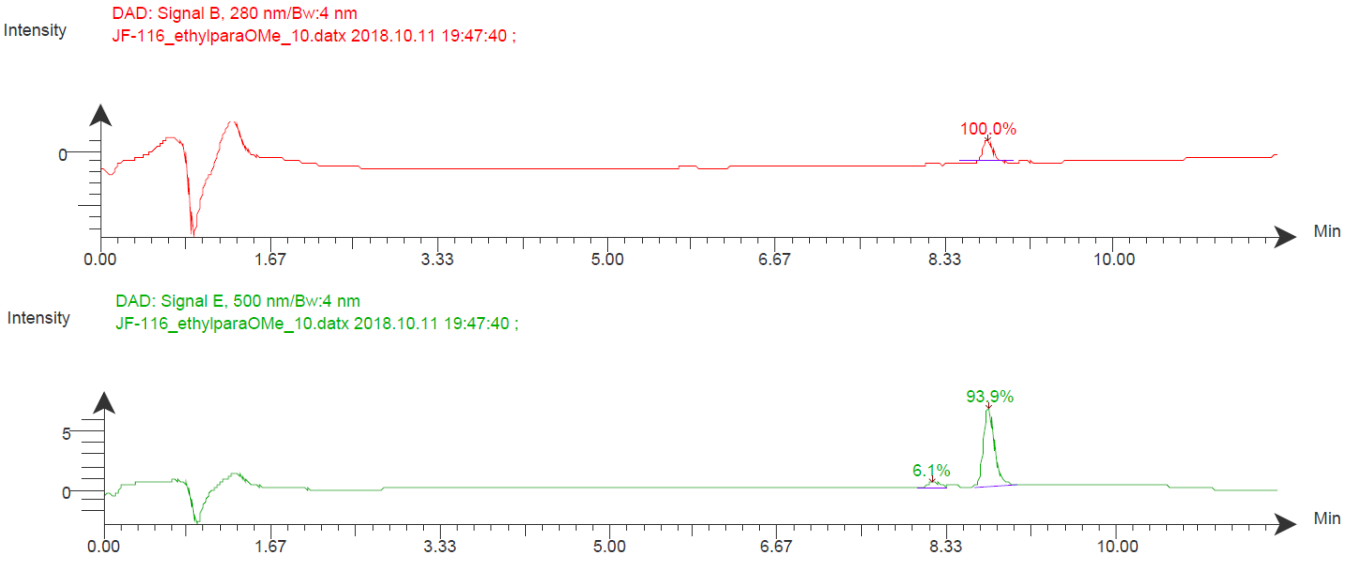

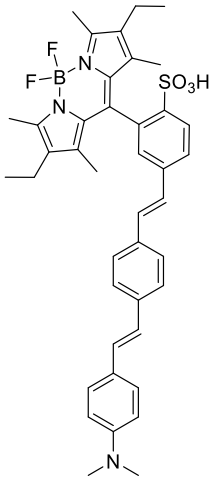

Ethyl BODIPY *m*-normal wire (15) To a flame-dried 10 mL Schlenk flask were added 1,3,5,7-tetramethyl-2,6-diethyl-*m*-bromo BODIPY **12** (51.6 mg, 0.09 mmol, 1 eq), molecular wire **4** (26.2 mg, 0.10 mmol, 1.1 eq), $Pd(OAc)_2$ (1.9 mg, 0.009 mmol, 9 mol%), and P(*o*-tol)$_3$ (5.2 mg, 0.017 mmol, 18 mol%). The flask was evacuated and backfilled with N_2 3x before addition of DMF (660 µL) and NEt_3 (330 µL). The Schlenk flask was sealed shut and heated to 70 °C overnight. The DMF was removed *in vacuo* and the residue dissolved in DCM (10 mL). Washed with water (3 x 10 mL), dried over Na_2SO_4, and concentrated under reduced pressure. Flash chromatography on silica gel (4% MeOH in DCM) yielded Et*m*H **15** as a reddish orange solid (17.3 mg, 26%).

^{1}H NMR (500 MHz, Methanol-d_4) δ 8.06 (d, *J* = 8.3 Hz, 1H), 7.77 (dd, *J* = 8.4, 1.9 Hz, 1H), 7.52 (d, *J* = 8.4 Hz, 2H), 7.47 (d, *J* = 8.4 Hz, 3H), 7.44 – 7.39 (m, 4H), 7.29 (d, *J* = 16.4 Hz, 1H), 7.19 (d, *J* = 16.4 Hz, 1H), 7.09 (d, *J* = 16.2 Hz, 1H), 6.93 (d, *J* = 16.3 Hz, 1H), 6.76 (d, *J* = 8.8 Hz, 3H), 2.96 (s, 8H), 2.47 (s, 6H), 2.34 (q, *J* = 7.5 Hz, 4H), 1.46 (s, 6H), 0.99 (t, *J* = 7.6 Hz, 6H). **^{13}C NMR** (700 MHz, Methanol-d_4) δ 153.5, 151.7, 143.6, 141.9, 141.6, 140.1, 139.7, 136.7, 134.9, 133.3, 132.6, 132.1, 130.5, 130.2, 128.7, 128.7, 128.3, 127.4, 127.3, 126.9, 124.9, 113.9, 40.8, 17.9, 15.1, 12.6, 11.93. **ESI-HR(-)**, calculated for $C_{41}H_{43}BF_2N_3O_3S^-$: 706.3092, found: 706.3077. **Analytical HPLC retention time:** 7.59 min. Estimated purity >99%.

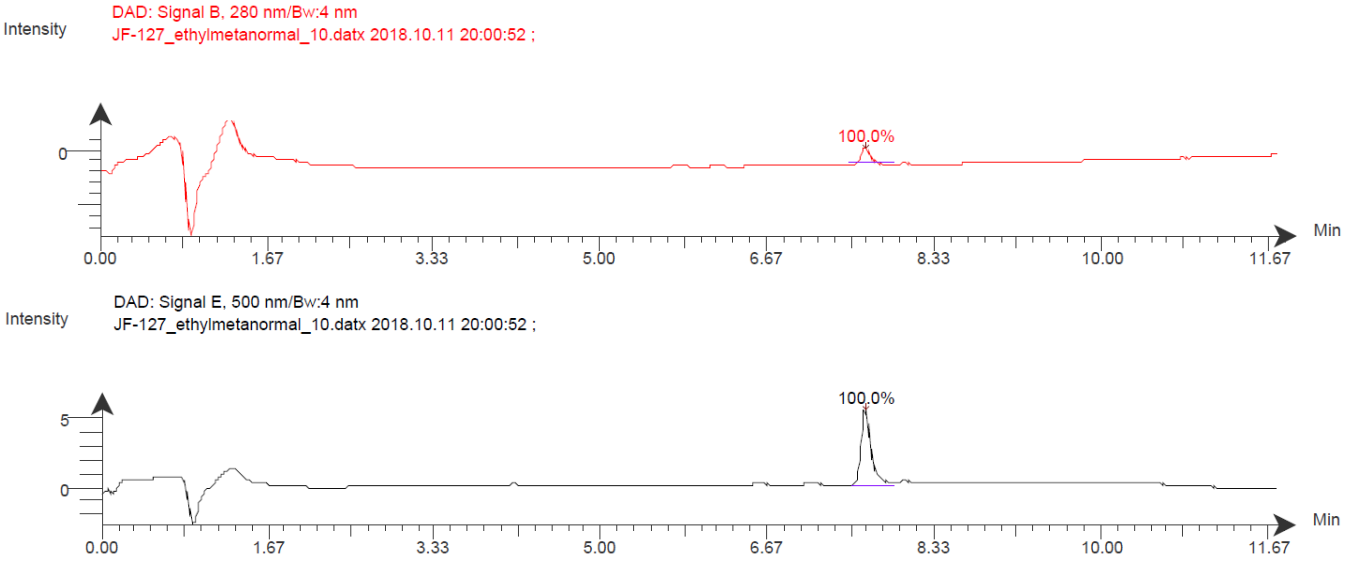

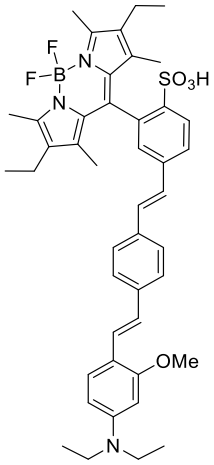

Ethyl BODIPY *m*-methoxy wire (16). To a flame-dried 10 mL Schlenk flask were added 1,3,5,7-tetramethyl-2,6-diethyl-*m*-bromo BODIPY **11** (49.3 mg, 0.09 mmol, 1 eq), methoxy molecular wire **14** (30.9 mg, 0.10 mmol, 1.1 eq), $Pd(OAc)_2$ (1.8 mg, 0.008 mmol, 9 mol%), and P(*o*-tol)$_3$ (5.0 mg, 0.016 mmol, 18 mol%). The flask was evacuated and backfilled with N_2 3x before addition of DMF (660 µL) and NEt_3 (330 µL). The Schlenk flask was sealed shut and heated to 70 °C overnight. The DMF was removed *in vacuo* and the residue dissolved in DCM (10 mL). Washed with water (3 x 10 mL), dried over Na_2SO_4, and concentrated under reduced pressure. Flash chromatography on silica gel (0 – 5% MeOH in DCM, gradient) yielded Et*m*OMe **16** as a reddish orange solid (20.0 mg, 29%).

^{1}H NMR (400 MHz, Methanol-d4) δ 8.06 (d, *J* = 8.3 Hz, 1H), 7.75 (dd, *J* = 8.3, 1.8 Hz, 1H), 7.47 (d, *J* = 8.2 Hz, 2H), 7.44 – 7.34 (m, 6H), 7.26 (d, *J* = 16.4 Hz, 1H), 7.14 (d, *J* = 16.4 Hz, 1H), 6.89 (d, *J* = 16.4 Hz, 1H), 6.33 (d, *J* = 9.1 Hz, 1H), 6.26 (d, *J* = 2.4 Hz, 1H), 3.86 (s, 3H), 3.40 (q, *J* = 7.1 Hz, 4H), 3.07 (q, *J* = 7.3 Hz, 4H), 2.65 (s, 10H), 2.47 (s, 6H), 2.33 (q, *J* = 7.5 Hz, 4H), 1.45 (s, 6H), 1.18 (dt, *J* = 8.6, 7.1 Hz, 12H), 0.98 (t, *J* = 7.5 Hz, 6H). **^{13}C NMR** (400 MHz, MeOD) δ 159.88, 153.62, 150.1, 143.21, 142.05, 141.56, 140.52, 140.25, 136.19, 134.78, 133.36, 132.59, 132.25, 130.43, 128.62, 128.49, 128.27, 127.46, 127.12, 126.56, 125.18, 124.35, 115.6, 106.17, 96.36, 55.87, 47.76, 45.70, 40.43 (DMSO), 17.87, 15.11, 13.00, 12.59, 11.95, 9.09 ppm. **ESI-HR(-)**, calculated for $C_{44}H_{49}BF_2N_3O_4S^-$: 764.3510, found: 764.3492. **Analytical HPLC retention time:** 6.95 min. Estimated purity >99%.

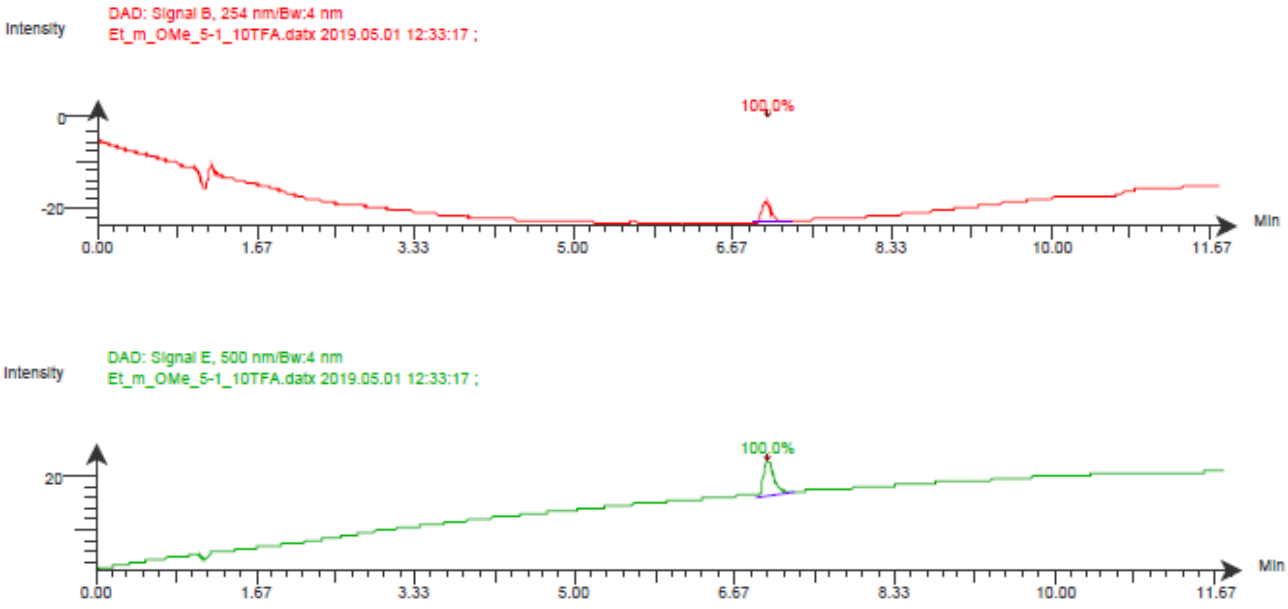

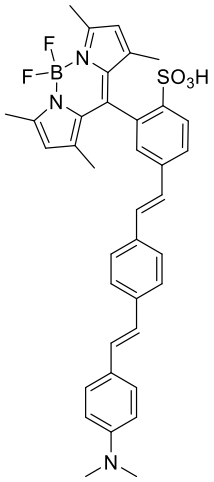

Tetramethyl BODIPY *m*-normal wire (17). To a flame-dried 10 mL Schlenk flask were added 1,3,5,7-tetramethyl-*m*-bromo BODIPY **12** (35.6 mg, 0.07 mmol, 1 eq), molecular wire **4** (18.1 mg, 0.07 mmol, 1.1 eq), $Pd(OAc)_2$ (0.15 mg, 0.0006 mmol, 9 mol%), and P(*o*-tol)$_3$ (0.4 mg, 0.0013 mmol, 18 mol%). The flask was evacuated and backfilled with N_2 3x before addition of DMF (440 µL) and NEt_3 (220 µL). The Schlenk flask was sealed shut and heated to 70 °C overnight. The DMF was removed *in vacuo* and the residue dissolved in DCM (10 mL). Washed with water (3 x 10 mL), dried over Na_2SO_4, and concentrated under reduced pressure. Flash chromatography on silica gel (0 – 4% MeOH in DCM, gradient) yielded TM*m*H **17** as an orange solid (23.1 mg, 56%).

^{1}H NMR (900 MHz, Methanol-*d*$_4$) δ 8.06 (d, *J* = 8.2 Hz, 1H), 7.77 (dd, *J* = 8.3, 1.9 Hz, 1H), 7.55 – 7.52 (m, 2H), 7.48 (dd, *J* = 9.3, 2.9 Hz, 2H), 7.43 – 7.39 (m, 3H), 7.30 (d, *J* = 16.3 Hz, 1H), 7.20 (d, *J* = 16.3 Hz, 1H), 7.09 (dd, *J* = 16.2, 2.9 Hz, 1H), 6.93 (d, *J* = 16.2 Hz, 1H), 6.77 – 6.73 (m, 2H), 5.99 (s, 2H), 2.96 (d, *J* = 1.6 Hz, 7H), 2.48 (s, 6H), 1.55 (s, 6H). **^{13}C NMR** (900 MHz, Methanol-*d*$_4$) 155.5, 151.9, 144.9, 143.4, 142.9, 142.0, 139.7, 136.6, 134.2, 133.3, 132.2, 130.5, 130.3, 128.7, 128.4, 128.3, 127.3, 126.8, 124.8, 121.6, 113.8, 40.8, 14.8, 14.6 ppm. **ESI-HR(-)**, calculated for $C_{37}H_{35}BF_2N_3O_3S^-$: 650.2466, found: 650.2457. **Analytical HPLC retention time:** 6.65 min. Estimated purity >99%.

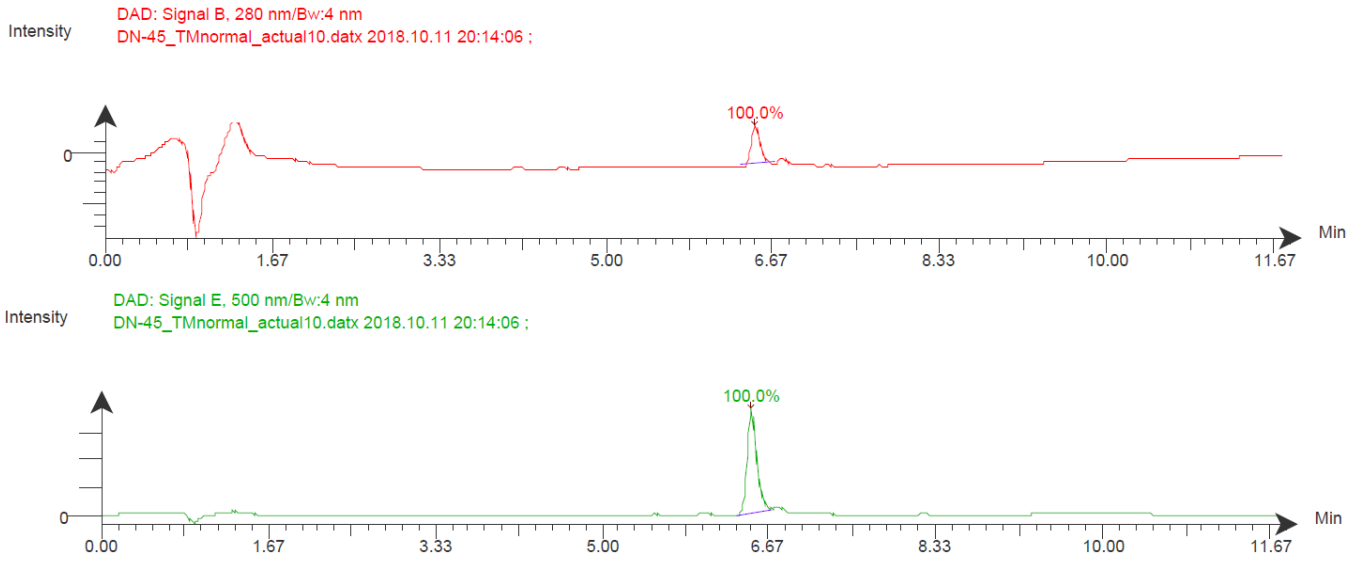

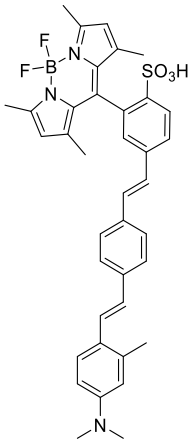

Tetramethyl BODIPY *m*-methyl wire (18). To a flame-dried 10 mL Schlenk flask were added 1,3,5,7-tetramethyl-*m*-bromo BODIPY **12** (50.4 mg, 0.10 mmol, 1 eq), methyl molecular wire **13** (30.2 mg, 0.11 mmol, 1.1 eq), $Pd(OAc)_2$ (1.2 mg, 0.005 mmol, 9 mol%), and P(*o*-tol)$_3$ (3.2 mg, 0.01 mmol, 18 mol%). The flask was evacuated and backfilled with N_2 3x before addition of DMF (700 µL) and NEt_3 (350 µL). The Schlenk flask was sealed shut and heated to 70 °C overnight. The DMF was removed *in vacuo* and the residue dissolved in DCM (10 mL). Washed with water (3 x 10 mL), dried over Na_2SO_4, and concentrated under reduced pressure. Flash chromatography on silica gel (1 – 4% MeOH in DCM, gradient) yielded TM*m*Me **18** as an orange solid (24 mg, 35%).

^{1}H NMR (700 MHz, DMSO-d_6) δ 7.88 (d, J = 8.2 Hz, 1H), 7.70 (d, J = 9.0 Hz, 1H), 7.58 – 7.51 (m, 5H), 7.39 – 7.31 (m, 3H), 7.26 (d, J = 16.4 Hz, 1H), 6.90 (d, J = 16.2 Hz, 1H), 6.59 (d, J = 8.6 Hz, 1H), 6.54 (d, J = 2.7 Hz, 1H), 6.04 (s, 2H), 3.32 (s, 6H), 2.92 (s, 7H), 2.43 (s, 6H), 2.37 (s, 3H), 1.45 (s, 6H). **^{13}C NMR** (900 MHz, DMSO-d_6) δ 152.8, 149.9, 144.9, 143.0, 138.5, 137.8, 136.5, 135.2, 131.5, 129.5, 128.9, 126.9, 126.5, 126.3, 126.2, 126.1, 125.9, 124.4, 123.7, 120.2, 113.7, 110.4, 53.4, 48.6, 39.9, 20.1, 18.0, 16.70, 14.1, 13.9 ppm. **ESI-HR(-)**, calculated for $C_{38}H_{37}BF_2N_3O_3S^-$: 664.2622, found: 664.2612. **Analytical HPLC retention time:** 6.50 min. Estimated purity 95%.

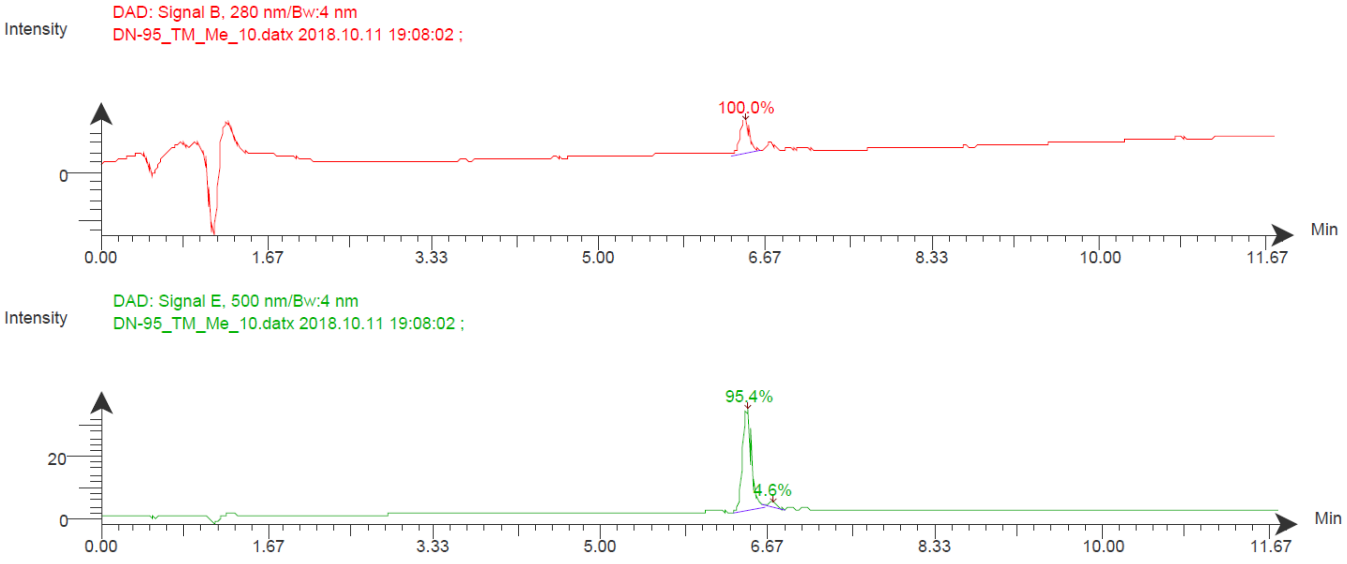

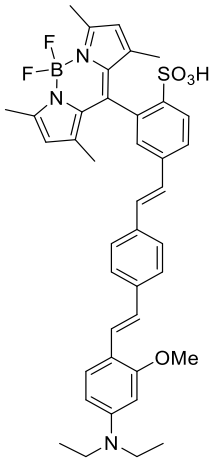

Tetramethyl BODIPY *m*-methoxy wire (19). To a flame-dried 10 mL Schlenk flask were added 1,3,5,7-tetramethyl-*m*-bromo BODIPY **12** (51.1 mg, 0.09 mmol, 1 eq), methoxy molecular wire **14** (30.2 mg, 0.10 mmol, 1.1 eq), $Pd(OAc)_2$ (1.1 mg, 0.005 mmol, 9 mol%), and P(*o*-tol)$_3$ (2.9 mg, 0.01 mmol, 18 mol%). The flask was evacuated and backfilled with N_2 3x before addition of DMF (630 µL) and NEt_3 (310 µL). The Schlenk flask was sealed shut and heated to 100 °C overnight. The DMF was removed *in vacuo* and the residue dissolved in DCM (10 mL). Washed with water (3 x 10 mL), dried over Na_2SO_4, and concentrated under reduced pressure. Flash chromatography on silica gel (0 – 4% MeOH in DCM, gradient) yielded TM*m*OMe **19** as an orange solid (30.5 mg, 62%).

^{1}H NMR (300 MHz, Methanol-d_4) δ 8.06 (d, J = 8.3 Hz, 1H), 7.75 (dd, *J* = 8.4, 1.9 Hz, 1H), 7.48 (d, *J* = 8.2 Hz, 2H), 7.45 – 7.33 (m, 5H), 7.26 (d, *J* = 16.4 Hz, 1H), 7.14 (d, *J* = 16.3 Hz, 1H), 6.89 (d, *J* = 16.5 Hz, 1H), 6.32 (dd, *J* = 8.7, 2.4 Hz, 1H), 6.24 (d, *J* = 2.3 Hz, 1H), 5.99 (s, 2H), 3.86 (s, 3H), 3.40 (q, *J* = 7.0 Hz, 4H), 2.48 (s, 6H), 1.53 (s, 6H), 1.18 (t, *J* = 7.0 Hz, 6H). **^{13}C NMR** (400 MHz, Methanol-d_4) δ 159.9, 155.5, 150.2, 144.9, 143.2, 142.9, 142.0, 140.6, 136.2, 134.1, 133.3, 132.3, 130.4, 128.3, 127.5, 127.1, 126.5, 125.2, 124.2, 121.6, 106.0, 96.2, 55.9, 45.6, 14.63, 14.56, 13.0 ppm. **ESI-HR(-)**, calculated for $C_{40}H_{41}BF_2N_3O_4S^-$: 708.2884, found: 708.2873. **Analytical HPLC retention time:** 6.16 min. Estimated purity 96%.

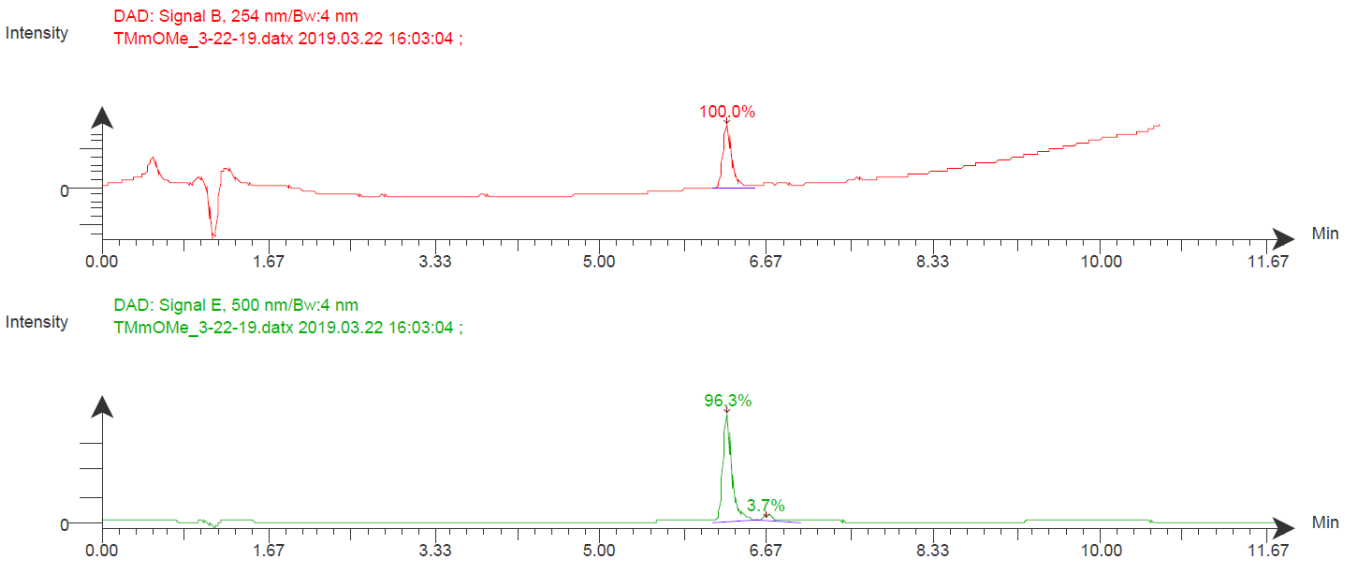

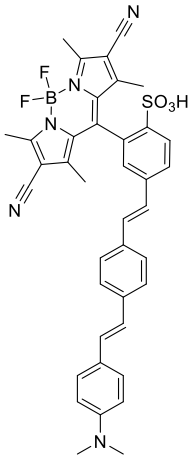

2,6-cyano BODIPY *m*-normal wire (22). To a flame-dried 4 mL dram vial were added 1,3,5,7-tetramethyl-2,6-cyano-*m*-bromo BODIPY **21** (29.2 mg, 0.05 mmol, 1 eq), molecular wire **4** (15.0 mg, 0.06 mmol, 1.1 eq) and $Pd(dba)_2$ (12.5 mg, 0.014 mmol, 25 mol%). The vial was evacuated and backfilled with N_2 3x before addition of 1M $P(tBu)_3$ in toluene (27 µL, 0.03 mmol, 50 mol%) and DMF (1.1 mL). The vial was sealed shut and heated to 70 °C overnight. The DMF was removed *in vacuo* and the residue dissolved in DCM (7 mL) and IPA (3 mL). Washed with water (3 x 10 mL), washed with sat. aq. sodium bicarbonate (10 mL), dried over Na_2SO_4, and concentrated under reduced pressure. Flash chromatography on silica gel (10% MeOH in DCM) yielded CN*m*H **22** as a yellowish solid (2.1 mg, 6%).

^{1}H NMR (400 MHz, Methanol-d_4) δ 8.11 (d, J = 8.3 Hz, 1H), 7.93 – 7.86 (m, 1H), 7.55 (d, J = 8.2 Hz, 2H), 7.52 – 7.45 (m, 3H), 7.45 – 7.32 (m, 3H), 7.23 (d, J = 16.4 Hz, 1H), 7.11 (d, J = 16.2 Hz, 1H), 6.93 (d, J = 16.3 Hz, 1H), 6.76 (d, J = 8.6 Hz, 2H), 2.97 (s, 6H), 2.67 (s, 6H), 1.74 (s, 6H). **^{13}C NMR** (400 MHz, Methanol-d_4) δ 159.6, 151.9, 151.0, 143.0, 142.8, 140.0, 136.5, 133.0, 131.8, 130.8, 130.4, 128.8, 128.7, 128.4, 127.3, 127.0, 126.3, 124.7, 114.7, 113.8, 49.6, 49.4, 49.2, 48.8, 48.6, 48.4, 40.7, 14.0, 13.7 ppm. **ESI-HR(-)**, calculated for $C_{39}H_{33}BF_2N_5O_3S^-$: 700.2371, found: 700.2356. **Analytical HPLC retention time:** 6.94 min. Estimated purity >99%.

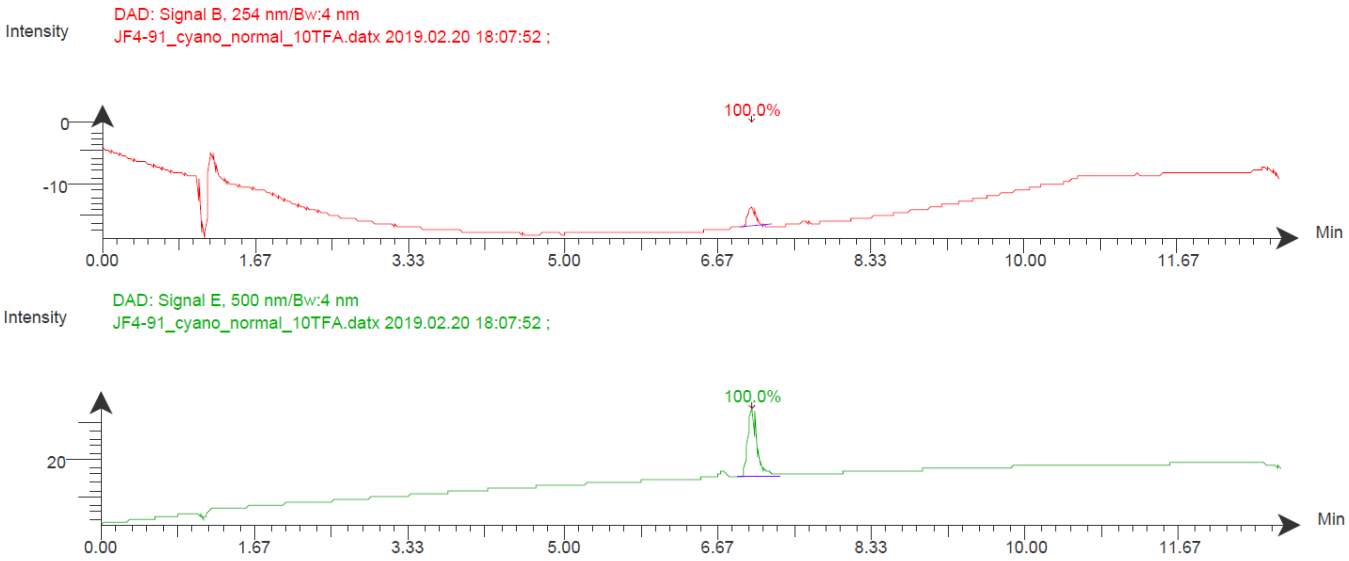

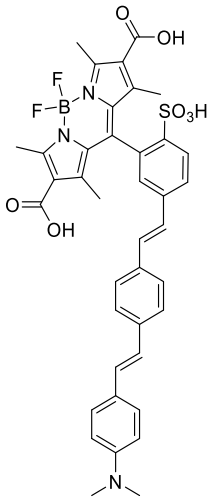

2,6-carboxy BODIPY m-normal wire (28). To a flame-dried 4 mL dram vial were added 1,3,5,7-tetramethyl-2,6-carboxy-*m*-bromo BODIPY **24** (42.6 mg, 0.07 mmol, 1 eq), molecular wire **4** (20.5 mg, 0.08 mmol, 1.1 eq) and $Pd_2(dba)_2$ (13.7 mg, 0.014 mmol, 20 mol%). The vial was evacuated and backfilled with N_2 3x before addition of 1M $P(tBu)_3$ in toluene (30 µL, 0.03 mmol, 50 mol%) and DMF (1.5 mL). The vial was sealed shut and heated to 70 °C overnight. The DMF was removed *in vacuo*. Preparatory thin layer chromatography (12% MeOH + 1% AcOH in DCM) yielded carboxy*m*H **28** as a yellow-orange solid (3.1 mg, 6%). This material was 93% pure by analytical HPLC. For NMR and spectroscopic characterization, a small amount was further purified by reverse phase preparative HPLC (10-100% MeCN in water, 0.05% formic acid additive).

^{1}H NMR (900 MHz, DMSO-d_6) δ 7.88 (d, *J* = 8.1 Hz, 1H), 7.74 (dd, *J* = 8.4, 1.8 Hz, 1H), 7.57 – 7.50 (m, 4H), 7.46 – 7.41 (m, 3H), 7.39 (d, *J* = 16.4 Hz, 1H), 7.27 (d, *J* = 16.4 Hz, 1H), 7.16 (d, *J* = 16.3 Hz, 1H), 6.96 (d, *J* = 16.3 Hz, 1H), 6.72 (d, *J* = 8.5 Hz, 2H), 2.93 (s, 7H), 2.71 (s, 6H), 1.73 (s, 6H). **ESI-HR(-)**, calculated for $C_{39}H_{35}BF_2N_3O_7S^-$: 738.2262, found: 738.2241. **Analytical HPLC retention time:** 5.30 min. Estimated purity >99%.

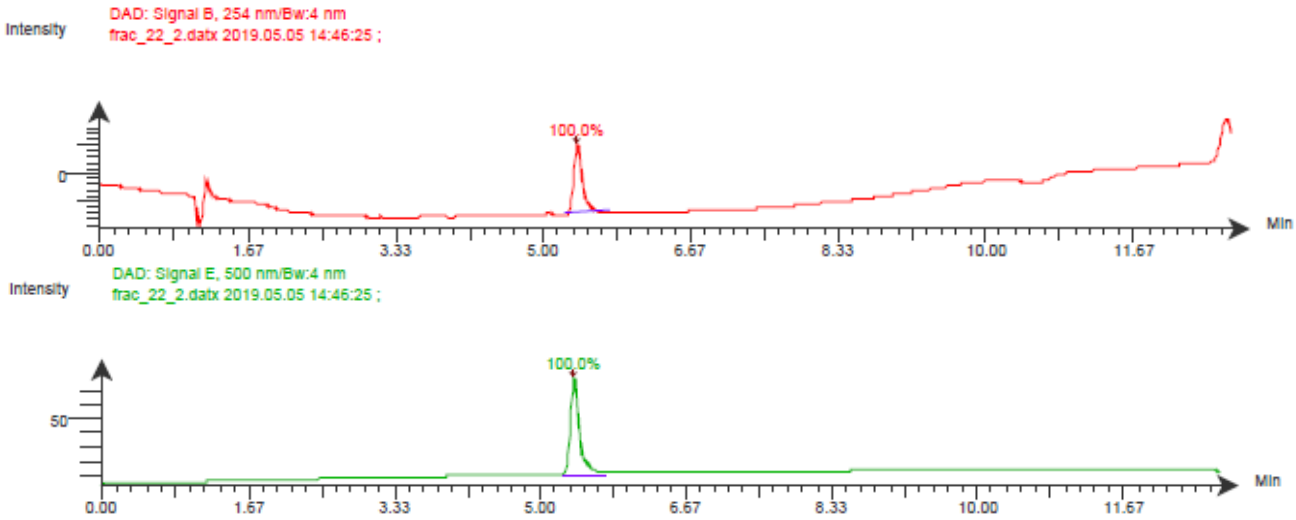

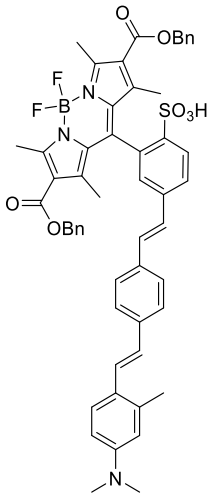

OBn methyl wire (26). To a flame-dried 10 mL Schlenk flask were added OBn BODIPY **24** (107 mg, 0.1 mmol, 1 eq), methoxy molecular wire **14** (41.3 mg, 0.16 mmol, 1.1 eq), $Pd(OAc)_2$ (2.9 mg, 0.013 mmol, 9 mol%), and P(*o*-tol)$_3$ (7.8 mg, 0.026 mmol, 18 mol%). The flask was evacuated and backfilled with N_2 3x before addition of DMF (2 mL) and NEt_3 (1 mL). The Schlenk flask was sealed shut and heated to 100 °C overnight. The DMF was removed *in vacuo* and the residue dissolved in DCM (10 mL). Washed with water (3 x 10 mL), dried over Na_2SO_4, and concentrated under reduced pressure. Flash chromatography on silica gel (3 – 7% MeOH in DCM, gradient) yielded OBn*m*Me **26** as an orange solid (39.3 mg, 30%).

^{1}H NMR (900 MHz, Methanol-*d*$_4$) δ 7.98 (d, *J* = 8.2 Hz, 1H), 7.59 (dd, *J* = 8.3, 1.8 Hz, 1H), 7.41 (d, *J* = 8.7 Hz, 1H), 7.34 (s, 4H), 7.30 (d, *J* = 7.1 Hz, 4H), 7.27 (td, *J* = 8.9, 8.1, 2.4 Hz, 6H), 7.25 – 7.21 (m, 2H), 7.16 (d, *J* = 1.7 Hz, 1H), 7.10 (d, *J* = 16.2 Hz, 1H), 6.99 (d, *J* = 16.2 Hz, 1H), 6.75 (d, *J* = 16.0 Hz, 1H), 6.54 (dd, *J* = 8.8, 2.6 Hz, 1H), 6.49 (d, *J* = 2.6 Hz, 1H), 5.16 (s, 4H), 2.86 (s, 6H), 2.74 (s, 7H), 2.32 (s, 3H), 1.69 (s, 6H). **^{13}C NMR** (900 MHz, Methanol-*d*$_4$) δ 165.6, 159.8, 151.6, 149.2, 147.3, 142.9, 142.2, 140.0, 138.0, 137.5, 136.2, 133.3, 133.3, 132.6, 130.7, 129.6, 129.3, 129.2, 128.3, 128.1, 127.7, 127.7, 127.4, 127.2, 126.5, 126.1, 126.0, 122.6, 118.2, 115.3, 112.0, 67.1, 49.9, 40.8, 30.8, 30.8, 30.7, 20.7, 15.42, 15.41, 15.39, 14.5, 14.2 ppm. **ESI-HR(-)**, calculated for $C_{54}H_{49}BF_2N_3O_7S^-$: 932.3358, found: 932.3369. **Analytical HPLC retention time:** 8.91 min.

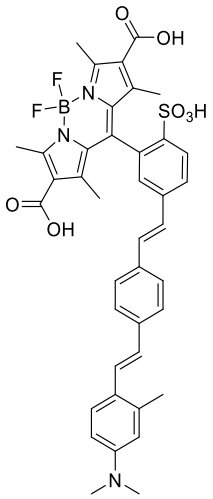

2,6-carboxy BODIPY *m*-Me wire (29). To a flame-dried 10 mL Schlenk flask were added $Pd(OAc)_2$ (1.4 mg, 0.019 mmol, 9 mol%). The flask was evacuated and backfilled with N_2 3x before addition of DCM (230 µL), Et_3SiH (26 µL, 0.161 mmol, 2.4 eq), and NEt_3 (3 µL, 0.019, 28 mol%). The mixture was stirred for 15 minutes at rt, then **26** (62.6 mg, 0.067 mmol, 1 eq) was dissolved in DCM and transferred to the

reaction via syringe (200µL + 200µL rinse). The Schlenk flask was sealed shut at room temperature for 4 hours. The reaction mixture was quenched with saturated aqueous NH_4Cl (2 mL), extracted with DCM (3 x 10 mL), dried over Na_2SO_4, and concentrated under reduced pressure. Preparatory thin layer chromatography (15% MeOH and 1% AcOH in DCM) yielded carboxy*m*Me **29** as a yellow-orange solid (8.8 mg, 31%).

^{1}H NMR (600 MHz, Methanol-d_4) δ 8.07 (d, J = 8.2 Hz, 1H), 7.81 (dd, J = 8.0, 1.6 Hz, 1H), 7.75 (dd, J = 7.8, 5.0 Hz, 1H), 7.57 – 7.43 (m, 6H), 7.35 (d, J = 16.2 Hz, 1H), 7.32 (d, J = 16.4 Hz, 1H), 7.21 (d, J = 8.3 Hz, 1H), 6.87 (d, J = 16.1 Hz, 1H), 6.64 (dd, J = 8.7, 2.8 Hz, 1H), 6.57 (d, J = 2.7 Hz, 1H), 2.94 (s, 6H), 2.74 (s, 7H), 2.39 (s, 3H), 1.80 (s, 6H). **ESI-HR(-)**, calculated for $C_{40}H_{37}BF_2N_3O_7S^-$: 752.2419, found: 752.2411. **Analytical HPLC retention time:** 5.28 min. Estimated purity >99%.

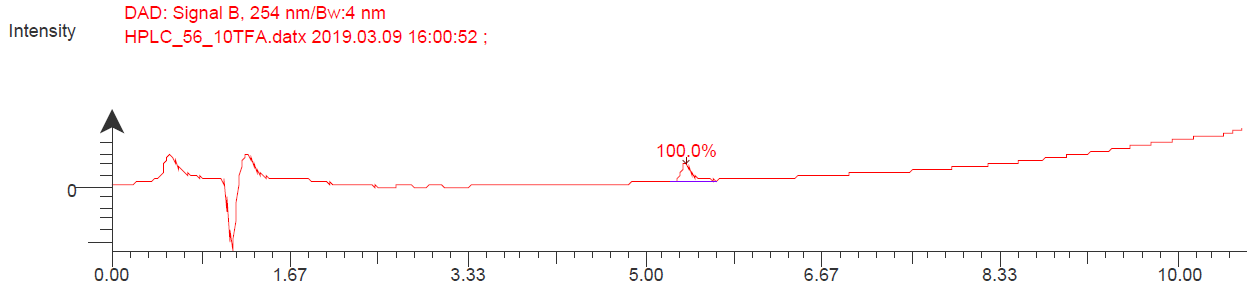

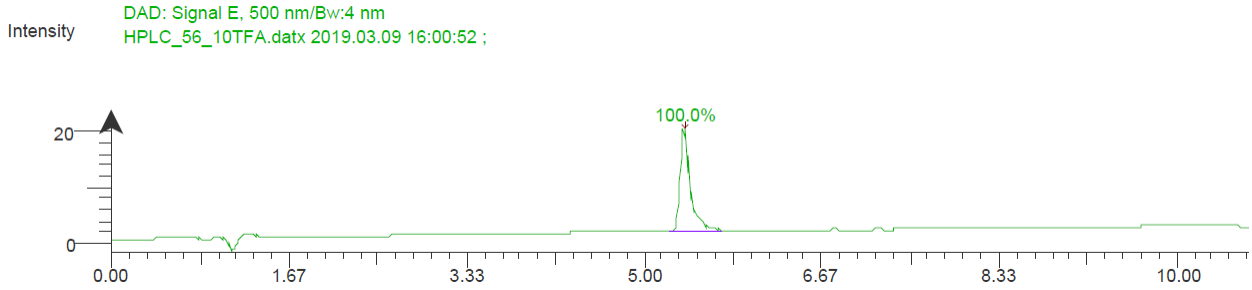

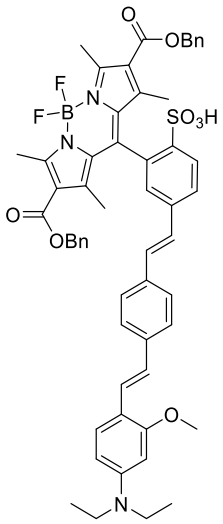

OBn methoxy wire (27). To a flame-dried 25 mL Schlenk flask were added OBn BODIPY **24** (608 mg, 0.81 mmol, 1 eq), methoxy molecular wire **14** (274 mg, 0.89 mmol, 1.1 eq), $Pd(OAc)_2$ (5.5 mg, 0.024 mmol, 3 mol%), and P(*o*-tol)$_3$ (14.8 mg, 0.049 mmol, 6 mol%). The flask was evacuated and backfilled with N_2 3x before addition of DMF (10.8 mL) and NEt_3 (5.4 mL). The schlenk flask was sealed shut and heated to 100 °C overnight. The DMF was removed *in vacuo* and the residue dissolved in DCM (10 mL). Washed with water (3 x 10 mL), dried over Na_2SO_4, and concentrated under reduced pressure. Flash

chromatography on silica gel (4 –10% MeOH in DCM, gradient) yielded OBn*m*OMe **27** as an orange solid (336.8 mg, 43%).

^{1}H NMR (400 MHz, Acetone-d_6) δ 8.06 (d, *J* = 8.3 Hz, 1H), 7.75 (d, *J* = 8.0 Hz, 1H), 7.56 (d, *J* = 8.1 Hz, 2H), 7.30 (s, 17H), 7.27 (d, *J* = 7.9 Hz, 1H), 6.97 (d, *J* = 16.4 Hz, 1H), 6.33 (dd, *J* = 8.7, 2.5 Hz, 1H), 6.29 (d, *J* = 2.4 Hz, 1H), 5.27 (s, 4H), 3.88 (s, 3H), 3.44 (q, *J* = 7.0 Hz, 4H), 2.77 (s, 7H), 1.86 (s, 7H), 1.17 (t, *J* = 7.0 Hz, 6H). **ESI-HR(-)**, calculated for $C_{56}H_{53}BF_2N_3O_8S^-$: 976.3620, found: 976.3606. **Analytical HPLC retention time:** 8.27 min.

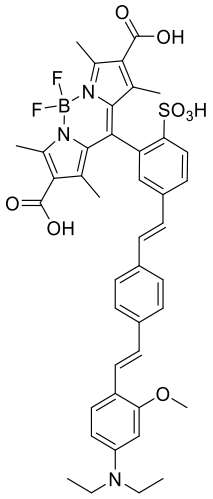

2,6-carboxy BODIPY *m*-methoxy wire (30). To a flame-dried 20 mL scintillation vial was added $Pd(OAc)_2$ (10.4 mg, 0.027 mmol). The vial was evacuated and backfilled with N_2 3x before addition of Et_3SiH (250 µL, 0.9 mmol), NEt_3 (20 µL, 0.086 mmol), and DCM (2.9 mL). This 5x stock solution was stirred at rt for 15 min. To another flame-dried 20 mL scintillation vial equipped with a stir bar was added **27** (67.2 mg, 0.07 mmol, 1 eq). The vial was evacuated and backfilled with N_2 3x before addition of the 1/5 of the stock solution total volume (640 µL). The vial was sealed and stirred at room temperature overnight. The reaction mixture was quenched with saturated aqueous NH_4Cl (3 mL), extracted with 3:1 DCM:IPA (3 x 10 mL), dried over Na_2SO_4, and concentrated under reduced pressure. Flash chromatography on silica gel (5 – 15% MeOH + 1% AcOH in DCM) yielded carboxy*m*OMe **30** as a yellow-orange solid (7.5 mg, 14%).

^{1}H NMR (500 MHz, DMSO-d_6) δ 7.86 (d, *J* = 8.2 Hz, 1H), 7.73 – 7.66 (m, 1H), 7.54 (d, *J* = 8.1 Hz, 2H), 7.43 (t, *J* = 8.4 Hz, 3H), 7.38 – 7.27 (m, 3H), 7.24 (d, *J* = 16.5 Hz, 1H), 6.92 (d, *J* = 16.4 Hz, 1H), 6.28 (dd, *J* = 8.9, 2.3 Hz, 1H), 6.20 (d, *J* = 2.3 Hz, 1H), 3.83 (s, 3H), 2.69 (s, 6H), 1.72 (s, 6H), 1.10 (d, *J* = 7.0 Hz, 6H). **ESI-HR(-)**, calculated for $C_{42}H_{41}BF_2N_3O_8S^-$: 796.2681, found: 796.2669. **Analytical HPLC retention time:** 5.19 min. Estimated purity >99%.

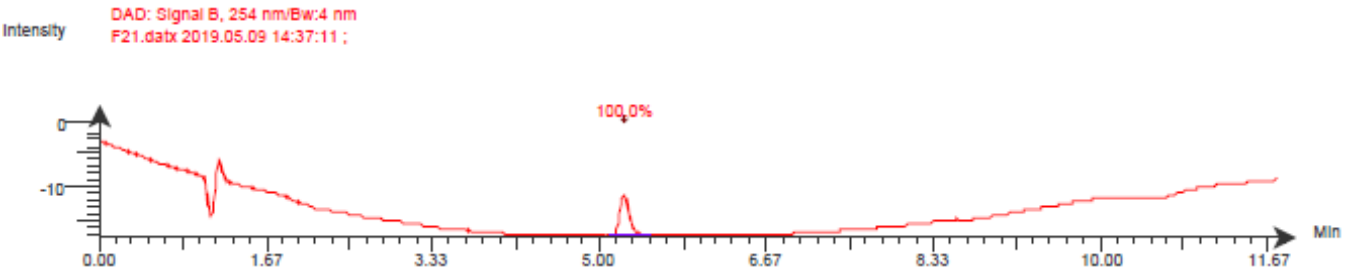

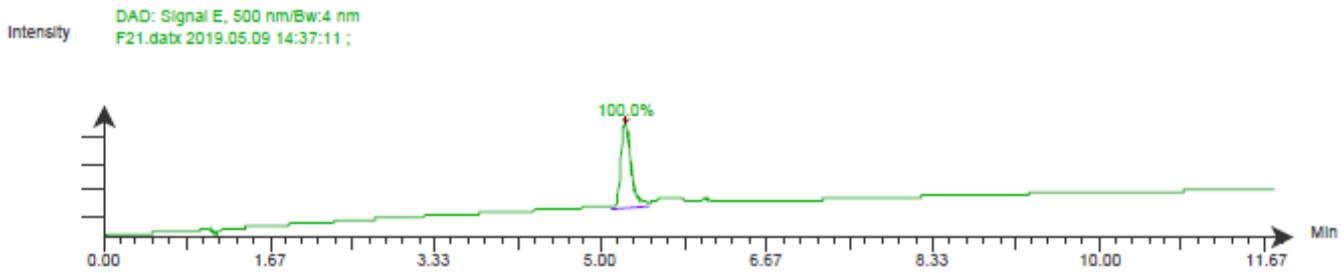

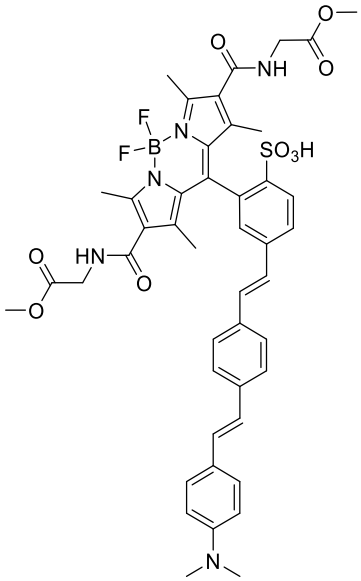

2,6-amide BODIPY *m*-normal wire (35). To a flame-dried 4 mL dram vial were added amide BODIPY **34** (15.6 mg, 0.02 mmol, 1 eq), molecular wire **4** (6.5 mg, 0.03 mmol, 1.1 eq), $Pd(OAc)_2$ (1.2 mg, 0.005 mmol, 25 mol%), and P(*o*-tol)$_3$ (3.3 mg, 0.011 mmol, 50 mol%). The vial was evacuated and backfilled with N_2 3x before addition of DMF (350 µL) and NEt_3 (150 µL). The dram vial was sealed shut and heated to 100 °C overnight. The DMF was removed *in vacuo* and the residue dissolved in DCM (10 mL). Washed with saturated NH_4Cl in water (10 mL), water (3 x 10 mL), dried over Na_2SO_4, and concentrated under reduced pressure. Flash chromatography on silica gel (10% MeOH in DCM) yielded amide*m*H **35** as a yellow-orange solid (4.1 mg, 21%).

^{1}H NMR (500 MHz, DMSO-d_6) δ 7.88 (d, *J* = 8.2 Hz, 1H), 7.74 (d, *J* = 8.5 Hz, 1H), 7.58 – 7.50 (m, 4H), 7.43 (d, *J* = 8.8 Hz, 2H), 7.36 (s, 2H), 7.28 (d, *J* = 16.5 Hz, 1H), 7.16 (d, *J* = 16.3 Hz, 1H), 6.96 (d, *J* = 16.4 Hz, 1H), 6.72 (d, *J* = 8.8 Hz, 2H), 3.99 – 3.86 (m, 4H), 3.62 (s, 6H), 2.93 (s, 6H), 2.55 (s, 6H), 1.55 (s, 6H). **ESI-HR(-)**, calculated for $C_{40}H_{41}BF_2N_3O_4S^-$: 880.3005, found: 880.2984. **Analytical HPLC retention time:** 5.47 min. Estimated purity >99%.

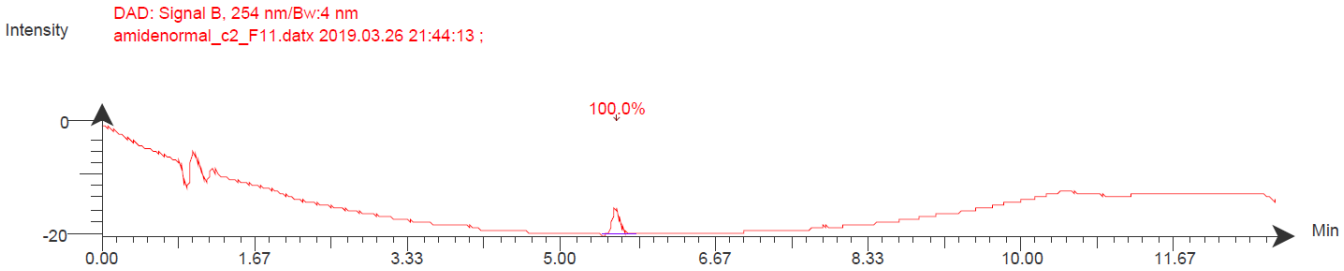

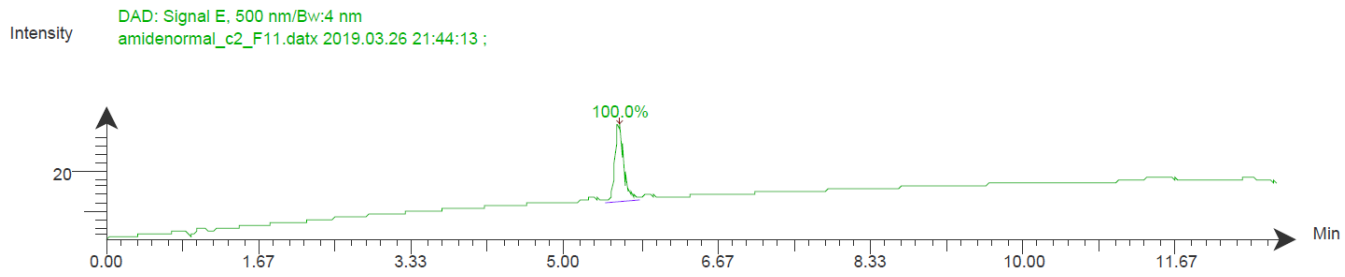

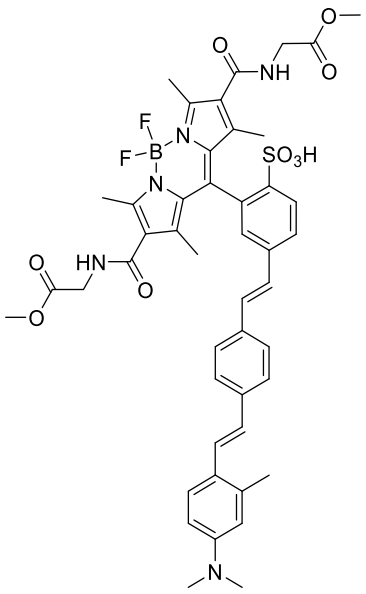

2,6-amide BODIPY m-Me wire (36). To a flame-dried 4 mL dram vial were added amide BODIPY **34** (21.0 mg, 0.03 mmol, 1 eq), methyl molecular wire **13** (9.3 mg, 0.04 mmol, 1.1 eq), $Pd(OAc)_2$ (1.7 mg, 0.007 mmol, 25 mol%), and P(*o*-tol)$_3$ (4.5 mg, 0.015 mmol, 50 mol%). The vial was evacuated and backfilled with N_2 3x before addition of DMF (400 µL) and NEt_3 (300 µL). The dram vial was sealed shut and heated to 100 °C overnight. The DMF was removed *in vacuo* and the residue dissolved in DCM (10 mL). Washed with water (10 mL), and the water layer was extracted with DCM (3 x 10 mL). The organics were combined, washed with brine (1 x 10 mL), dried over Na_2SO_4, and concentrated under reduced pressure. Flash chromatography on silica gel (15%-20% MeOH in DCM) yielded amide*m*Me **6** as a yellow-orange solid (8.7 mg, 34%).

^{1}H NMR (400 MHz, Methanol-*d*$_4$) δ 8.10 (d, *J* = 8.3 Hz, 1H), 7.84 (dd, *J* = 8.4, 1.9 Hz, 1H), 7.59 – 7.46 (m, 6H), 7.35 (dd, *J* = 16.3, 8.3 Hz, 2H), 7.23 (d, *J* = 16.4 Hz, 1H), 6.88 (d, *J* = 16.1 Hz, 1H), 6.64 (dd, *J* = 8.8, 2.7 Hz, 1H), 6.58 (d, *J* = 2.6 Hz, 1H), 4.05 (d, *J* = 2.5 Hz, 4H), 3.72 (s, 6H), 2.95 (s, 6H), 2.62 (s, 6H), 2.40 (s, 3H), 1.68 (s, 6H). **^{13}C NMR** (700 MHz, Methanol-*d*$_4$) δ 171.73, 168.41, 155.64, 151.91, 146.24, 143.29, 142.58, 140.22, 138.07, 136.78, 133.51, 133.15, 132.70, 129.35, 129.33, 128.49, 127.91, 127.82, 127.54, 127.26, 126.78, 126.34, 49.68, 42.17, 40.91, 13.61, 13.31, 13.29. **ESI-HR(-)**, calculated for $C_{46}H_{47}BF_2N_5O_9S^-$: 894.3161, found: 894.3149. **Analytical HPLC retention time:** 5.24 min. Estimated purity >99%.

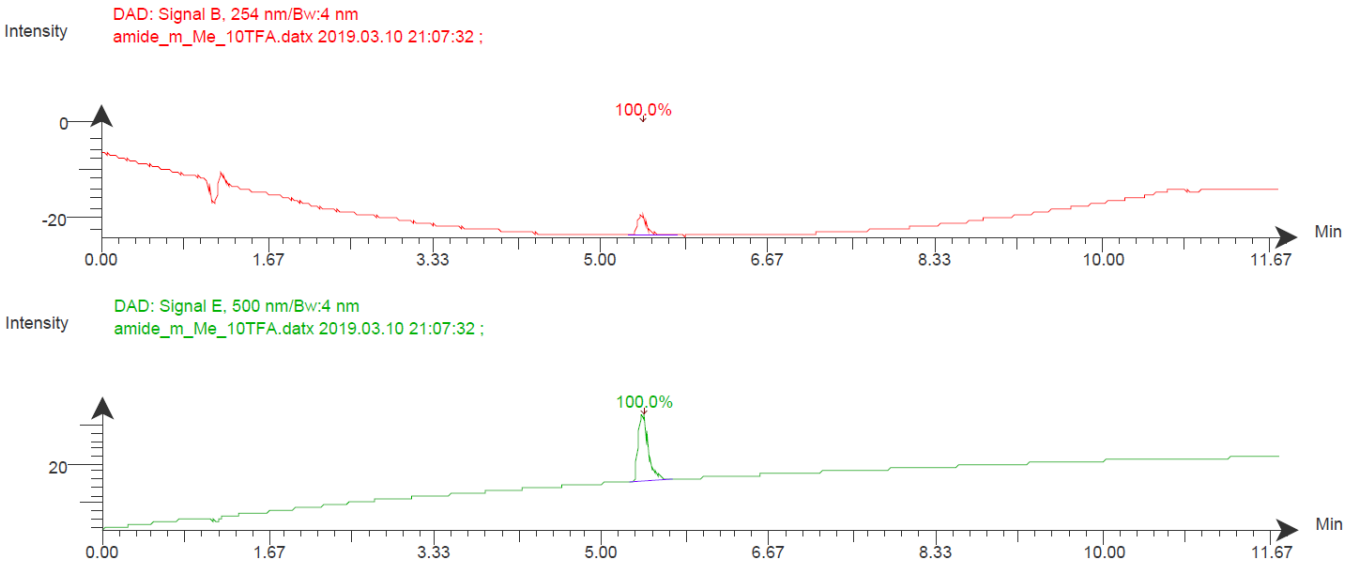
Intensity
DAD: Signal B, 254 nm/Bw:4 nm
amide_m_Me_10TFA.datx 2019.03.10 21:07:32 ;
100.0%
0
-20
0.00
1.67
3.33
5.00
6.67
8.33
10.00
11.67
Min
Intensity
DAD: Signal E, 500 nm/Bw:4 nm
amide_m_Me_10TFA.datx 2019.03.10 21:07:32 ;
100.0%
20
0.00
1.67
3.33
5.00
6.67
8.33
10.00
11.67
Min

Spectra of Compounds

JF3-120_ethylpBrclean.1.fid — AVB-400 ZBO Proton starting parameters. 6/11/03 RN

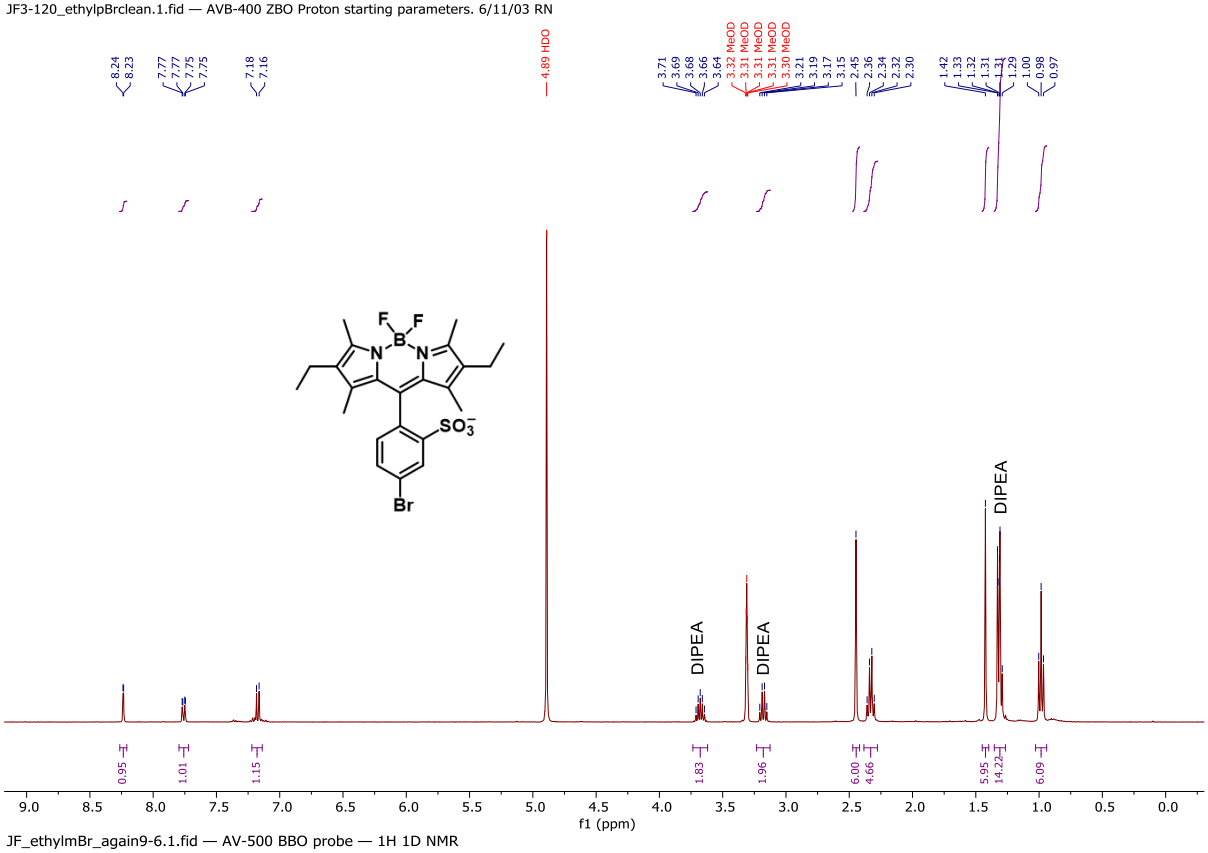

JF_ethylmBr_again9-6.1.fid — AV-500 BBO probe — 1H 1D NMR

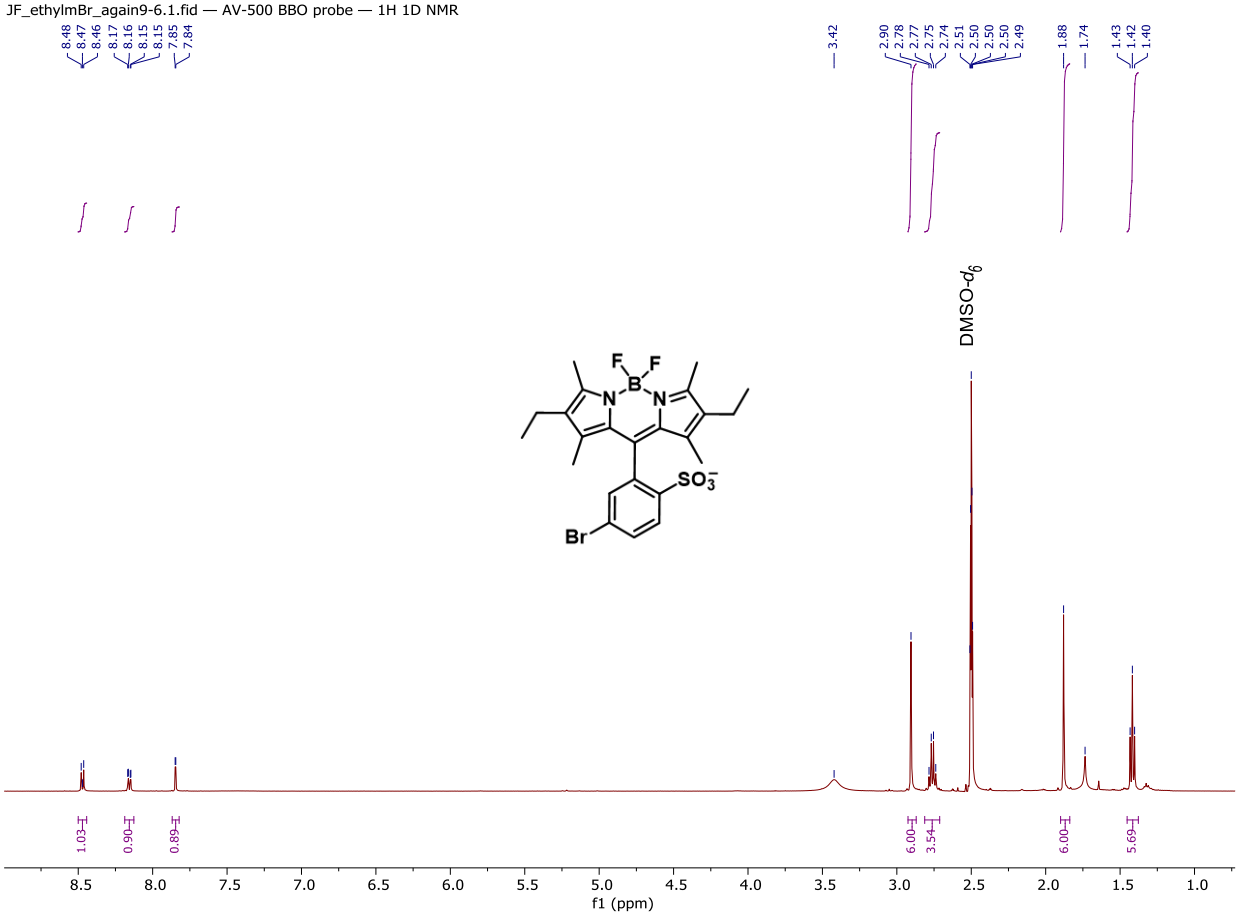

JF_TMmBr_again9-6.1.fid — AV-500 BBO probe — 1H 1D NMR

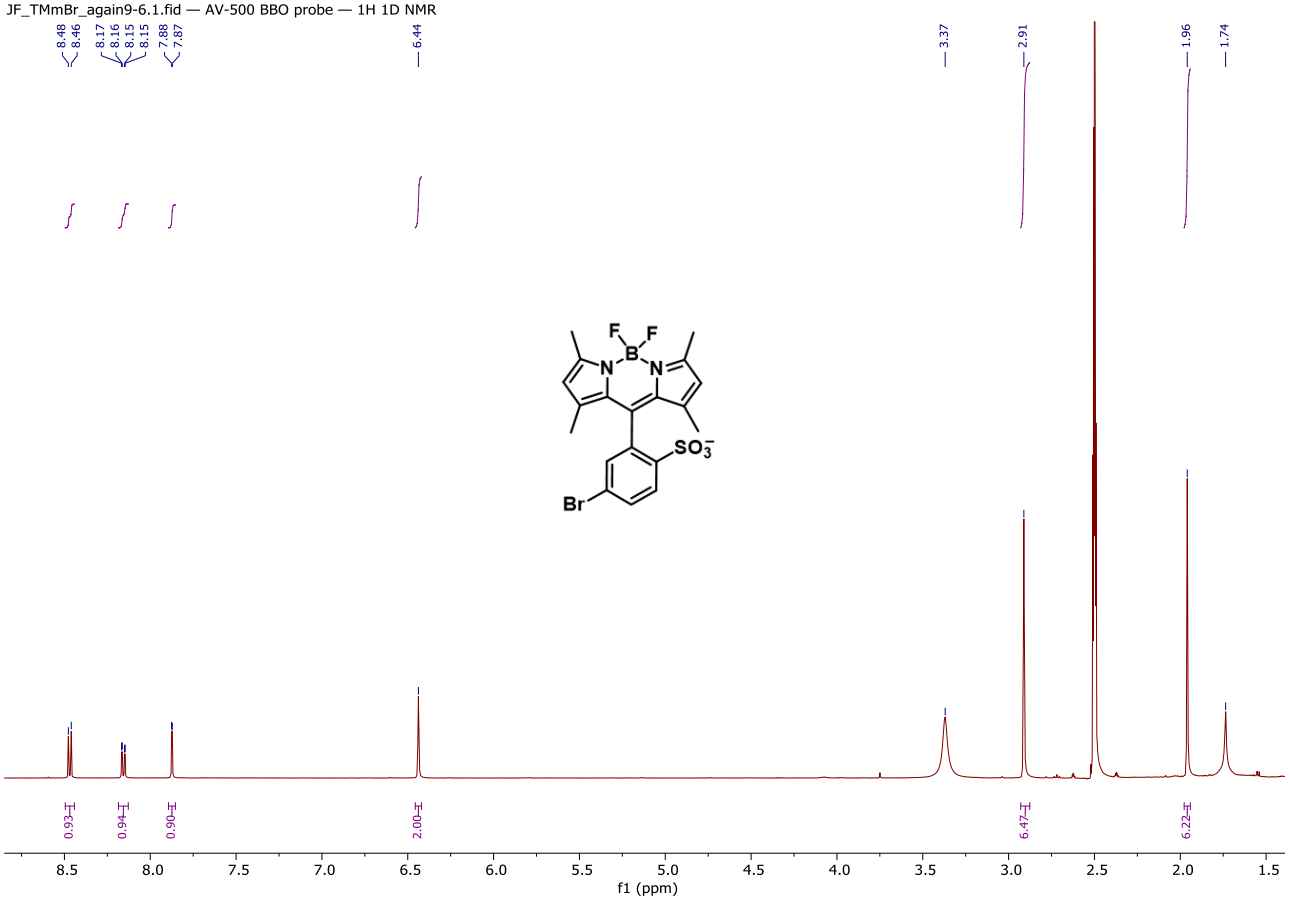

dcBODIPY_FA_HPLC_vial2.1.fid — AVB-400 ZBO Proton starting parameters. 6/11/03 RN

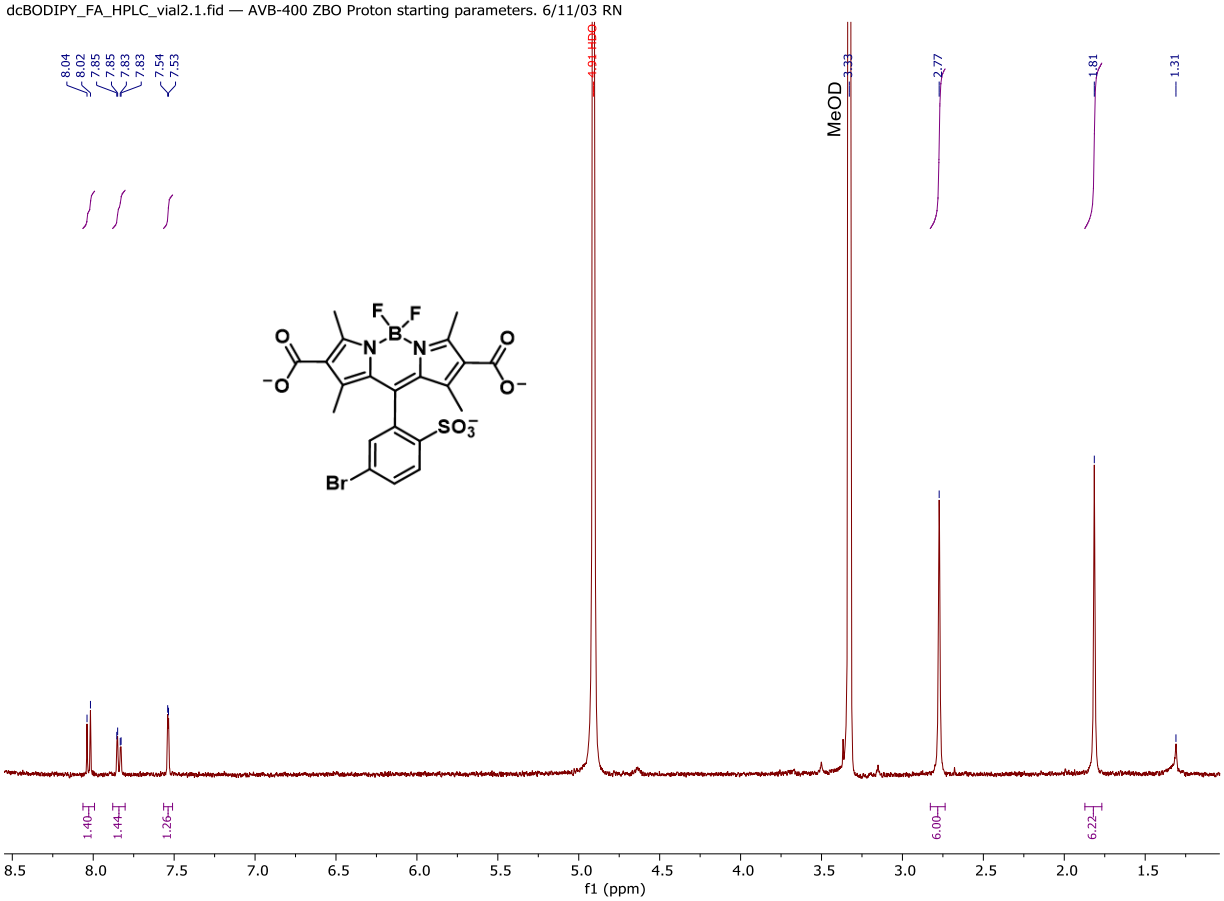

JF3-32_bottom.1.fid — AV-600 ZBO proton starting parameters 11/16/08 RN

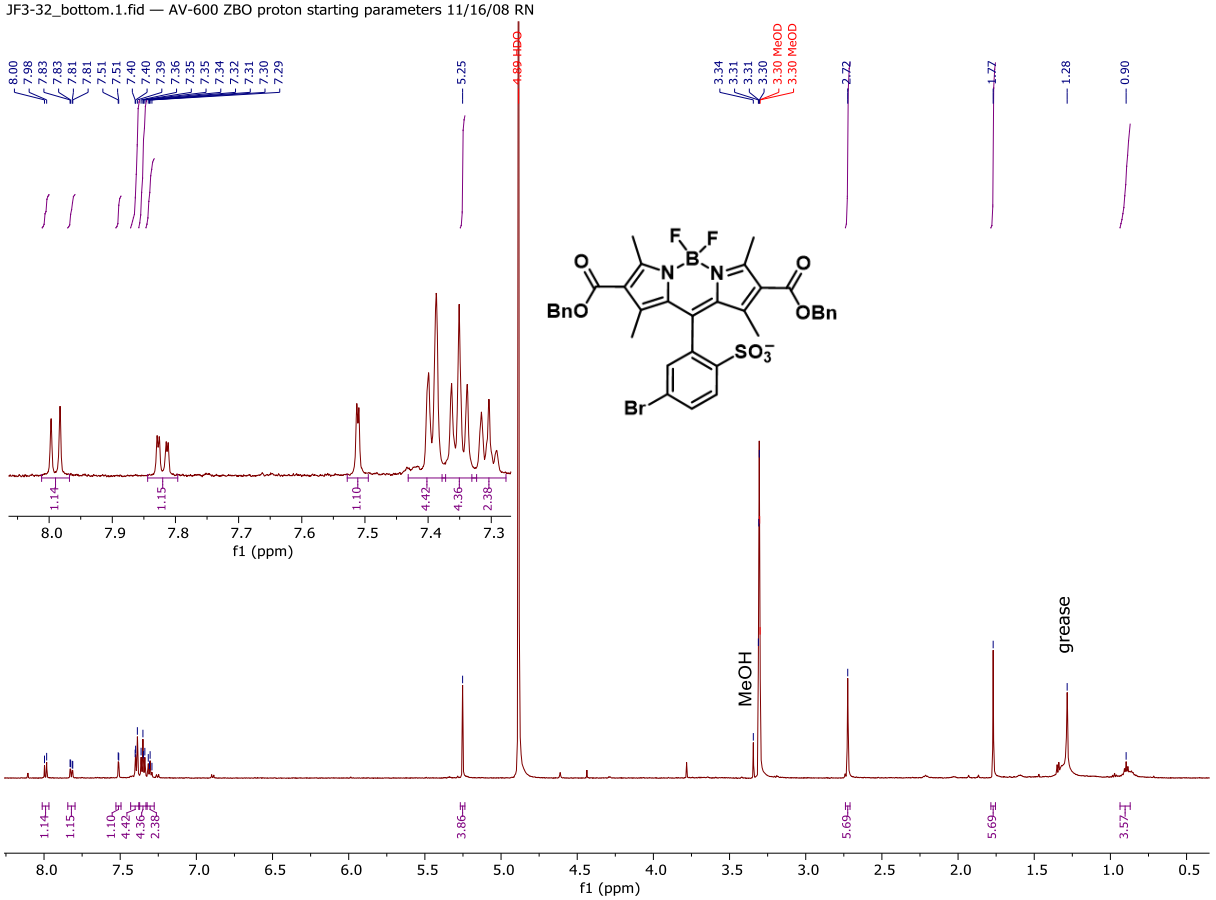

JF4-75_amideHPLCed.1.fid — AV-700 starting parameters for 1D 1H — TXI probe - HC 08/22/2018 — p1=14.88 us @ -6 dB (13 dB attenuator at the amplifier)

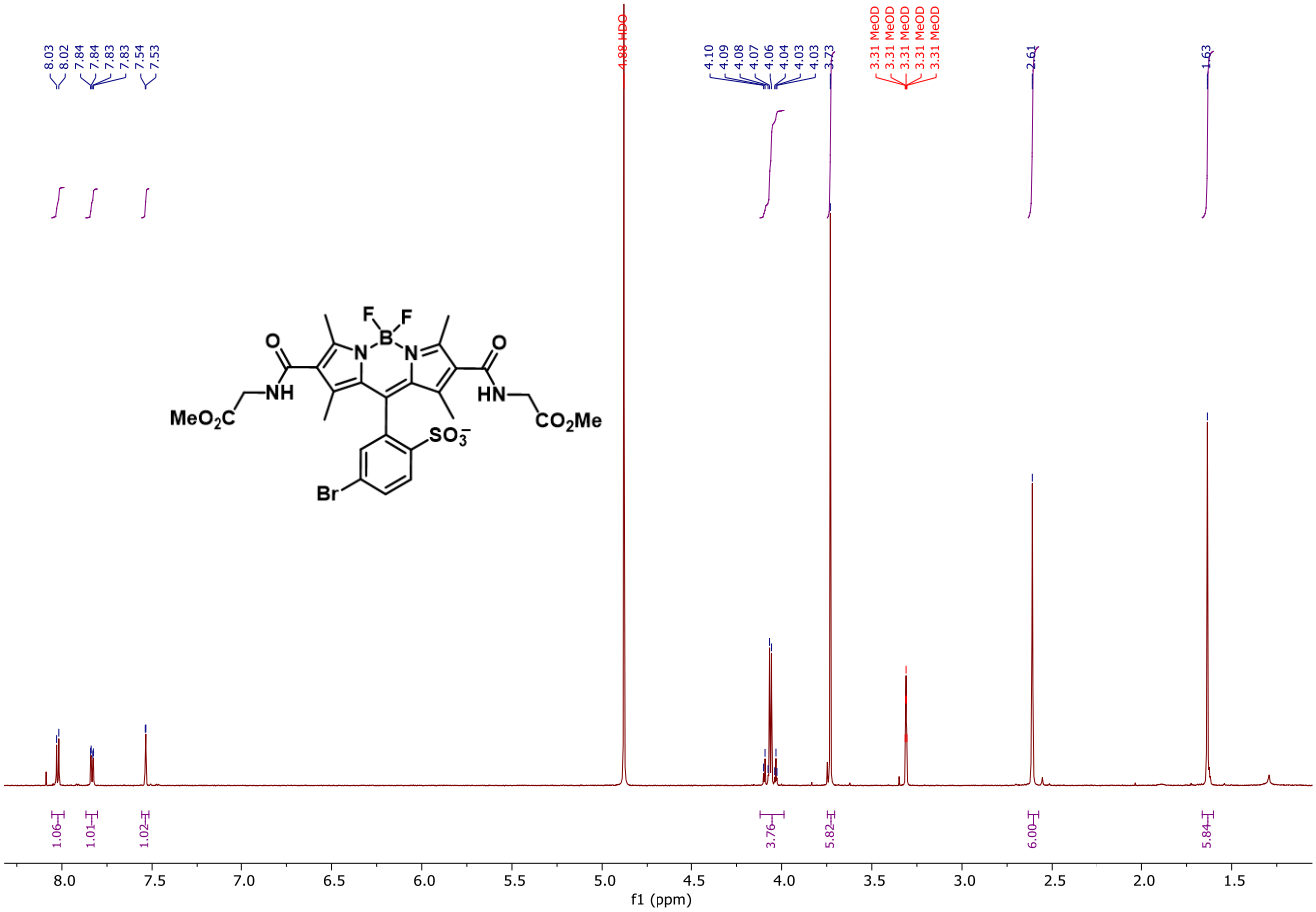

EK-51_cyano_clean.2.fid — AVB-400 ZBO Proton starting parameters. 6/11/03 RN

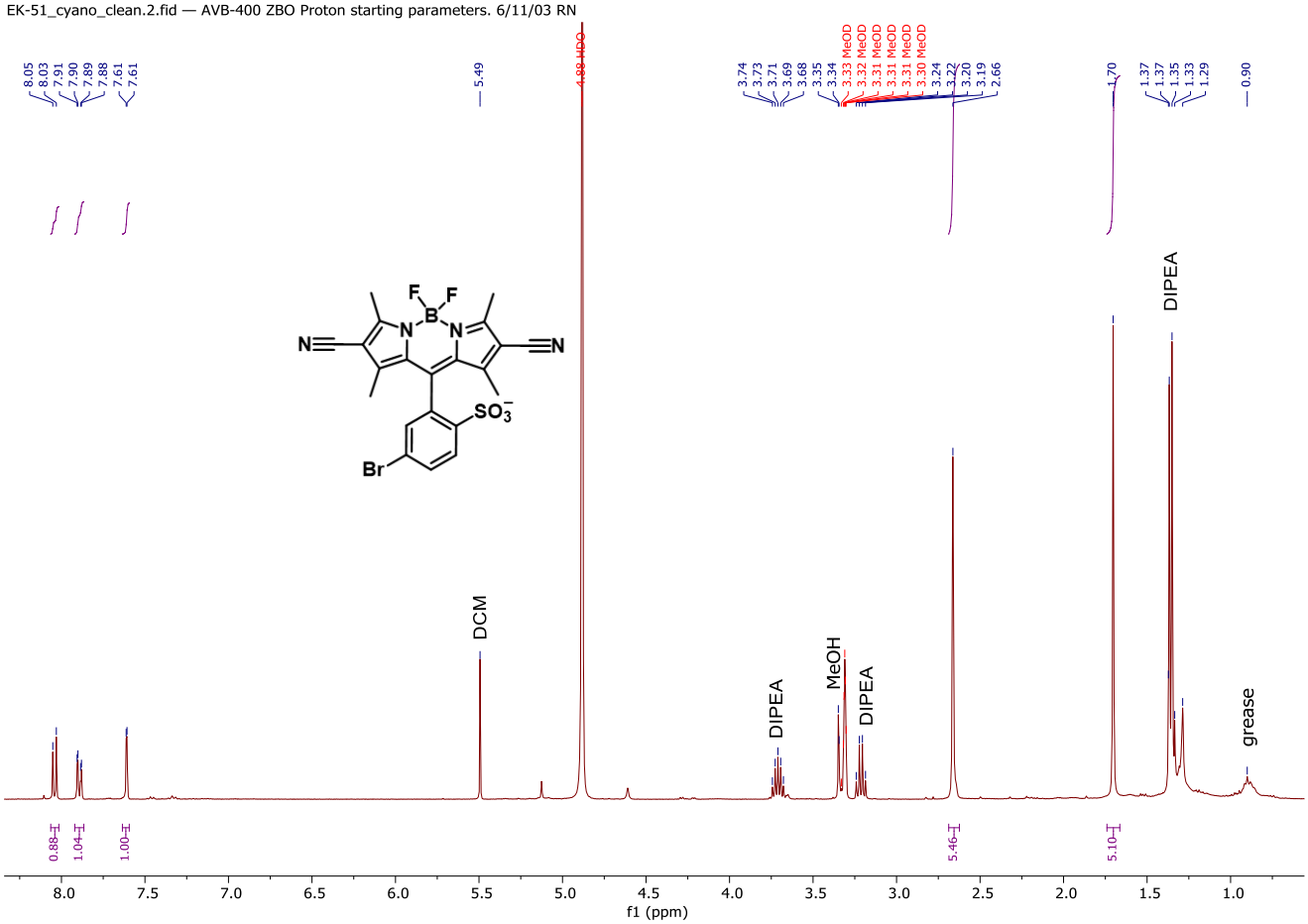

VHpdt1.1.fid — AVB-400 ZBO Proton starting parameters. 6/11/03 RN

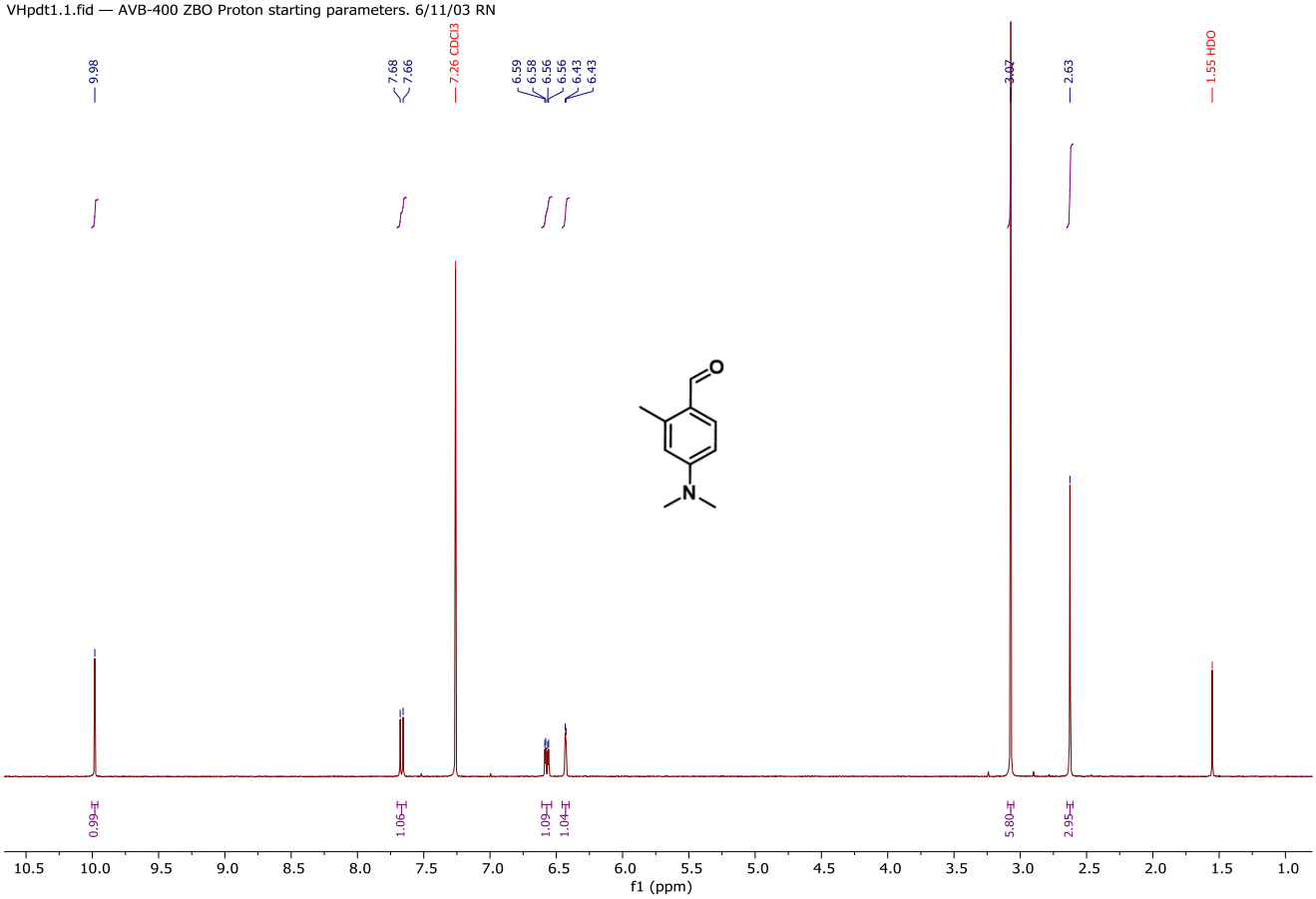

JF4-37_styrene.1.fid
AVQ-400 QNP Proton starting parameters. 7/16/03. Revised 7/22/03 RN

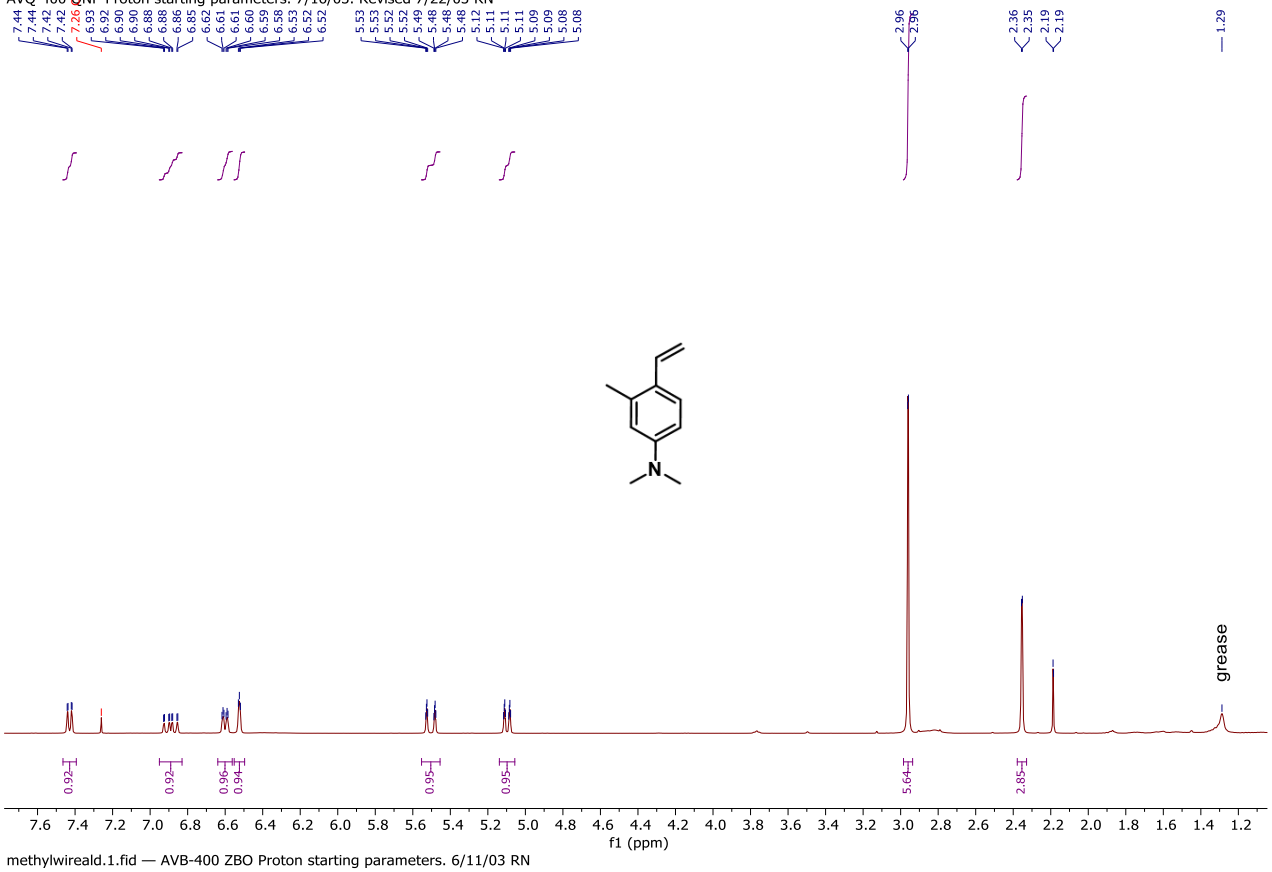

methylwireald.1.fid — AVB-400 ZBO Proton starting parameters. 6/11/03 RN

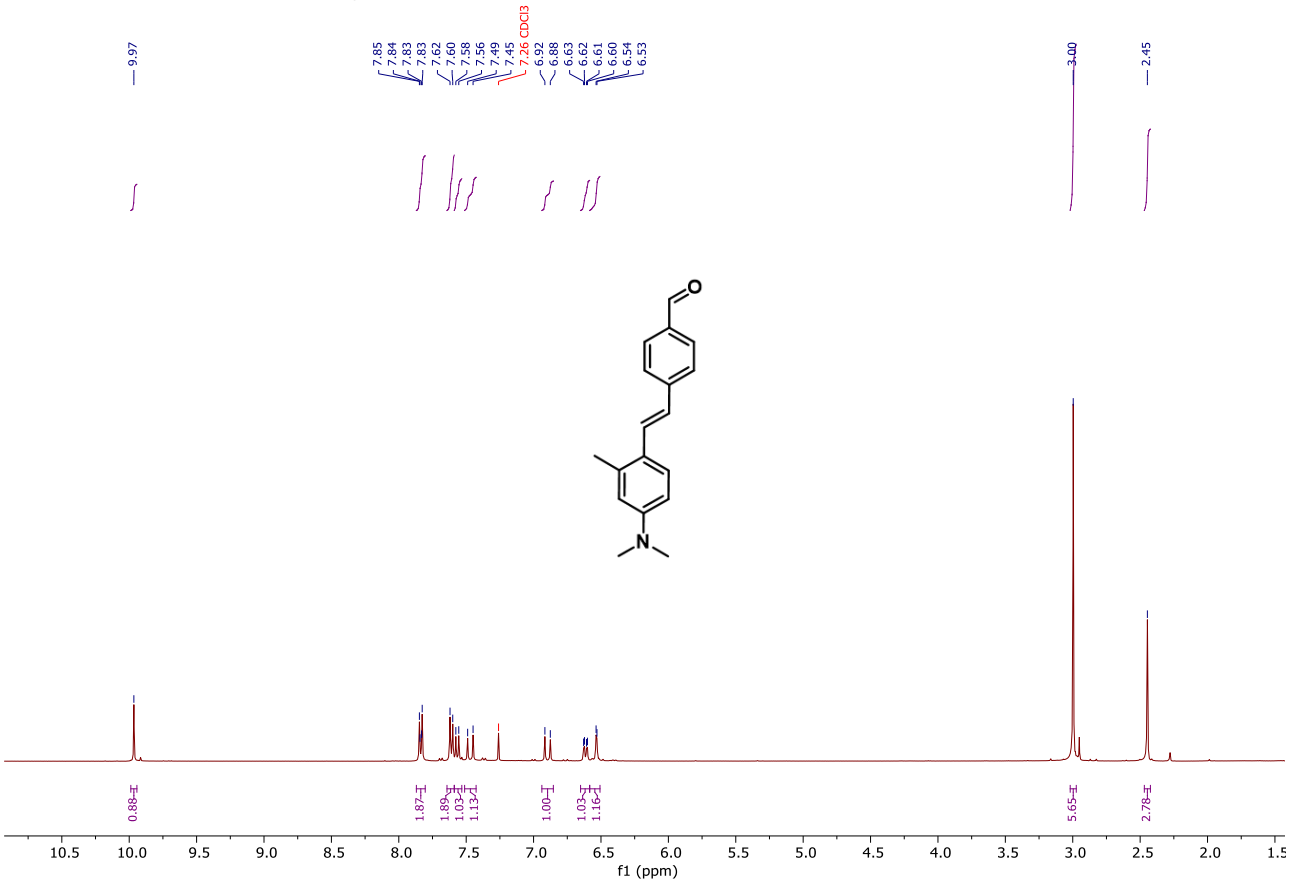

JF-methylwire.1.fid — AVB-400 ZBO Carbon Starting paramters 6/11/03 RN

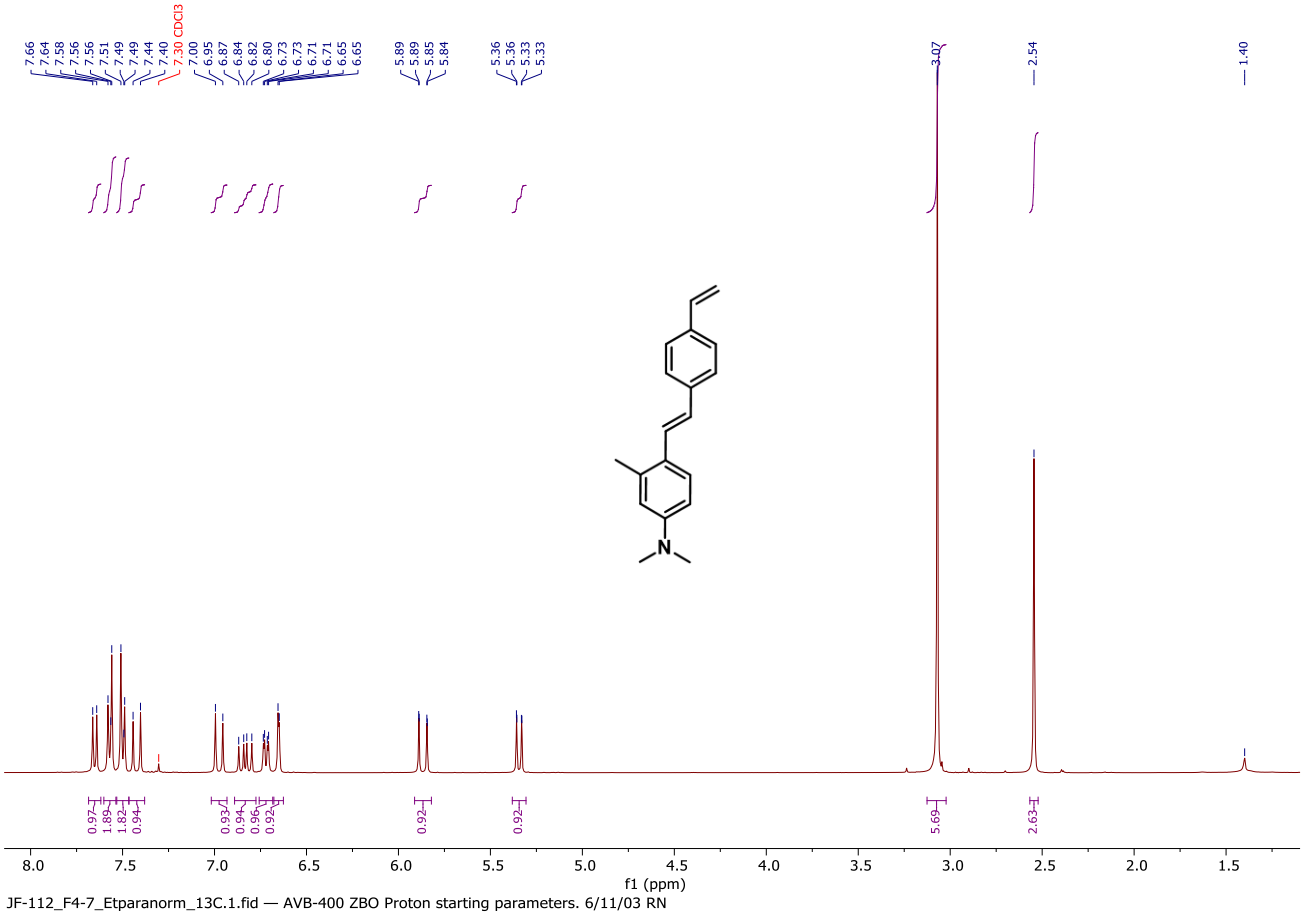

JF-112_F4-7_Etparanorm_13C.1.fid — AVB-400 ZBO Proton starting parameters. 6/11/03 RN

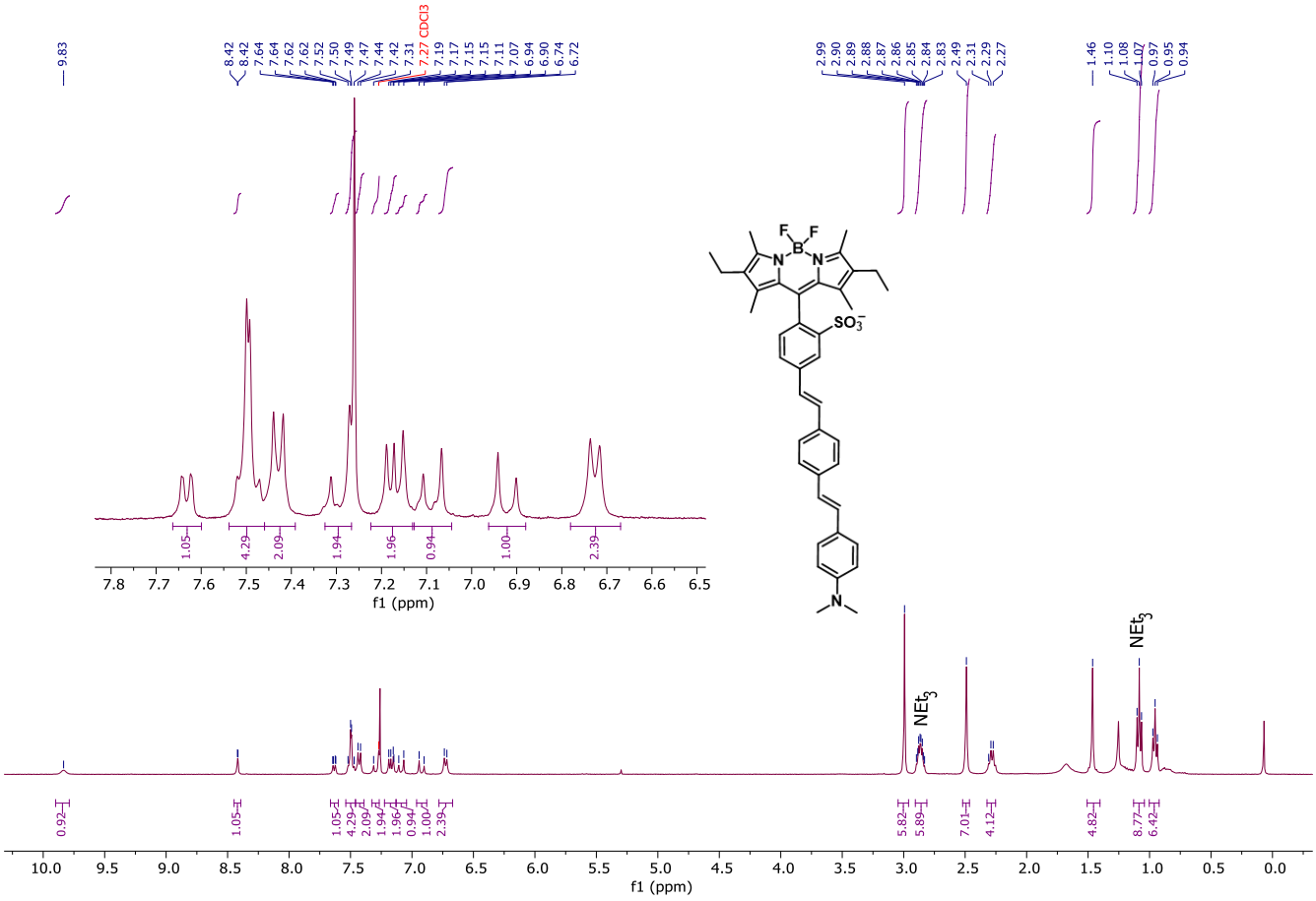

DN-78_EtpOMe.1.fid — AVB-400 ZBO Proton starting parameters. 6/11/03 RN

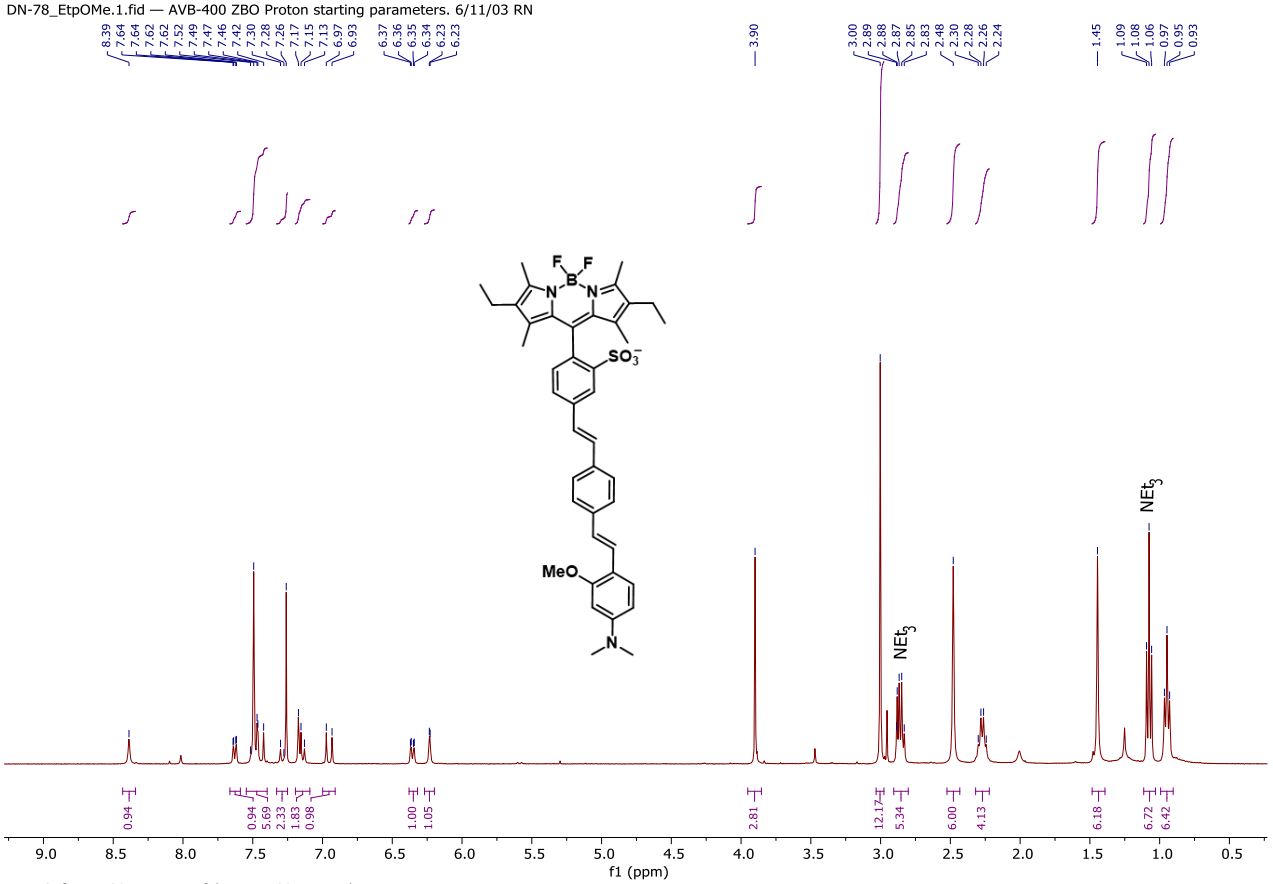

JF4-73_frac15-20_Etmnor.4.fid — AV-500 TBI probe — 1H 1D NMR

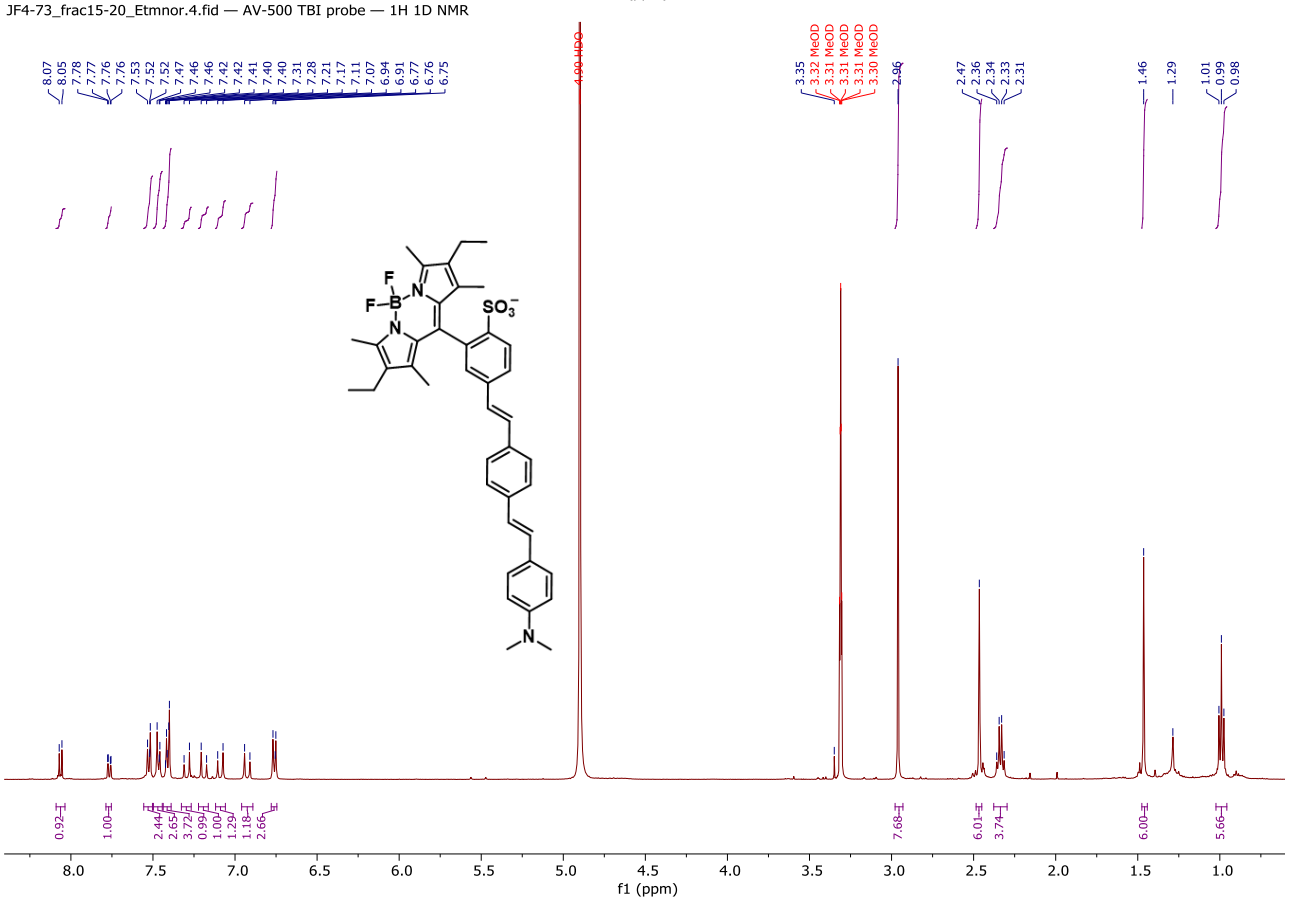

PZ-37_c2_F14-20.1.fid — AVB-400 ZBO Proton starting parameters. 6/11/03 RN

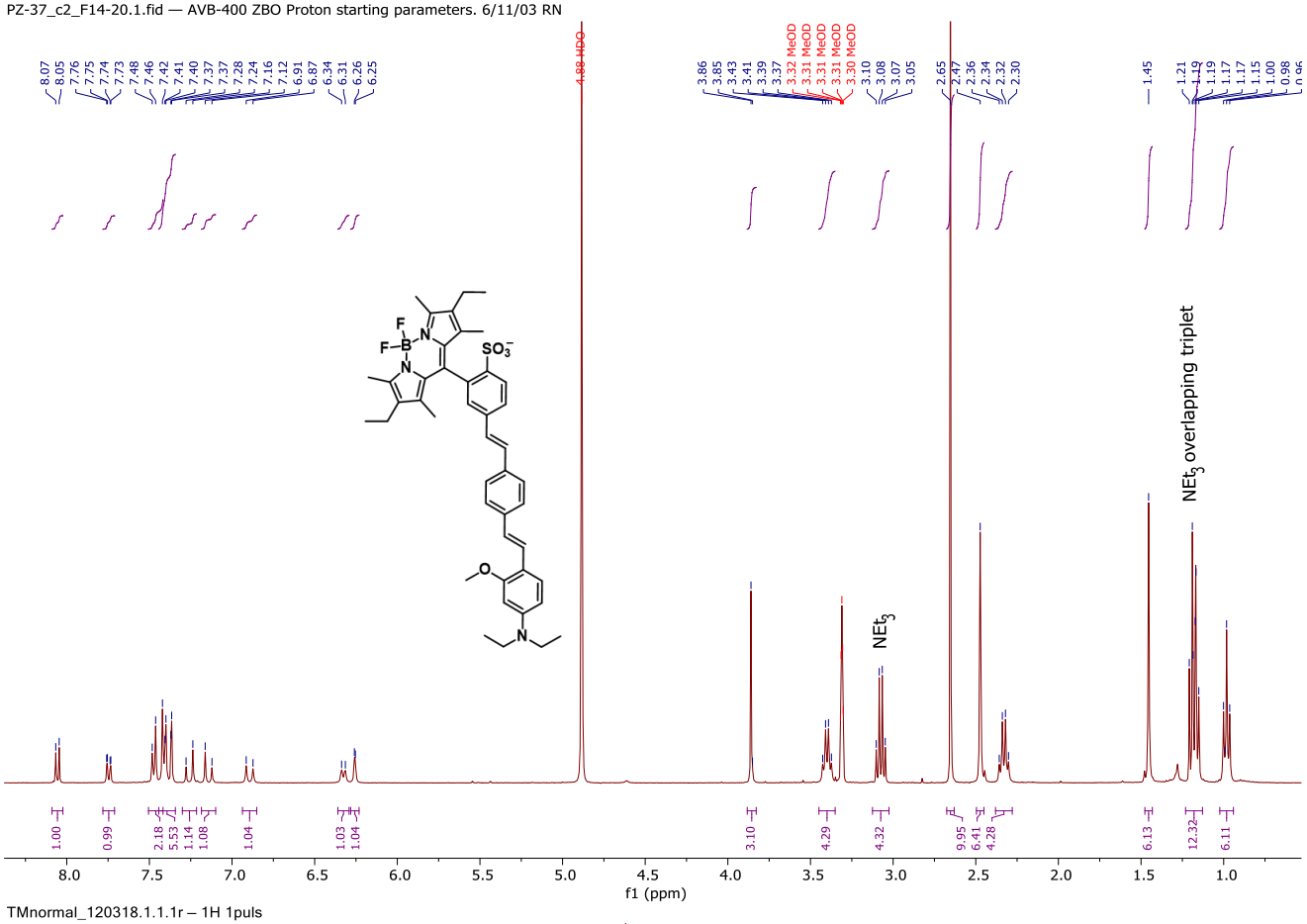

TMnormal_120318.1.1.1r – 1H 1puls

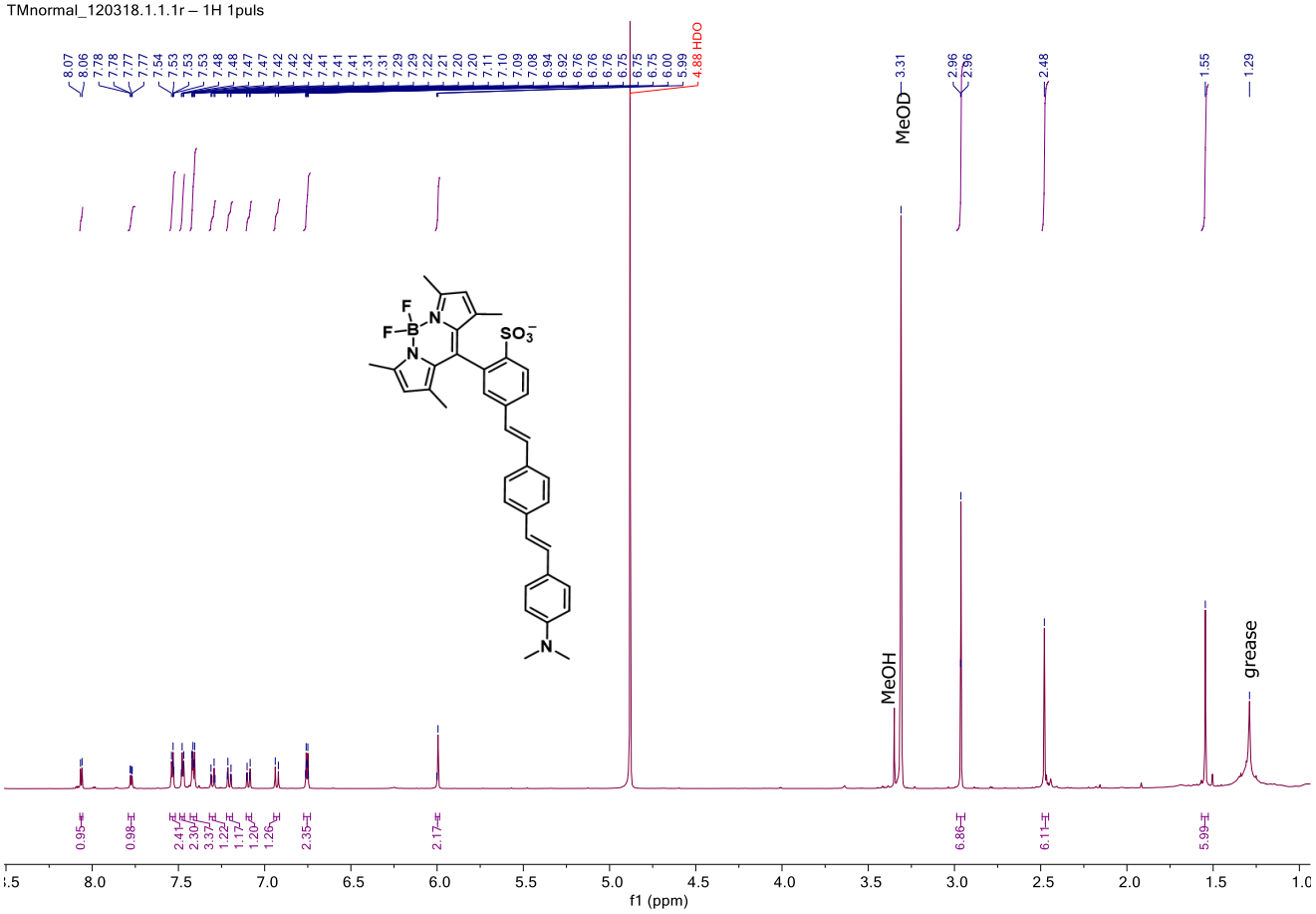

DN-95_c2_TMmMe_DMSO.2.fid — AVQ-400 QNP Proton starting parameters. 7/16/03. Revised 7/22/03 RN

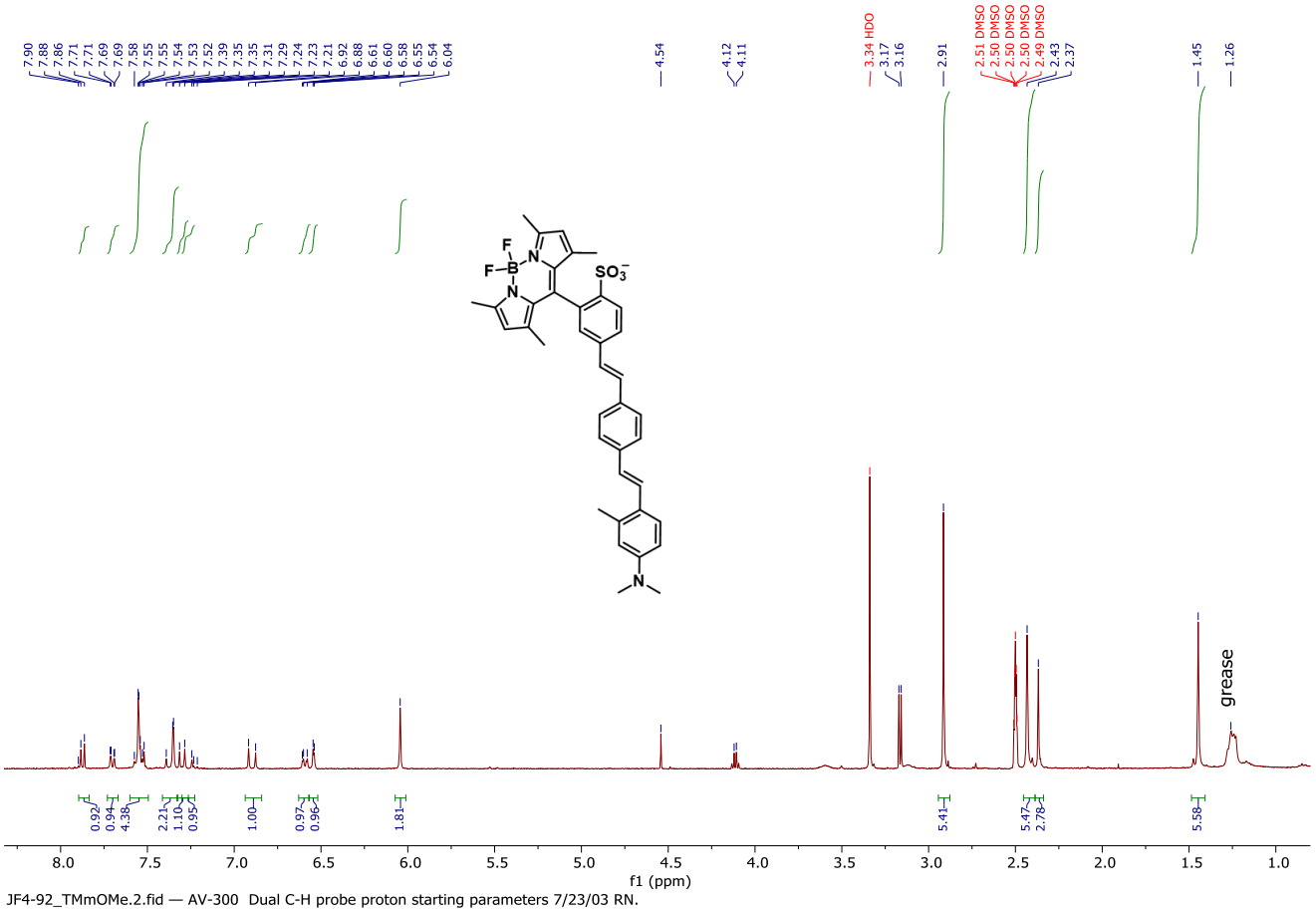

JF4-92_TMmOMe.2.fid — AV-300 Dual C-H probe proton starting parameters 7/23/03 RN.

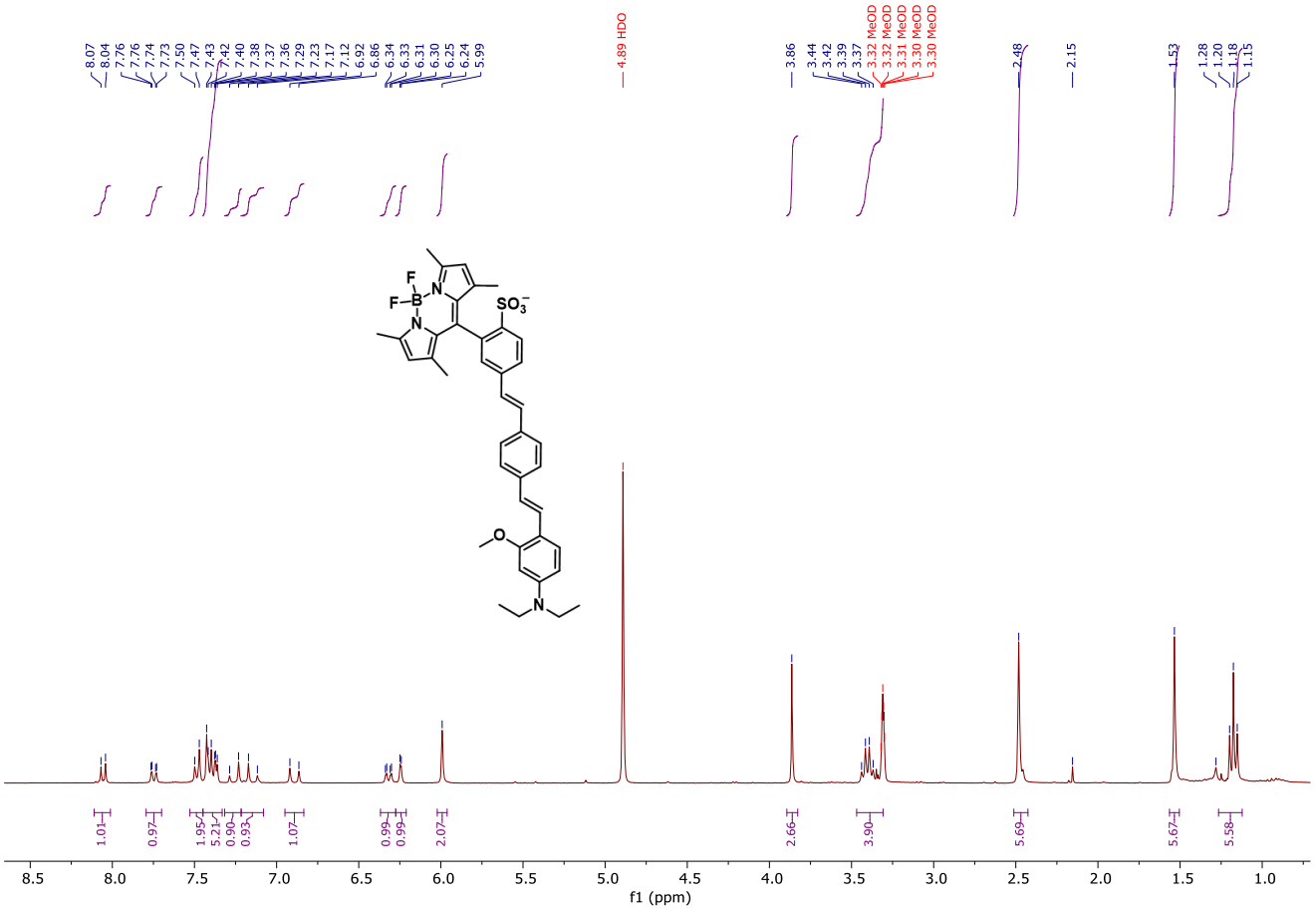

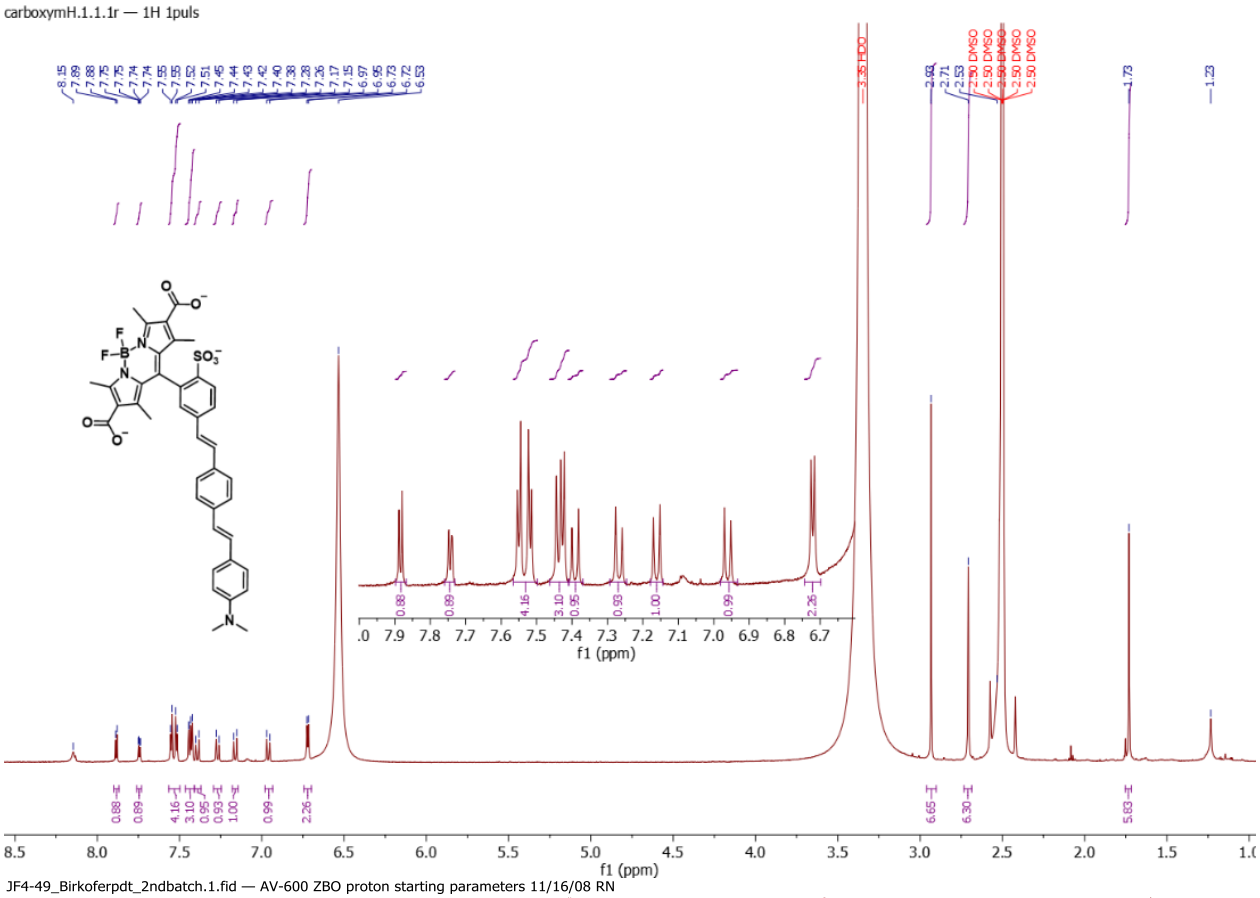
carboxymH.1.1.1r — 1H 1puls
f1 (ppm)

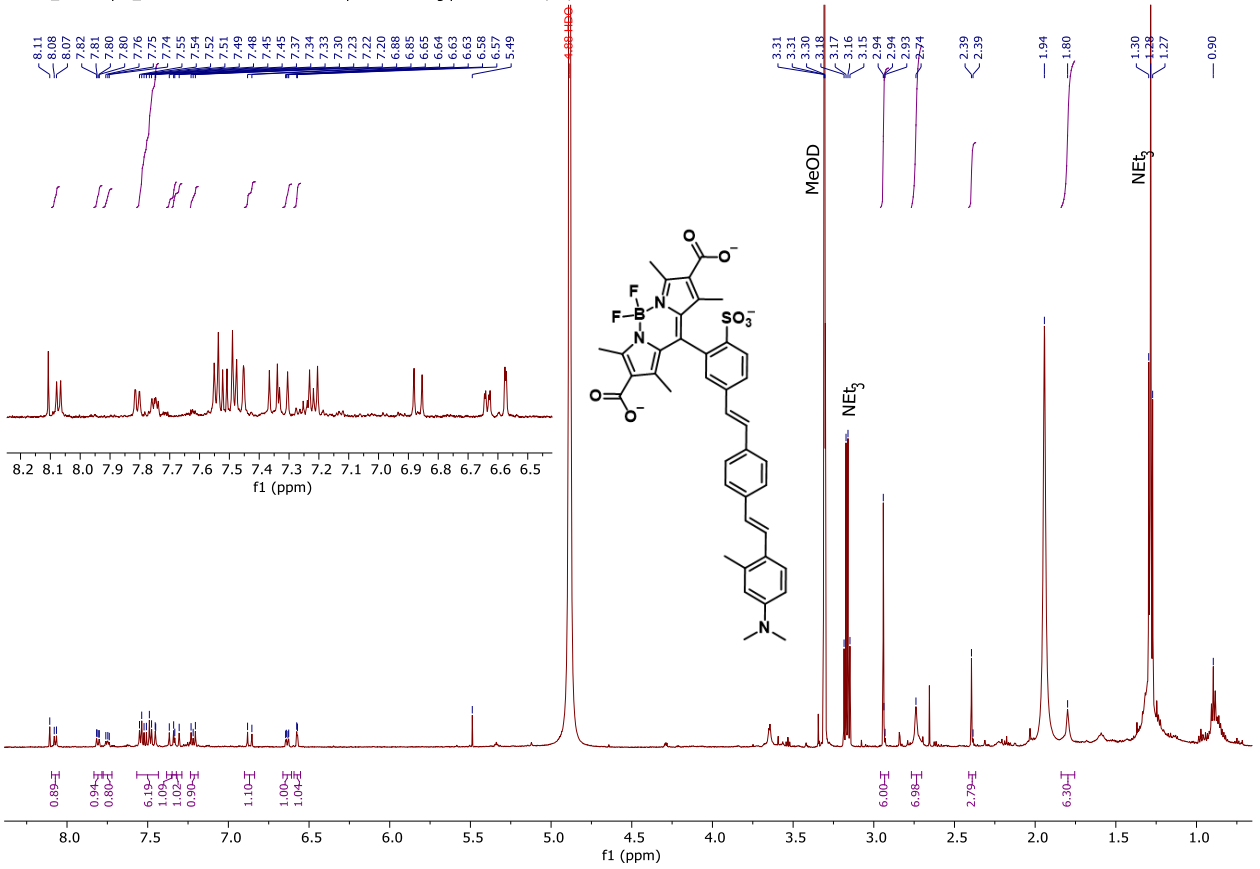
JF4-49_Birkoferpdt_2ndbatch.1.fid — AV-600 ZBO proton starting parameters 11/16/08 RN
MeOD
NEt3
NEt3
f1 (ppm)

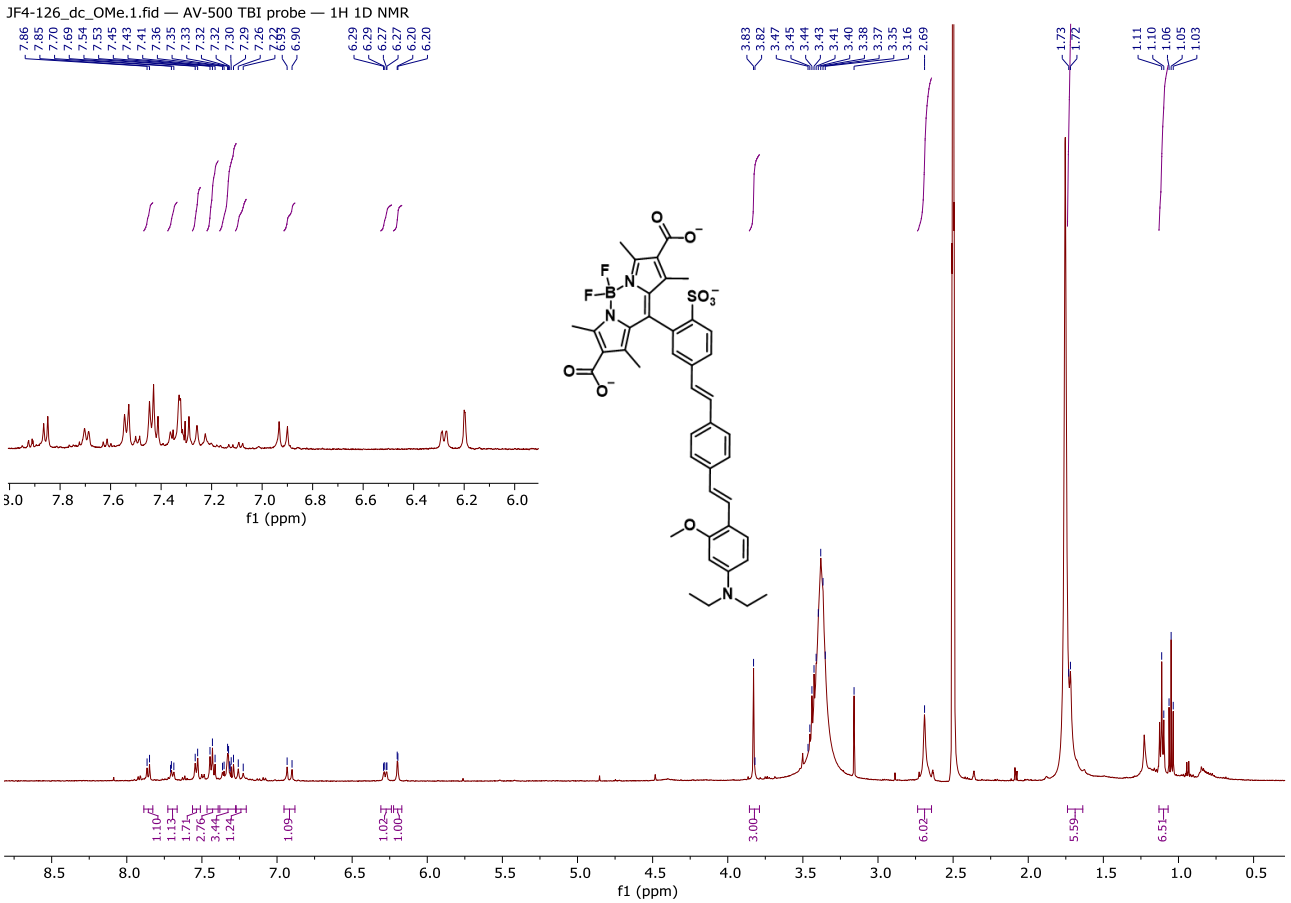
JF4-126_dc_OMe.1.fid — AV-500 TBI probe — 1H 1D NMR
f1 (ppm)

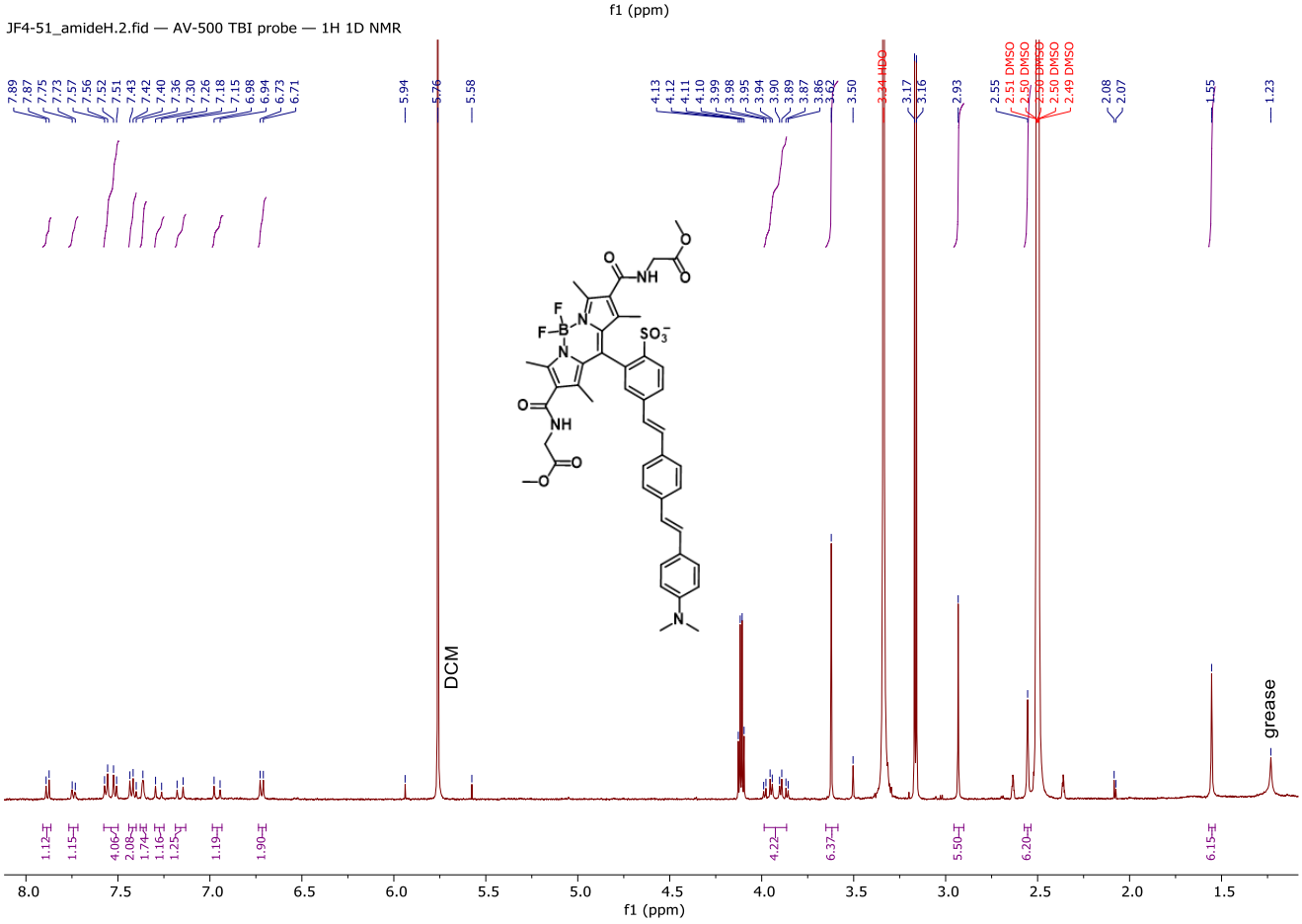
JF4-51_amideH.2.fid — AV-500 TBI probe — 1H 1D NMR
DCM
grease
f1 (ppm)

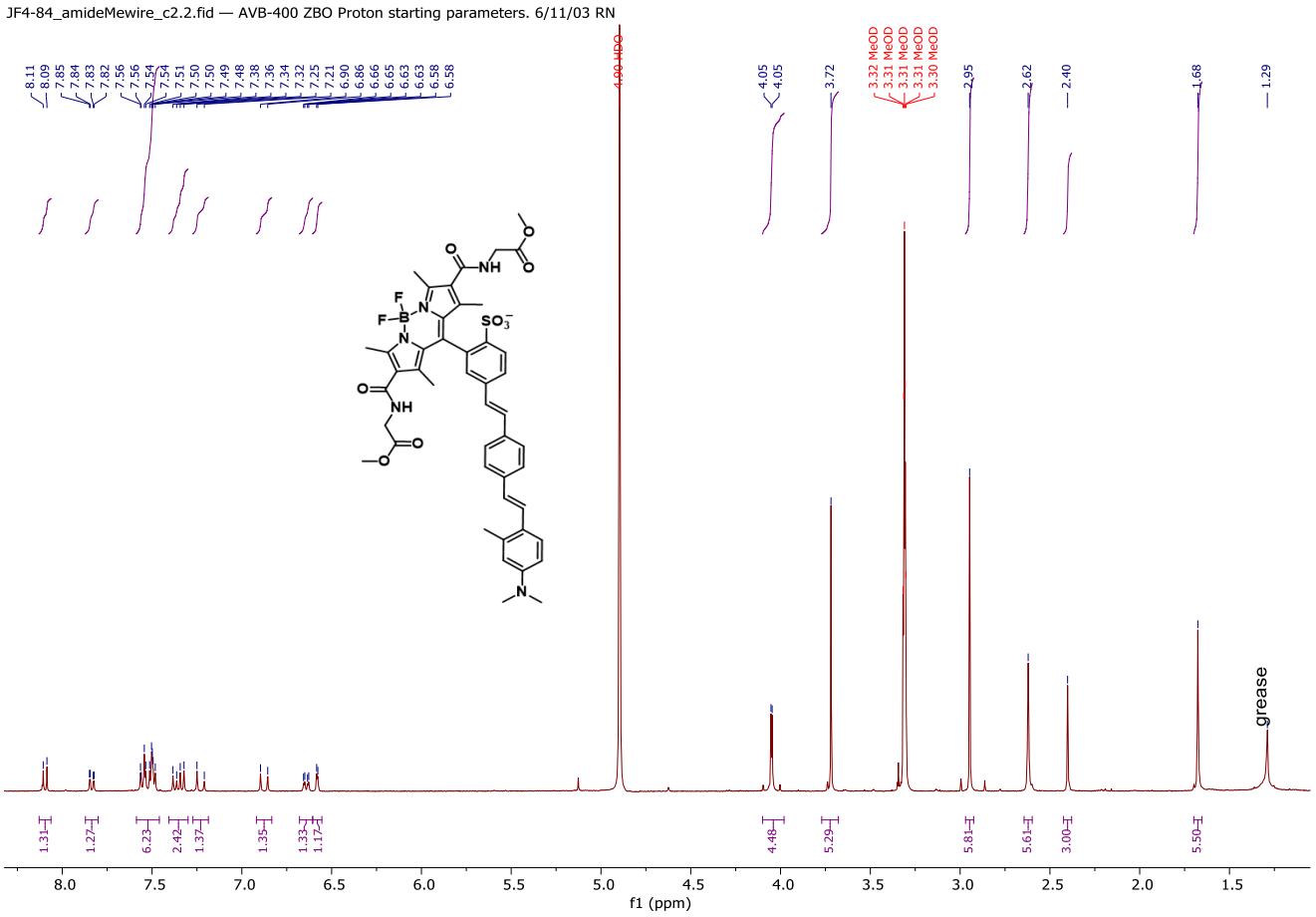

References

1. Frisch, M. J.; Trucks, G. W.; Schlegel, H. B.; Scuseria, G. E.; Robb, M. A.; Cheeseman, J. R.; Scalmani, G.; Barone, V.; Petersson, G. A.; Nakatsuji, H.; Li, X.; Caricato, M.; Marenich, A. V.; Bloino, J.; Janesko, B. G.; Gomperts, R.; Mennucci, B.; Hratchian, H. P.; Ortiz, J. V.; Izmaylov, A. F.; Sonnenberg, J. L.; Williams; Ding, F.; Lipparini, F.; Egidi, F.; Goings, J.; Peng, B.; Petrone, A.; Henderson, T.; Ranasinghe, D.; Zakrzewski, V. G.; Gao, J.; Rega, N.; Zheng, G.; Liang, W.; Hada, M.; Ehara, M.; Toyota, K.; Fukuda, R.; Hasegawa, J.; Ishida, M.; Nakajima, T.; Honda, Y.; Kitao, O.; Nakai, H.; Vreven, T.; Throssell, K.; Montgomery Jr., J. A.; Peralta, J. E.; Ogliaro, F.; Bearpark, M. J.; Heyd, J. J.; Brothers, E. N.; Kudin, K. N.; Staroverov, V. N.; Keith, T. A.; Kobayashi, R.; Normand, J.; Raghavachari, K.; Rendell, A. P.; Burant, J. C.; Iyengar, S. S.; Tomasi, J.; Cossi, M.; Millam, J. M.; Klene, M.; Adamo, C.; Cammi, R.; Ochterski, J. W.; Martin, R. L.; Morokuma, K.; Farkas, O.; Foresman, J. B.; Fox, D. J. *Gaussian 16 Rev. B.01*, Wallingford, CT, 2016.

2. Chai, J. D.; Head-Gordon, M., Long-range corrected hybrid density functionals with damped atom-atom dispersion corrections. *Phys Chem Chem Phys* **2008,** *10* (44), 6615-6620.

3. Weigend, F.; Ahlrichs, R., Balanced basis sets of split valence, triple zeta valence and quadruple zeta valence quality for H to Rn: Design and assessment of accuracy. *Phys Chem Chem Phys* **2005,** *7* (18), 3297-3305.